European Journal of Taxonomy 909: 1–63
https://doi.org/10.5852/ejt.2023.909.2351
ISSN 2118-9773
www.europeanjournaloftaxonomy.eu
2023 · Huber *et al.*

Monograph

urn:lsid:zoobank.org:pub:A48BD2B3-DC40-45BD-9968-F04890A1C5C5

Andean giants: *Priscula* spiders from Ecuador, with notes on species groups and egg-sac troglomorphism (Araneae: Pholcidae)

Bernhard A. HUBER [1*], Guanliang MENG [2], Nadine DUPÉRRÉ [3], Jonas ASTRIN [4] & Mauricio HERRERA [5]

[1,2,4] Zoological Research Museum Alexander Koenig, LIB, Bonn, Germany.
[3] Museum of Nature Hamburg, LIB, Hamburg, Germany.
[5] Instituto Nacional de Biodiversidad, Sección Invertebrados, Quito, Ecuador.

[*] Corresponding author: b.huber@leibniz-lib.de
[2] Email: G.Meng@leibniz-lib.de
[3] Email: n.duperre@leibniz-lib.de
[4] Email: J.Astrin.ZFMK@uni-bonn.de
[5] Email: mauricio.herrera@biodiversidad.gob.ec

[1] urn:lsid:zoobank.org:author:33607F65-19BF-4DC9-94FD-4BB88CED455F
[2] urn:lsid:zoobank.org:author:3B848D35-BC61-496E-9A39-7774B3BF237E
[3] urn:lsid:zoobank.org:author:F15E1FF2-2DF5-479A-AD10-8076CE96E911
[4] urn:lsid:zoobank.org:author:50661540-FD30-4ABA-8415-6B3069105E93
[5] urn:lsid:zoobank.org:author:35508EDA-A02C-4B00-BDA2-B516CF61DE21

Abstract. The Andean genus *Priscula* Simon, 1893 includes the largest Neotropical pholcid spiders, but due to their mostly cryptic lifestyle they remain poorly collected and poorly studied. Many species available in collections remain undescribed and nothing has been published about the phylogeny and the biology of the genus. Here, we deal with a recent collection of *Priscula* spiders from Ecuador, the country of origin of the type species, *P. gularis* Simon, 1893. We describe eight new species, collected at 17 localities at altitudes from 640–3160 m, all based on males and females: *P. azuay* sp. nov., *P. llaviucu* sp. nov., *P. espejoi* sp. nov., *P. esmeraldas* sp. nov., *P. chapintza* sp. nov., *P. pastaza* sp. nov., *P. bonita* sp. nov., and *P. lumbaqui* sp. nov. We use a sample of approximately 26 species-level taxa, mostly from Ecuador and Venezuela, to propose a first hypothesis about relationships within the genus. Our data (mainly CO1) suggest the existence of five species groups, three of which are represented in Ecuador. The cave-dwelling *P. pastaza* sp. nov. is only slightly troglomorphic (paler than usual; anterior median eyes strongly reduced or lost) but differs dramatically from forest-dwelling congeners in its biology: it hangs fully exposed in its web during the day; it produces egg sacs with only 6–7 eggs (average in 15 other species: 42 eggs); and it produces the largest eggs relative to body size of all studied species.

Keywords. CO1 barcode, cave-dwelling, taxonomy, egg size, egg number, Venezuela.

Huber B.A., Meng G., Dupérré N., Astrin J. & Herrera M. 2023. Andean giants: *Priscula* spiders from Ecuador, with notes on species group and egg-sac troglomorphism (Aranea: Pholcidae). *European Journal of Taxonomy* 909: 1–63. https://doi.org/10.5852/ejt.2023.909.2351

Introduction

With body lengths of ~7 mm and leg spans of over 12 cm, some species of *Priscula* Simon, 1893 are the largest known pholcid spiders in the Neotropics. Similar sizes are only reached by some representatives of the Old World genus *Artema* Walckenaer, 1837 and by some species of the North and Central American genus *Ixchela* Huber, 2000 (Huber 2021). Despite their size, most species of *Priscula* are usually difficult to find, at least during the day. Large parts of their conspicuous webs are usually hidden in dark sheltered spaces at ground level, and the spiders themselves spend the day deep within the cavities under logs and overhangs, among roots, in tussocks, or in holes in the ground. Geographically, *Priscula* is largely restricted to the tropical Andes, ranging from Bolivia to Venezuela (Huber 2000). A single species is known to range into northern Argentina (Huber 2014), and one undescribed species has been collected on the Island of Trinidad (B.A. Huber, unpubl. data).

Only a single morphological synapomorphy (male palpal tarsal organ on a turret) has previously been proposed (Huber 2000), but the monophyly of the genus appears beyond doubt. Representatives of *Priscula* are easily distinguished from all other indigenous Neotropical pholcids by the combination of size and globose to higher than long abdomen. The only superficially similar spiders in the Neotropics are two introduced species [*Artema atlanta* Walckenaer, 1837 and *Physocyclus globosus* (Taczanowski, 1874)] that can easily be distinguished from *Priscula* by details of the male chelicerae, male palp, and female epigynum (Huber 2000).

While the assignment of a given specimen to *Priscula* is thus usually easy and unproblematic, the relationships to other genera remain mysterious. A first morphological cladistic analysis (Huber 2000) assigned *Priscula* to "holocnemines", a group that included what are currently Arteminae and Smeringopinae. Molecular data later suggested instead an affinity either with Modisiminae (Bruvo-Mađarić *et al.* 2005; Eberle *et al.* 2018) or with Modisiminae + Arteminae (Eberle *et al.* 2018). Recent data on sperm ultrastructure also found similarities between *Priscula* and certain Modisiminae (Dederichs *et al.* 2022). Such an affinity makes sense geographically, as both *Priscula* and Modisiminae are restricted to the New World. However, our latest molecular (UCE) data (G. Meng, B.A. Huber, L. Podsiadlowski, unpubl. data) point instead to a sister-group relationship between *Priscula* and the Old World genus *Artema*. In sum, the morphological distinctness and the problematic phylogenetic placement together suggest that *Priscula* might be an ancient and possibly relict element of the Neotropical fauna.

Current data suggest that the highest species diversity of *Priscula* is concentrated in Venezuela. However, this is very likely biased and due to the extensive revisions of Venezuelan species by González-Sponga (1999) and Huber & Villarreal (2020). Unpublished data suggest a comparable diversity in Colombia, Ecuador, and Peru. The present paper is a first effort to close this gap, treating recent collections of *Priscula* spiders from Ecuador, a country from which only one species has previously been known: the type species *P. gularis* Simon, 1893.

Material and methods

Material examined

The morphological part of his study is based on the examination of more than 100 adult specimens from Ecuador deposited in the following collections: Instituto Nacional de Biodiversidad, Quito, Ecuador (INABIO; MECN codes); Museo de Zoología, Pontificia Universidad Católica, Quito, Ecuador (QCAZ); Zoologisches Forschungsmuseum Alexander Koenig, Bonn, Germany (ZFMK); and Zoological Museum Hamburg, Germany (ZMH). The molecular part is based on the specimens listed in Tables 1–2 as well as on previously published data (see below).

Table 1 (continued on the next page). Geographic origins of sequenced specimens. Newly sequenced specimens, sorted by Code. For geographic origins of previously sequenced specimens included in our analyses (codes starting with CH, JA, P, S) see Eberle *et al.* (2018).

Code	Country	Admin.	Locality	Lat.	Long.
BH62	Venezuela	Mérida	near Escaguey, NE Mérida	8.6918	-70.9950
BH63	Venezuela	Mérida	Mucuy, along Lago Suero trail	8.6260	-71.0365
BH64	Venezuela	Mérida	El Valle, along river	8.7030	-71.0770
BH66	Venezuela	Trujillo	between Boconó and Burbusay	9.3945	-70.2674
BH69	Venezuela	Aragua	between Maracay and Puerto Colombia	10.4304	-67.5998
BH70	Venezuela	Mérida	El Valle, along river	8.7030	-71.0770
BH75	Venezuela	Aragua	Henri Pittier N.P., Rancho Grande	10.3500	-67.6840
BH77	Venezuela	Monagas	between Cueva del Guacharo and Salto la Palia	10.1750	-63.5580
BH78	Venezuela	Lara	Yacambú N.P.	9.7080	-69.5830
BH79	Venezuela	Falcón	E Curimagua, Cuevas de Acarite	11.1737	-69.6280
BH80	Venezuela	Lara	between Coro and Barquisimeto, El Rodeo	10.7240	-69.3008
BH81	Venezuela	Mérida	between Mérida and Barinas, ‘site 2’	8.8645	-70.6182
BH82	Venezuela	Trujillo	near Boconó, Laguna Negra	9.3054	-70.1752
BH121	Venezuela	Trujillo	between Boconó and Burbusay	9.3945	-70.2674
BH126	Venezuela	Miranda	El Ávila N.P., between Sabas Nieves and La Silla	10.5245	-66.8566
BH127	Venezuela	Aragua	Henri Pittier N.P., Rancho Grande	10.3500	-67.6840
BH129	Venezuela	Lara	between Coro and Barquisimeto, El Rodeo	10.7240	-69.3008
BH130	Venezuela	Lara	between Barquisimeto and Boconó	9.5906	-69.8343
BH132	Venezuela	Aragua	Colonia Tovar, above town	10.4144	-67.3005
BH133	Venezuela	Aragua	Colonia Tovar, at Cerro Picacho	10.4080	-67.3080
BH134	Venezuela	Aragua	Henri Pittier N.P.	10.3500	-67.7200
BH143	Trinidad		Cerro Aripo	10.7120	-61.2355
BH148	Trinidad		Cerro Aripo	10.7120	-61.2355
EB003	Ecuador	Cotopaxi	San Francisco de Las Pampas	-0.4228	-78.9543
EB004	Ecuador	Cotopaxi	San Francisco de Las Pampas	-0.4228	-78.9543
EB020	Ecuador	Chimborazo	Vía Guano-Ilapo	-1.6037	-78.5907
EB032	Ecuador	Azuay	between Guayaquil and Cuenca, ‘loc. 2’	-2.7060	-79.4350
EB042	Ecuador	Pichincha	between San Juan and Chiriboga, ‘site 2’	-0.2327	-78.7497

Table 1 (continued). Geographic origins of sequenced specimens. Newly sequenced specimens, sorted by Code. For geographic origins of previously sequenced specimens included in our analyses (codes starting with CH, JA, P, S) see Eberle *et al*. (2018).

Code	Country	Admin.	Locality	Lat.	Long.
EB070	Ecuador	Azuay	between Guayaquil and Cuenca, 'loc 2'	-2.7060	-79.4350
EB077	Ecuador	Cañar	S Zhud	-2.4790	-78.9978
EB078	Ecuador	Cañar	S Zhud	-2.4790	-78.9978
EB083	Ecuador	Chimborazo	Desierto de Palmira	-2.0750	-78.7580
EB084	Ecuador	Tungurahua	S Baños	-1.4134	-78.4340
EB090	Ecuador	Pastaza	Cavernas del Anzu, in Caverna de los Continentes	-1.4067	-78.0449
EB095	Ecuador	Pastaza	Cavernas del Anzu, in Cueva Copa del Mundo	-1.4054	-78.0433
EB096	Ecuador	Pastaza	Cavernas del Anzu, at Cueva Copa del Mundo	-1.4054	-78.0433
EB107	Ecuador	Napo	Antisana N.P.	-0.6409	-77.8086
EB110	Ecuador	Napo	Gruta de Los Tayos, in canyon	-0.2186	-77.7402
EB115	Ecuador	Sucumbíos	near Lumbaquí	0.0349	-77.3106
EB119	Ecuador	Sucumbíos	near La Bonita	0.4740	-77.5580
EB121	Ecuador	Sucumbíos	between La Bonita and Santa Barbara	0.6470	-77.4910
EB127	Ecuador	Carchi	near El Ángel	0.6178	-77.9261
EB161	Venezuela	Táchira	SE Pregonero, near La Trampa	7.9236	-71.7152
EB162	Argentina	Tucumán	W of Embalse El Cadillal	-26.6133	-65.2251
EB164	Venezuela	Mérida	above Mesa Bolívar	8.4670	-71.6140
EB165	Venezuela	Miranda	El Ávila N.P., near La Julia	10.5164	-66.8089
EB166	Venezuela	La Guaira	El Limón, 'site 2'	10.4774	-67.2819
EB167	Venezuela	Mérida	near La Carbonera	8.6276	-71.3688
EB169	Venezuela	La Guaira	El Limón, 'site 1'	10.4788	-67.3010
EB171	Ecuador	Pastaza	Cueva de Los Tallos	-1.9512	-77.7885
EB172	Ecuador	Pastaza	Cueva de Los Tallos	-1.9512	-77.7885
EB173	Ecuador	Cotopaxi	San Francisco de Las Pampas	-0.4199	-79.0062
EB176	Ecuador	Azuay	between Guayaquil and Cuenca, 'loc. 2'	-2.7060	-79.4350
EB177	Ecuador	Azuay	between Guayaquil and Cuenca, 'loc. 1'	-2.6640	-79.4450
EB178	Ecuador	Azuay	between Guayaquil and Cuenca, 'loc. 2'	-2.7060	-79.4350
EB179	Ecuador	Azuay	between Guayaquil and Cuenca, 'loc. 2'	-2.7060	-79.4350

Table 2 (continued on the next page). GenBank accession numbers of newly sequenced specimens, sorted by Code. For accession numbers of previously sequenced specimens included in our analyses (codes starting with CH, JA, S) see Supplementary Table S1 and Eberle *et al.* (2018).

Code	Species	Vial	CO1	28S
BH62	*P. andinensis*	Ven18-218	OQ301935	
BH63	*P. andinensis*	Ven18-220	OQ301936	
BH64	*P. andinensis*	Ven18-226	OQ301937	
BH66	*P. andinensis*	Ven18-215	OQ301938	
BH69	*P. salmeronica*	Ven18-239	OQ301939	
BH70	*P. ulai*	Ven18-225	OQ301940	
BH75	*P. venezuelana*	Ven02/100-29	OQ301941	
BH77	*P. paila*	Ven02/100-24	OQ301942	
BH78	*P. lagunosa*	Ven02/100-59	OQ301943	
BH79	*P. acarite*	Ven18-196	OQ301944	
BH80	*P. acarite*	Ven18-197	OQ301945	
BH81	*P.* sp.-light	Ven18-237	OQ301946	
BH82	*P.* sp.-light	Ven18-208	OQ301947	
BH121	*P. andinensis*	Ven18-215	OQ301951	
BH126	*P. venezuelana*	Ven18-148	OQ301953	
BH127	*P. venezuelana*	Ven02/100-30	OQ301954	
BH129	*P. acarite*	Ven18-197	OQ301957	
BH130	*P. andinensis*	Ven18-205	OQ301952	
BH132	*P. venezuelana*	Ven02/100-09	OQ301955	
BH133	*P. venezuelana*	Ven02/100-44	OQ301956	
BH134	*P.* sp.	Ven02/100-33	OQ301948	
BH143	*P.* Tri11	Tri24female	OQ301949	
BH148	*P.* Tri11	Tri24male	OQ301950	OQ311352
EB003	*P. esmeraldas*	Dup009	OQ301958	
EB004	*P. esmeraldas*	Dup010	OQ301959	
EB020	*P. gularis*?	Dup086	OQ301960	
EB032	*P. azuay*?	Ecu038female	OQ301961	
EB042	*P.* Ecu5	Ecu124	OQ301962	
EB070	*P. espejoi*	Ecu154	OQ301963	
EB077	*P.* cf. *gularis*	Ecu162	OQ301964	
EB078	*P. llaviucu*	Ecu163	OQ301965	
EB083	*P. gularis*?	Ecu167	OQ301966	
EB084	*P.* cf. *gularis*	Ecu168	OQ301967	
EB090	*P. pastaza*	Ecu174	OQ301968	
EB095	*P. pastaza*	Ecu183	OQ301969	
EB096	*P. bonita*?	Ecu184	OQ301970	
EB107	*P. bonita*	Ecu201	OQ301971	
EB110	*P. bonita*	Ecu205	OQ301972	

Table 2 (continued). GenBank accession numbers of newly sequenced specimens, sorted by Code. For accession numbers of previously sequenced specimens included in our analyses (codes starting with CH, JA, S) see Supplementary Table S1 and Eberle *et al.* (2018).

Code	Species	Vial	CO1	28S
EB115	*P. lumbaqui*	Ecu210	OQ301973	
EB119	*P. bonita*	Ecu214	OQ301974	
EB121	*P. bonita*	Ecu216	OQ301975	
EB127	*P.* cf. *gularis*	Ecu222	OQ301976	
EB161	*P. andinensis*	Ven20-118	OQ301932	
EB162	*P. binghamae*?	Arg171	OQ301931	
EB164	*P. bolivari*	Ven20-130	OQ301930	
EB165	*P.* cf. *limonensis*	Ven20-182	OQ301929	
EB166	*P. limonensis*	Ven20-175	OQ301928	
EB167	*P. piapoco*?	Ven20-110	OQ301927	
EB169	*P. salmeronica*	Ven20-166	OQ301922	
EB171	*P. chapintza*	Dup148	OQ301920	
EB172	*P. chapintza*	Dup156	OQ301923	
EB173	*P.* Dup55	Dup170	OQ301924	
EB176	*P. espejoi*	Ecu39	OQ301925	
EB177	*P. espejoi*	Ecu151B	OQ301926	OQ311349
EB178	*P. espejoi*	Ecu154B		OQ311350
EB179	*P. azuay*	Ecu38male	OQ301921	

Taxonomy and Morphology

Taxonomic descriptions follow the style of recent publications on Pholcidae (e.g., Huber 2022; based on Huber 2000). The sequence of descriptions is as in Figs 1–2. Measurements were done on a dissecting microscope with an ocular grid and are in mm unless noted otherwise; eye measurements are ± 5 µm. Photos were made with a Nikon Coolpix 995 digital camera (2048 × 1536 pixels) mounted on a Nikon SMZ 18 stereo microscope or a Leitz Dialux 20 compound microscope. CombineZP (https://combinezp.software.informer.com/) was used for stacking photos. Drawings are partly based on photos that were traced on a light table and later improved under a dissecting microscope, or they were directly drawn with a Leitz Dialux 20 compound microscope using a drawing tube. Cleared epigyna were stained with chlorazol black. Distribution maps were generated with ArcMap 10.0.

Abbreviations

ALE = anterior lateral eye(s)
ALS = anterior lateral spinneret(s)
AME = anterior median eye(s)
a.s.l. = above sea level
L/d = length/diameter
PLE = posterior lateral eye(s)
PME = posterior median eye(s)
PMS = posterior median spinneret(s)

Abbreviations used in figures only are explained in the figure legends.

Molecular data and analyses

Taxon sampling

We used eleven species from Eberle *et al.* (2018): four *Priscula* species and seven outgroup taxa representing Modisiminae, Arteminae, and Ninetinae. To this we newly added 56 *Priscula* specimens (Tables 1–2, Supplementary Table S1).

Gene sampling

For the taxa taken from previous studies, we used all available sequences (CO1 barcode, 12S, 16S, 18S, 28S, and H3; or a subset of these). For the newly added taxa, we sequenced 55 CO1 barcodes and three 28S genes. In total, there were 111 sequences and 67 specimens (Supplementary Table S1).

DNA extraction, amplification and sequencing

One leg each of specimens stored in non-denatured pure ethanol (~99%) at -20°C was used for DNA extraction. Extracted genomic DNA is deposited at and available from the LIB Biobank, Museum Koenig, Bonn. For DNA extractions, a Qiagen (Hilden, Germany) BioSprint96 magnetic bead extractor and corresponding

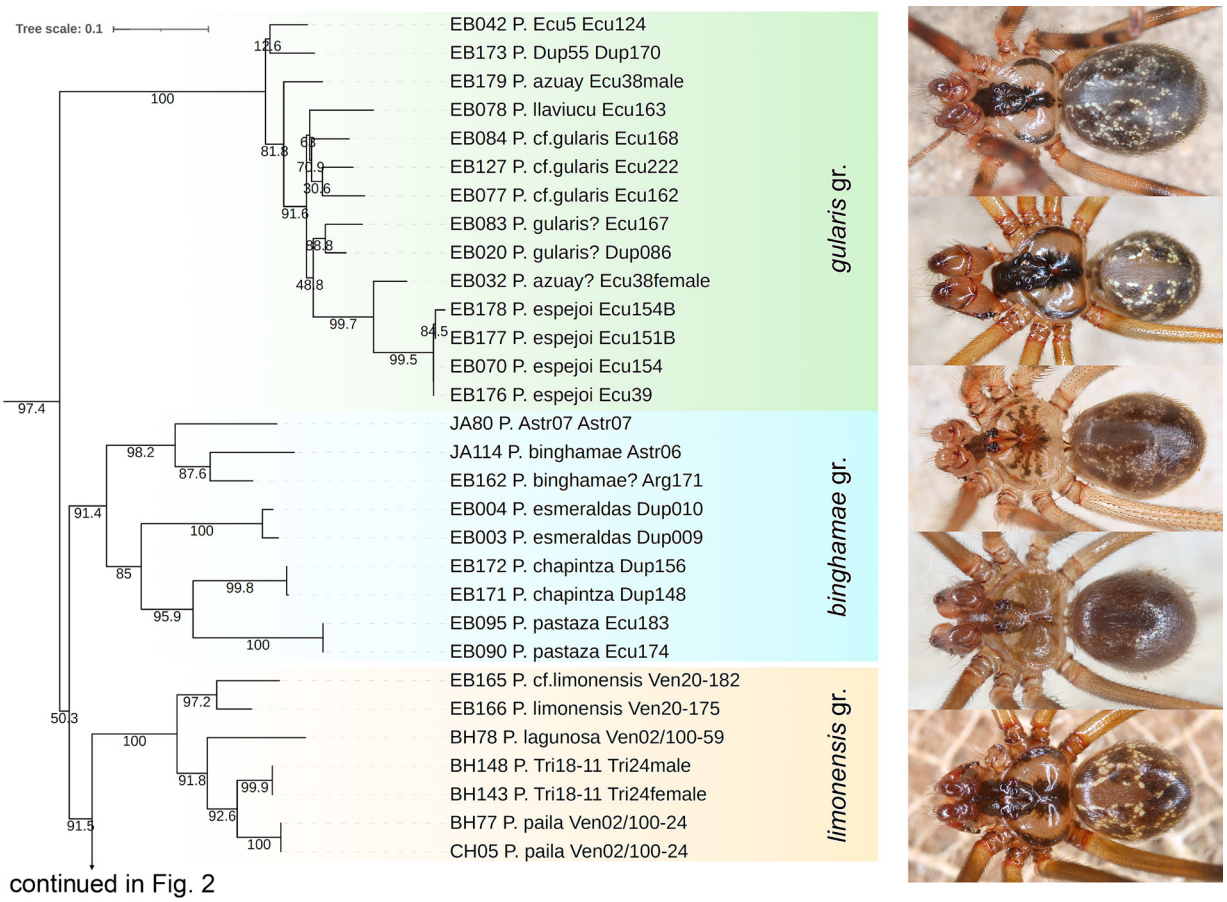

Fig. 1; continued in Fig. 2. Relationships of *Priscula* derived from an unpartitioned analysis of molecular data using IQ-Tree and the ClipKIT kpic-smart-gap trimming strategy. Numbers on the branches are SH-aLRT supports (%). The tree shows only the ingroup. For the complete tree (incl. outgroups), and for clade support using different partitioning and alignment strategies, see Supplementary Figures S1–S3. Photos on the right, from top: *Priscula llaviucu* Huber sp. nov.; *P. espejoi* Huber sp. nov.; *P. binghamae* (Chamberlin, 1916); *P. pastaza* Huber sp. nov.; *P.* "Tri18-11".

kits were used, following the manufacturer's specifications. CO1 primers used were LCO1490-JJ and HCO2198-JJ (Astrin & Stüben 2008), with versions JJ2 (Astrin *et al.* 2016) as backup. The 20 µl reaction volume consisted of 5 µl H_2O, 1 µl DNA template, 2 µl Q-Solution, 10 µl Qiagen Multiplex-Mix, 1 µl forward primer, and 1 µl reverse primer. The PCR procedure was: (1) 95°C for 15 minutes; (2) denaturation at 94°C for 35 seconds; (3) annealing at 55°C (-1°C per cycle down to 40°C, then 25 cycles at 45°C) for 90 seconds; (4) elongation at 72°C for 90 seconds; (5) final elongation at 72°C for 10 minutes, followed by cooling at 10°C. The settings (incl. primers and PCR conditions) for 28S were the same as in Eberle *et al.* (2018). PCR products were sent for bidirectional Sanger sequencing to BGI (Hong Kong, China).

DNA sequence alignment and editing

The newly sequenced CO1 barcodes and 28S sequences were assembled with GENEIOUS R7 (Kearse *et al.* 2012). Taxonomic assignments of the assembled sequences were checked by: (1) blasting assembled sequences against a local NT database; (2) the identification engine of the Barcode of Life Data System (BOLD) (http://www.boldsystems.org/index.php; Ratnasingham & Hebert 2007; Yang *et al.* 2020).

Multiple sequence alignment (MSA)

For the protein-coding genes CO1 and H3, DNA sequences were translated into protein sequences using BioPython (version 1.78) (Cock *et al.* 2009) with invertebrate mitochondrial genetic code and standard genetic code, respectively. Next, protein-MSAs were constructed using the mafft-linsi algorithm of

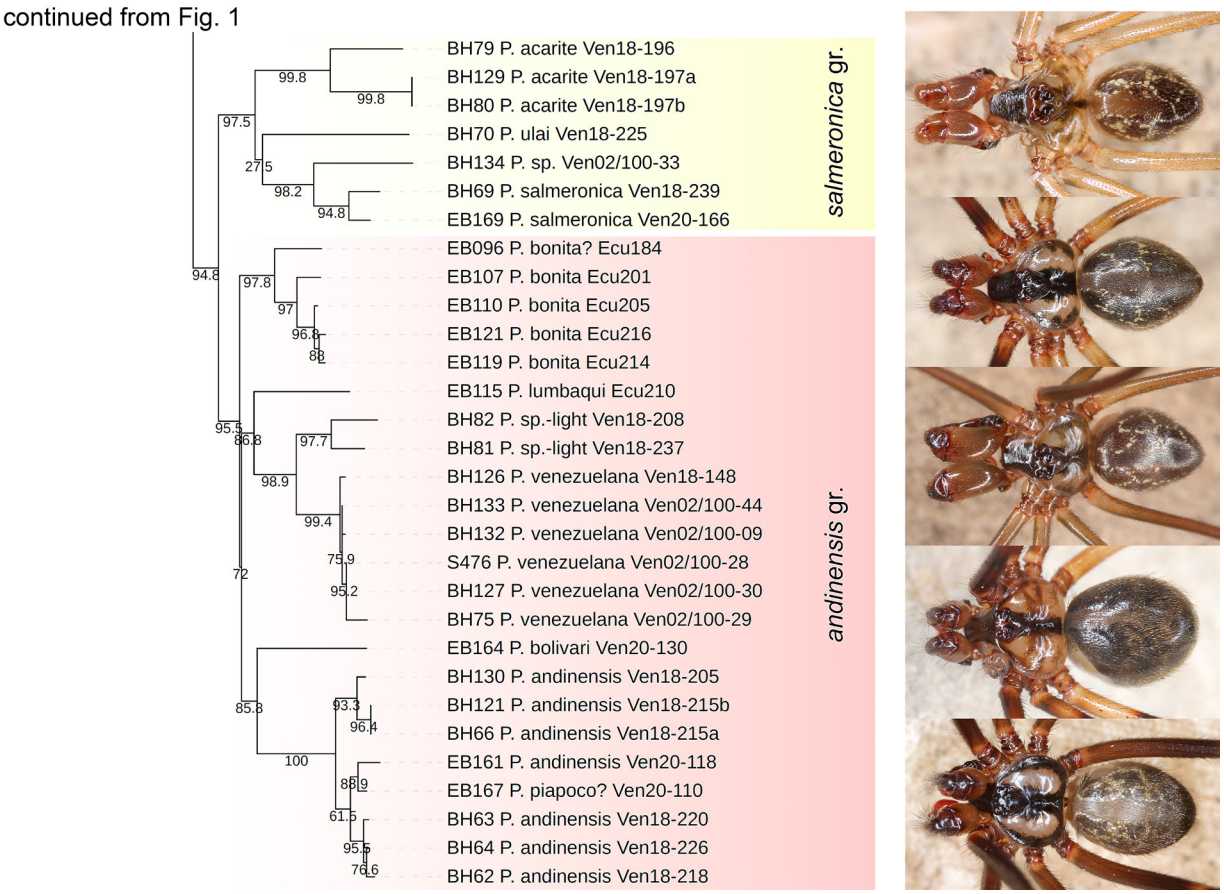

Fig. 2. Relationships of *Priscula*; continued from Fig. 1. Photos on the right, from top: *P. salmeronica* González-Sponga, 1999; *P. bonita* Huber sp. nov.; *P. lumbaqui* Huber sp. nov.; *P. venezuelana* Simon, 1893; *P. andinensis* González-Sponga, 1999.

MAFFT (version 7.487) (Katoh & Standley 2013), which then assisted in the construction of nucleotide level MSAs with pal2nal.pl (Suyama *et al.* 2006). This helps avoid the introduction of biologically meaningless frameshifts to the alignments (Suyama *et al.* 2006). The alignments of rRNA genes (12S, 16S, 18S, and 28S) were constructed based on secondary structure information using the mafft-xinsi algorithm in MAFFT (version 7.487) (Katoh & Standley 2013) and MXSCARNA (Tabei *et al.* 2008). Poorly aligned regions in the MSAs were then trimmed with Gblocks (version 0.91b) (Talavera & Castresana 2007) (-b5=h), TrimAl (version 1.4.rev15) (Capella-Gutiérrez *et al.* 2009) (-automated 1) and ClipKIT (version 1.1.3) (Steenwyk *et al.* 2020), respectively. In the ClipKIT program, we tested different trimming strategies (--modes gappy, kpi, kpic, kpic-gappy, kpic-smart-gap, kpi-gappy, kpi-smart-gap, smart-gap).

Phylogenetic inference

Maximum-likelihood trees were constructed based on concatenated alignments (trimmed or untrimmed) using IQ-TREE (version 2.1.3) (Minh *et al.* 2020). For comparison, both partitioned (by locus) and unpartitioned analyses were performed. To overcome local optima during heuristics, we performed ten

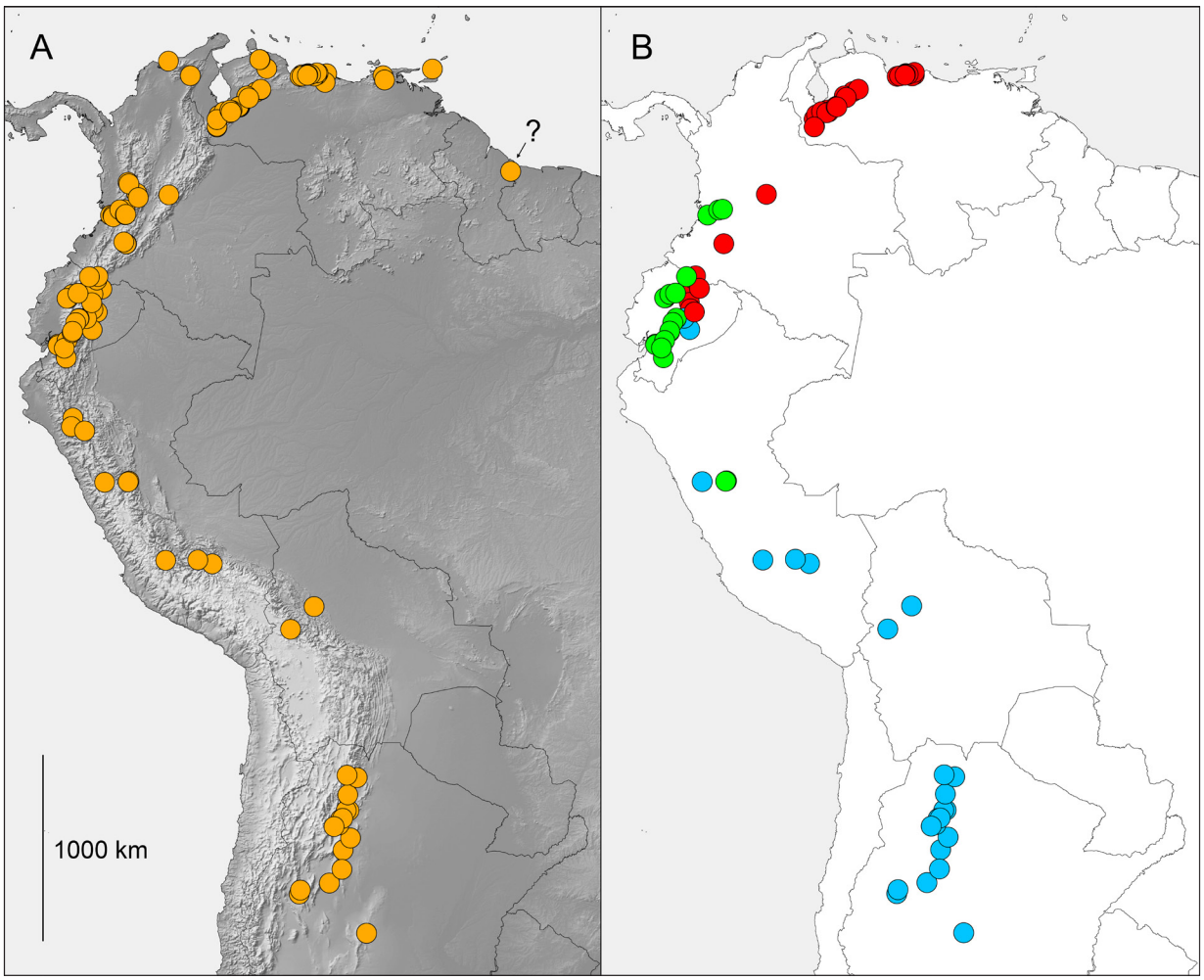

Fig. 3. Known distribution of *Priscula*. **A**. Map showing all known records, including unpublished material available in collections (B.A. Huber, unpubl. data). Note that the type locality of *P. taruma* in Guyana is dubious (see text for details). **B**. Known distributions of the three species groups represented in Ecuador. Red: *andinensis* group; green: *gularis* group; blue: *binghamae* group; see text for further details.

independent IQ-TREE runs (--runs 10), with a smaller perturbation strength (-pers 0.2) and larger number of stop iterations (-nstop 500). Branch supports were evaluated with 2000 ultrafast bootstrap (UFBoot) (Minh *et al.* 2013) with the risk of potential model violations considered (-B 2000 -bnni). The SH-aLRT branch test (Guindon *et al.* 2010) was performed using 2000 bootstrap replicates (-alrt 2000). Best-fitting substitution models were automatically determined by the ModelFinder algorithm (Kalyaanamoorthy *et al.* 2017) in IQ-TREE (-m MFP for unpartitioned anlayses, -m MFP+MERGE for partitioned analyses). Using the untrimmed CO1 alignment and the Kimura 2-parameter model (Kimura 1980), a NJ tree and K2P genetic distances between different specimens were calculated with MEGA (version 11.0.13) (Tamura *et al.* 2021). Tree visualizations were finished with iTOL (Letunic & Bork 2021).

Results

Taxonomy

Order Araneae Clerck, 1757
Family Pholcidae C.L. Koch, 1850
Genus ***Priscula*** Simon, 1893

General notes

The genus was revised in Huber (2000) and the diagnosis and general description given there are still largely valid (see below for amendments of description). Since then, the genus has received little attention, with only two further publications contributing to our knowledge of the group. Huber & Villarreal (2020) reported new species from Venezuela, and Huber (2014) added a few records for *P. binghamae* (Chamberlin, 1916) from Argentina.

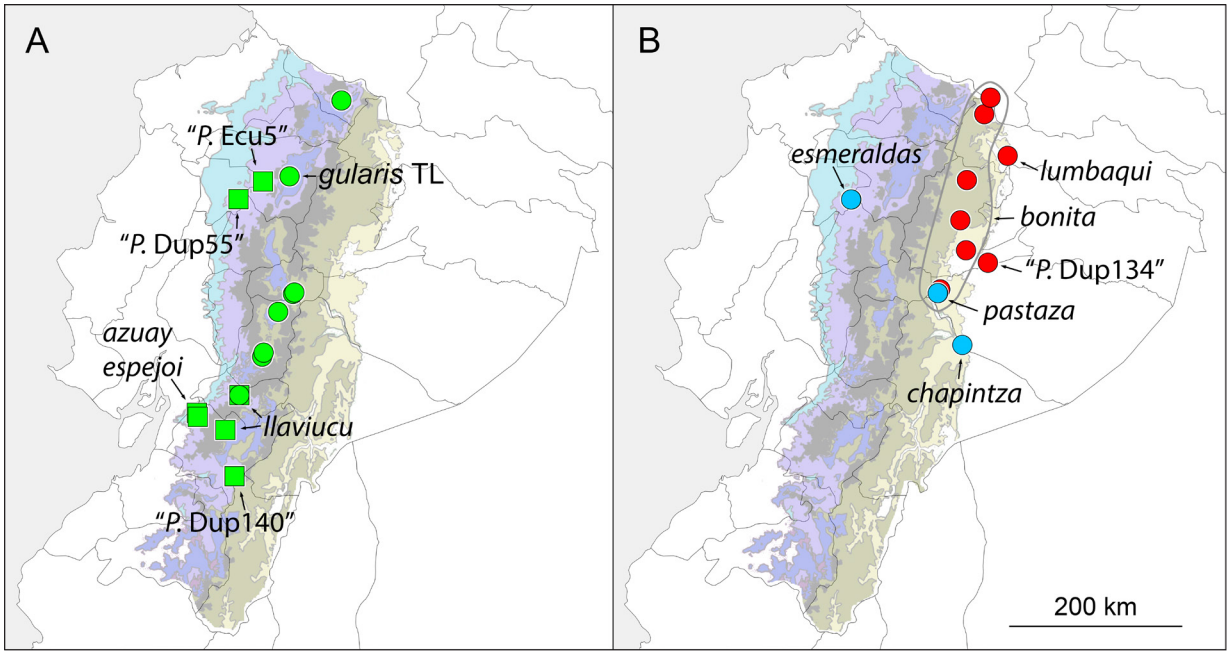

Fig. 4. Known distribution of *Priscula* in Ecuador. **A**. Representatives of the *gularis* group. Circles: *P. gularis* (TL = type locality) and specimens treated herein as "*P. gularis*?" and "*P.* cf. *gularis*". Squares: other Ecuadorian representatives of the *gularis* group. **B**. Representatives of the *andinensis* group (red) and *binghamae* group (blue) in Ecuador. The background colors indicate biogeographic regions of Ecuador (as far as relevant for *Priscula*, i.e., Andean regions from western foothill forests to eastern foothill forests), taken from Torres-Carvajal *et al.* (2019).

The species described in Huber & Villarreal (2020) and the new species described below largely fit the genus description given in Huber (2000). The following amendments complement the genus description: 1) ocular area in males sometimes with strong hair brushes between eye triads; (2) male clypeus unmodified in shape, but rim often more strongly sclerotized than in female; (3) abdomen ventrally in front of spinnerets sometimes with sclerite or pair of sclerites; (4) male chelicerae consistently with whitish lateral area; (5) male palpal femur sometimes with ventral process at about half length; (6) main bulbal process not always spiraling but sometimes of simpler shape; (7) tibia 1 L/d: 23–73; (8) prolateral trichobothrium on tibia 1 present.

Molecular analyses

The results of the molecular analyses are shown in Figs 1–2 and in Supplementary Figs S1–S4 and Supplementary Table S2. Details are presented in the Species groups section below (phylogenetic aspects) as well as within the individual species descriptions (barcoding aspects).

Species groups

The relationships of *Priscula* to other genera were not the focus of the present study and will soon be addressed using molecular (UCE) data (G. Meng, B.A. Huber, L. Podsiadlowski, unpubl. data). Within *Priscula*, our molecular data suggest five species groups (Figs 1–2) that are consistently and sometimes highly supported. For morphological support for these groups and for possible assignments of species not included in the molecular dataset, see Discussion.

***gularis* group**

This group includes the type species *P. gularis* Simon, 1893, and three of the newly described species: *P. azuay* sp. nov., *P. espejoi* sp. nov., and *P. llaviucu* sp. nov. It always received high support (SH-aLRT supports: 92–100) and was in most analyses (except when using TrimAl and Gblocks) resolved as the sister of the other four groups (see Fig. S2). Internal relationships varied but two undescribed species ("*P.* Ecu5" and "*P.* Dup55") were consistently resolved either as paraphyletic 'basal' species or together as sister of the remaining species. Among the latter, *P. azuay* was again consistently resolved as sister to the rest. All sequenced species in this group are from Ecuador.

***binghamae* group**

This group includes the southernmost known species, *P. binghamae*, an undescribed species from Peru ("*P.* Astr07"), and three of the newly described species from Ecuador: *P. esmeraldas* sp. nov., *P. chapintza* sp. nov., and *P. pastaza* sp. nov. The group received reasonable to high support (78–94) and was in most analyses resolved as the sister of the three following groups; only TrimAl and Gblocks resolved the *binghamae* group as sister to all other groups. The three species from Ecuador were always resolved as monophyletic (79–96), always in the same topology: *P. esmeraldas* + (*P. chapintza* + *P. pastaza*).

***limonensis* group**

The species included in this group are from the Cordillera de la Costa and the Cordillera de Mérida in Venezuela, and from the Island of Trinidad. The group received reasonable to high support (86–100); it always formed a monophylum with the following two groups (79–84), as their sister. Internal relationships were consistently resolved in the same topology.

***salmeronica* group**

The species included in this group are restricted to Venezuela, where they occur in the Cordillera de la Costa and in the Cordillera de Mérida. The group received reasonable to high support (86–98) and always formed a monophylum with the *andinensis* group (82–96). Internal relationships varied, except that *P. salmeronica* González-Sponga, 1999 was consistently resolved as sister to an undescribed species ("*P.* Ven02/100-33").

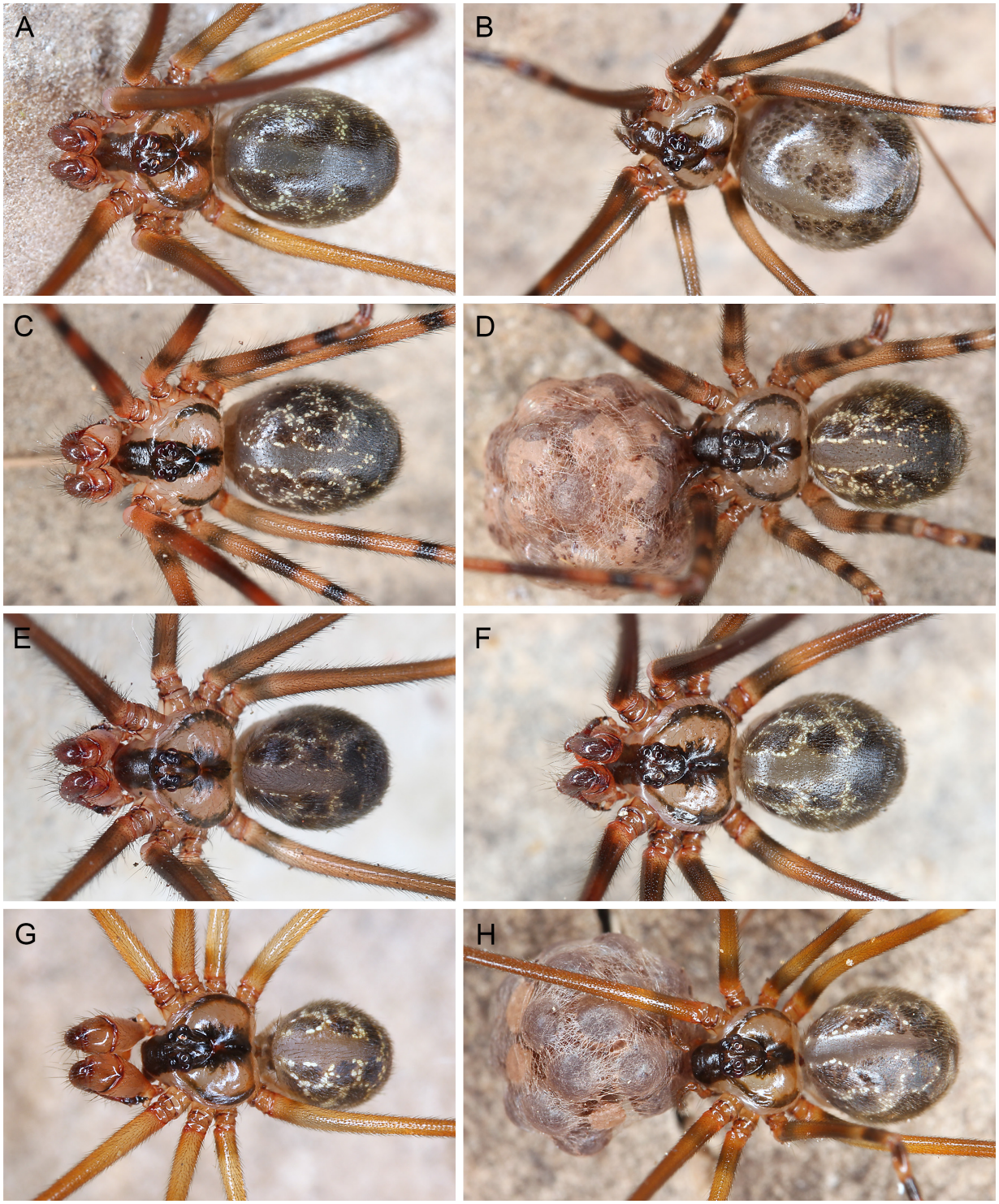

Fig. 5. *Priscula* spp., *gularis* group, live specimens. **A–B**. *P. azuay* Huber sp. nov.; male and female from Guayaquil-Cuenca, 'loc. 2'. **C–D**. *P. llaviucu* Huber sp. nov.; male and female with egg-sac from Cajas National Park. **E–F**. *P.* cf. *gularis*; males from near Zhud and from near Baños. **G–H**. *P. espejoi* Huber sp. nov.; male and female with egg-sac from Guayaquil-Cuenca, 'loc. 1'.

***andinensis* group**

This group includes two of the newly described species: *P. bonita* sp. nov. and *P. lumbaqui* sp. nov. Geographically, it ranges from the eastern side of the Central Andes in Ecuador to the Cordillera de la Costa in Venezuela. The group received modest to high support in most analyses (81–99; only TrimAl in partitioned analysis lower: 72) and was consistently resolved as sister to the *salmeronica* group (82–96). Internal relationships varied, except that *P. venezuelana* Simon, 1893 was consistently resolved as sister to an undescribed Venezuelan species ("*P.* sp.-light") (84–100), and *P. bolivari* Huber, 2020 was consistently resolved as sister to *P. andinensis* González-Sponga, 1999 (mostly 78–87; only TrimAl in unpartitioned analysis lower: 33). The two new Ecuadorian species were never resolved as sister taxa.

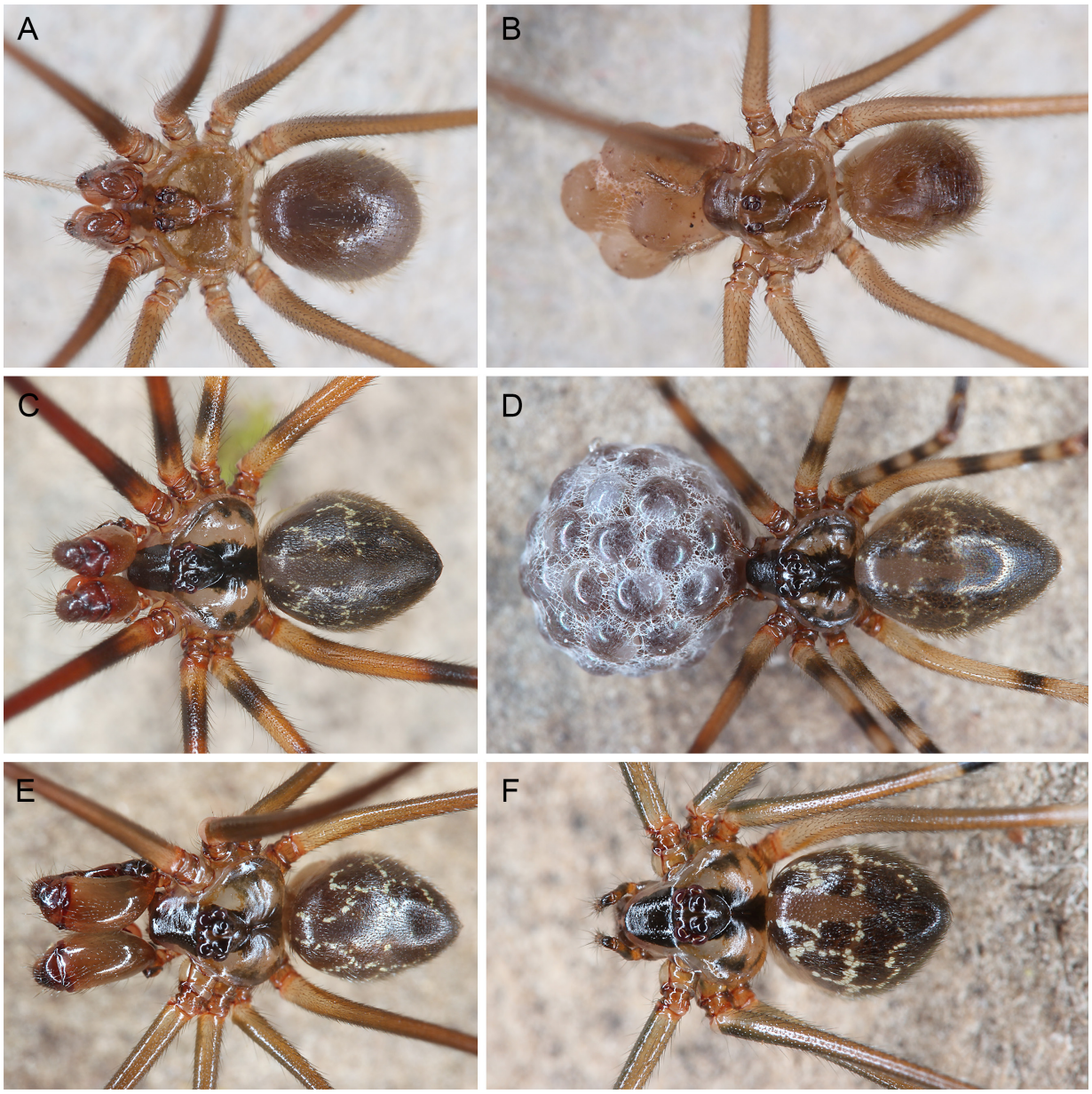

Fig. 6. *Priscula* spp., *binghamae* and *andinensis* groups, live specimens. **A–B**. *P. pastaza* Huber sp. nov.; male and female with egg-sac from Cavernas del Anzu Forest Reserve. **C–D**. *P. bonita* Huber sp. nov.; male from La Bonita-Santa Barbara and female with egg-sac from Gruta de los Tayos. **E–F**. *P. lumbaqui* Huber sp. nov.; male and female from near Lumbaqui.

Distribution

Priscula is a tropical Andean genus (Figs 3–4), ranging from northern Argentina to the Island of Trinidad (whose Northern Range is an outlier of the Venezuelan Andes). Many records are from high elevations (79% of all known records > 1000 m a.s.l.; 32% > 2000 m). A notable geographic outlier is *P. taruma* Huber, 2000, supposedly collected in Guyana, East Berbice-Corentyne, "Canje Ikuruwa River". In the original description (Huber 2000), the label coordinates were incorrectly shown as degrees and minutes, while in fact they should be read as decimal degrees: 5.70° N, 57.50° W (which marks a spot between Canje River and Ikuruwa Lake; approximately 10–20 m a.s.l.). This species is known from a single male specimen, and it continues to be the only record of *Priscula* from the entire Guyana Shield. This record might thus result from mislabeling and should be doubted until the presence of *Priscula* is confirmed from this locality or region.

Natural history

Most of the species newly described below were found in sheltered spaces like deep holes at ground level, tunnels under roads, deep within large grass tussocks, or in thick mosses covering tree trunks (see individual natural history sections below). This cryptic lifestyle is probably correlated with their general dark coloration (Eberle *et al.* 2018; Figs 5–6). Most known *Priscula* species share the dark coloration and thus probably also the cryptic lifestyle (for a few known exceptions, see Discussion). Anecdotal observations (B.A. Huber, unpublished data on an unidentified species in Merenberg Reserve, Colombia) suggest that some or many of these species may be nocturnal, abandoning their hideaways in the darkness and spending the night in exposed parts of their webs. The cave-dwelling *P. pastaza* (Fig. 6A–B), by contrast, was found hanging from the center of its exposed web during the day, suggesting that visual predators account for the reclusive day-lives of forest-dwelling species. This may be related to a further observation regarding cave-dwelling versus forest-dwelling species: two *P. pastaza* egg-sacs contained only six and seven eggs, respectively, while egg-sacs of 15 further species contained an average of 42 eggs (data from Huber & Villarreal 2020; Huber & Eberle 2021; and herein). This relationship persisted when egg numbers were corrected for body size (female carapace width) (Fig. 7A): *P. pastaza* had by far the lowest value (4.2), followed by a Venezuelan species that lives in cave entrances (*P. acarite* Huber, 2020: 10.0); in the other 14 studied species, this value ranged from 13.5–32.7 (mean 20.7). Egg size ranged from 0.81–1.22 mm

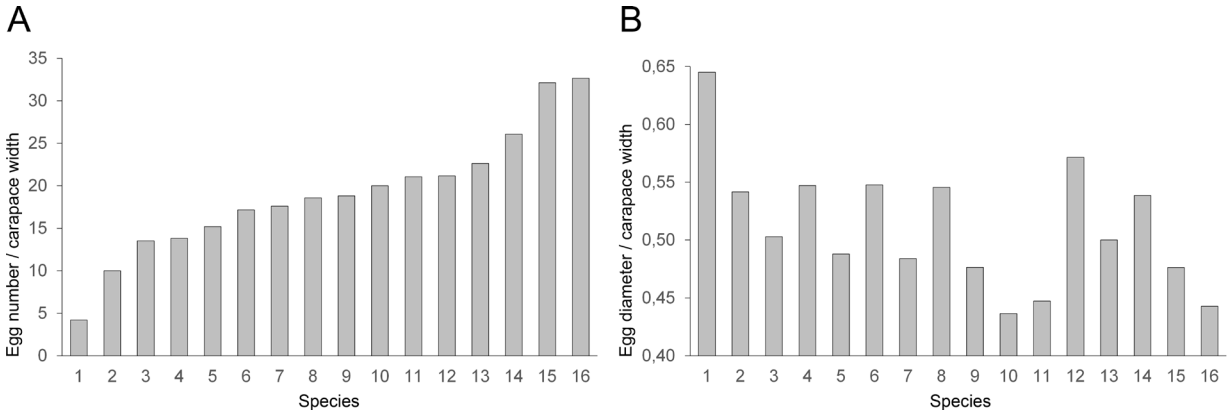

Fig. 7. Egg numbers and sizes in 16 species of *Priscula*. **A**. Mean egg numbers per egg-sac corrected for body size (egg number / female carapace width in mm), in ascending order. **B**. Egg diameter corrected for body size (female carapace width), in same order as previous diagram. Species (number of egg sacs studied in parentheses): 1. *P. pastaza* Huber sp. nov. (2); 2. *P. acarite* (1); 3. *P.* "Tri18-11" (1); 4. *P. ulai* (2); 5. *P. piapoco* (1); 6. *P. bonita* Huber sp. nov. (2); 7. *P. binghamae* (2); 8. *P. espejoi* Huber sp. nov. (3); 9. *P. salmeronica* (1); 10. *P. andinensis* (2); 11. *P. paila* (2); 12. *P.* cf. *gularis* (ZFMK Ar 24091) (2); 13. *P. esmeraldas* Huber sp. nov. (1); 14. *P. llaviucu* Huber sp. nov. (1); 15. *P. lumbaqui* Huber sp. nov. (1); 16. *P. venezuelana* (2). Data from Huber & Villarreal (2020), Huber & Eberle (2021), and herein.

(N = 16 species, 25 egg-sacs). The eggs of *P. pastaza* were of medium size (1.00 mm) but, corrected for body size, *P. pastaza* had the largest eggs (Fig. 7B).

Composition

The genus now includes 28 described species, most of them from Venezuela (currently 13 described species) and Ecuador (nine species). Unpublished material shows that the genus is also diverse in Colombia (only three described species) and Peru (two described species).

Priscula azuay Huber sp. nov.
urn:lsid:zoobank.org:act:7433AF78-D32F-4BED-810D-55A2102A705C
Figs 5A–B, 8–11

Diagnosis

Distinguished from known congeners by details of procursus (Fig. 9A–C; distinctive dorsal distal membrane larger than in similar *P. espejoi* sp. nov.; short distal ventral sclerite; without retrolateral process), genital bulb (Fig. 9D–F; main bulbal process long and slender, gradually narrowing at tip), epigynum (Fig. 11A–B; in lateral view without anterior bulge, similar to *P. llaviucu* sp. nov. but posterior bulge weaker than in *P. llaviucu*), and female internal genitalia (Fig. 10C; pore plates roughly triangular, narrower anteriorly than posteriorly and converging anteriorly – apparently indistinguishable from *P. espejoi*). From *P. espejoi* also distinguished by male chelicerae (Fig. 10A–B; frontal apophyses in 'regular' more proximal position).

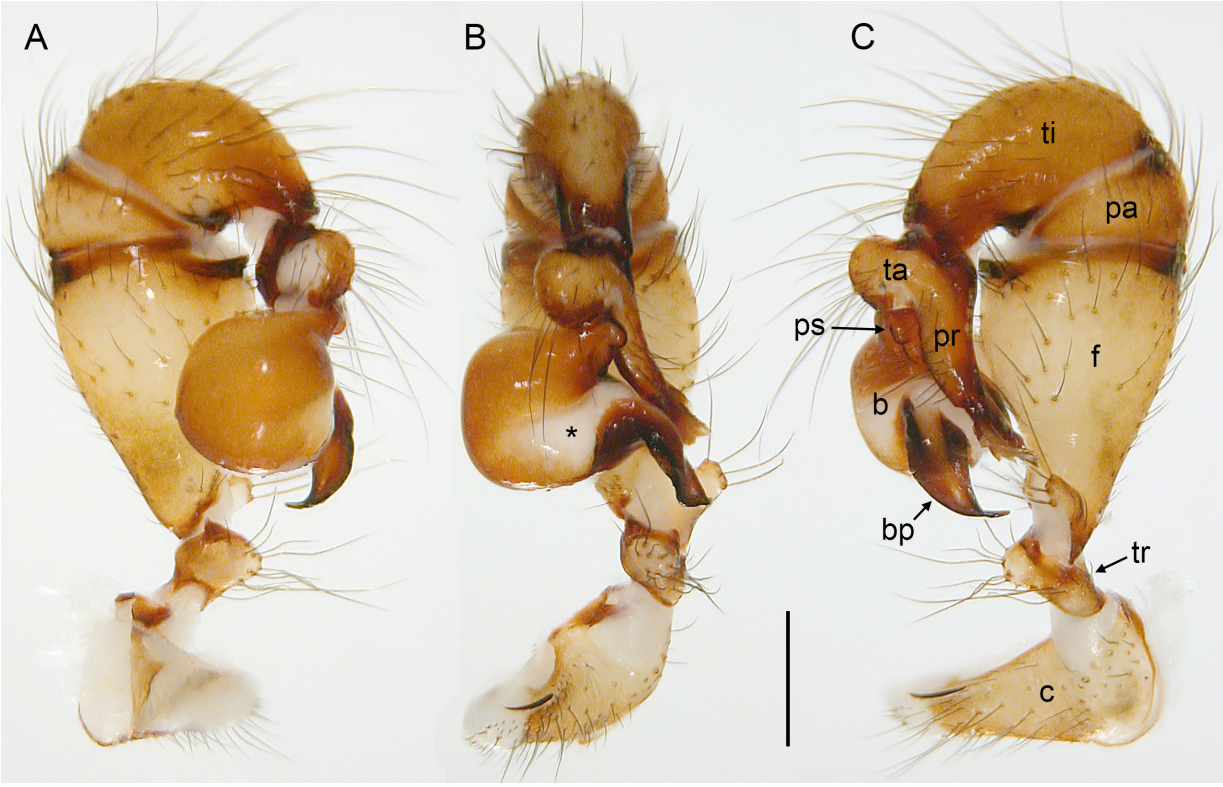

Fig. 8. *Priscula azuay* Huber sp. nov.; male paratype from between Guayaquil and Cuenca, 'loc. 2', ZFMK Ar 24098; left male palp, prolateral, dorsal, and retrolateral views; asterisk marks whitish area on genital bulb. Abbreviations: b = genital bulb; bp = main bulbal process; c = coxa; f = femur; pa = patella; pr = procursus; ps = proximal bulbal sclerite; ta = tarsus; ti = tibia; tr = trochanter. Scale line: 0.5 mm.

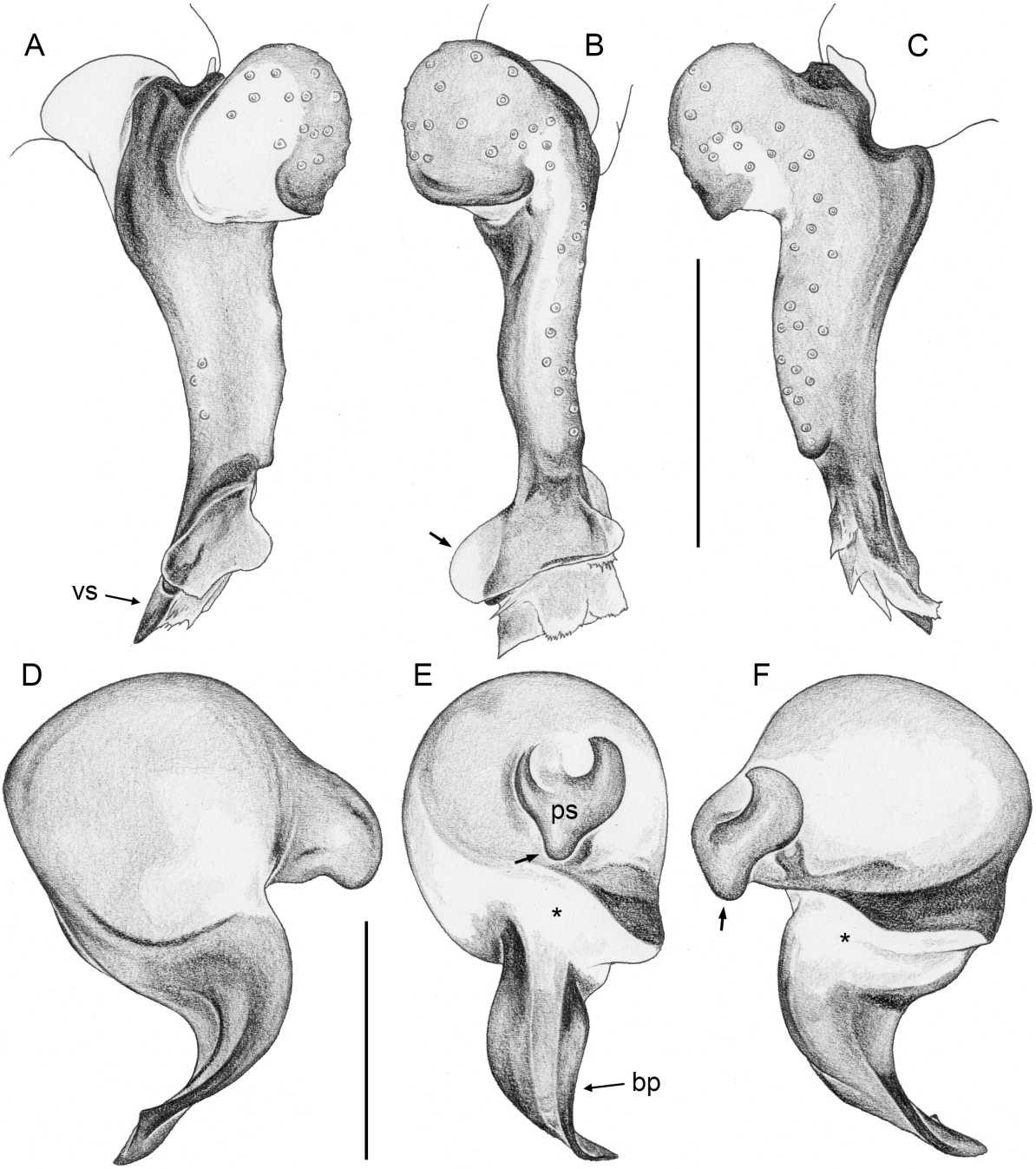

Fig. 9. *Priscula azuay* Huber sp. nov.; male paratype from between Guayaquil and Cuenca, 'loc. 2', ZFMK Ar 24098. **A–C.** Left tarsus and procursus, prolateral, dorsal, and retrolateral views; arrow points at distinctive dorsal distal membrane. **D–F.** Left genital bulb, dorsal, retrolateral, and ventral views; arrows point at process on proximal bulbal sclerite; asterisks mark whitish area on genital bulb. Abbreviations: bp = main bulbal process; ps = proximal bulbal sclerite; vs = ventral sclerite. Scale lines: 0.5 mm.

Etymology

The species name is derived from the type locality, noun in apposition.

Type material

Holotype

ECUADOR – **Azuay** • 1 ♂; between Guayaquil and Cuenca, 'loc. 2'; 2.706° S, 79.435° W; 2400 m a.s.l.; 21 Sep. 2021; B.A. Huber and M. Herrera leg.; MECN-ARAC-26-T.

Paratypes

ECUADOR – **Azuay** • 1 ♂, 1 ♀; same collection data as for holotype; MECN-ARAC-27-T, in ZFMK Ar 24098.

Note

The female paratype is assigned with some hesitation to this species. Its genetic distance to the holotype is 9.3%, while its distance to an unambiguous *P. espejoi* sp. nov. male is only 7.1%. However, two other sequenced females collected at the same locality had a much lower distance to the *P. espejoi* male (0.0–0.2%); those females are thus considered conspecific with the *P. espejoi* male, and the single female described here is tentatively assigned to *P. azuay* sp. nov.

Description

Male (holotype)

Measurements. Total body length 6.2, carapace width 2.4. Distance PME–PME 200 µm; diameter PME 230 µm; distance PME–ALE 130 µm; distance AME–AME 30 µm; diameter AME 65 µm. ALE and PLE larger than PME (diameters 270 µm). Leg 1: 48.8 (12.5+1.1+12.3+20.0+2.9), tibia 2: 9.5, tibia 3: 6.9, tibia 4: 9.2; tibia 1 L/d: 52.

Color (in ethanol). Carapace pale ochre-yellow, with brown median mark and lateral bands, ocular area and clypeus also dark brown; sternum brown with some lighter marks; legs ochre-yellow, with dark rings subdistally on femora and proximally and subdistally on tibiae; abdomen gray, dorsally and

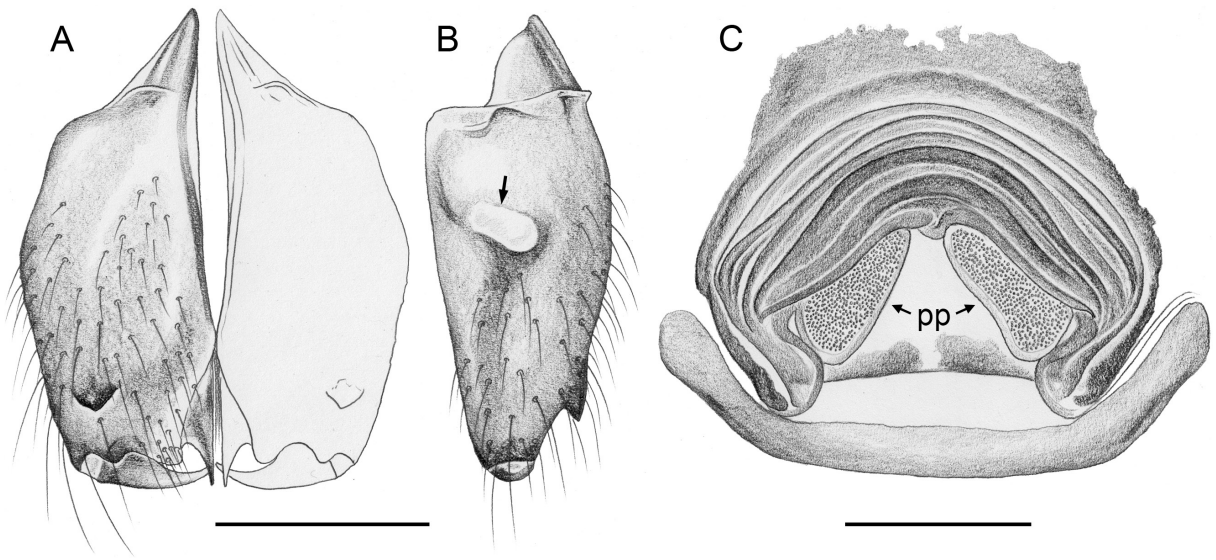

Fig. 10. *Priscula azuay* Huber sp. nov.; male and female paratypes from between Guayaquil and Cuenca, 'loc. 2', ZFMK Ar 24098. **A–B.** Male chelicerae, frontal and lateral views; arrow points at whitish area. **C.** Cleared female genitalia, dorsal view. Abbreviation: pp=pore plates. Scale lines: 0.5 mm.

laterally densely covered with black marks and small white marks in-between, ventrally with distinct brown plate in front of gonopore.

Body. Habitus as in Fig. 5A. Ocular area raised, without hump on posterior side, with stronger hairs at median side of each ocular triad. Deep thoracic groove. Clypeus unmodified except sclerotized rim. Sternum wider than long (1.55/1.15), unmodified. Abdomen higher than long, dorso-posteriorly rounded.

Chelicerae. As in Fig. 10A–B, with short entapophyses, pair of small frontal apophyses in relatively proximal position, without stridulatory ridges.

Palps. As in Fig. 8A–C; coxa unmodified, trochanter with low whitish rounded ventral protrusion, femur large, proximally with distinct retrolateral process, ventrally without process at half-length, distal ventral rim protruding, in ventral view with wide excavation; patella ventrally reduced to strongly sclerotized narrow rim; tibia small relative to femur; procursus (Fig. 9A–C) dorsally with small subdistal hump, distally with distinctive membranous elements and short ventral (slightly prolateral) spine; genital bulb (Fig. 9D–F) with distinctive process on proximal sclerite, with whitish area on retrolateral-ventral side, large spiraling main bulbal process.

Legs. Without spines; with curved hairs on metatarsi 1–3, some weakly curved hairs also on tibiae 1–2; with few short vertical hairs; retrolateral trichobothrium of tibia 1 at 5%; prolateral trichobothrium

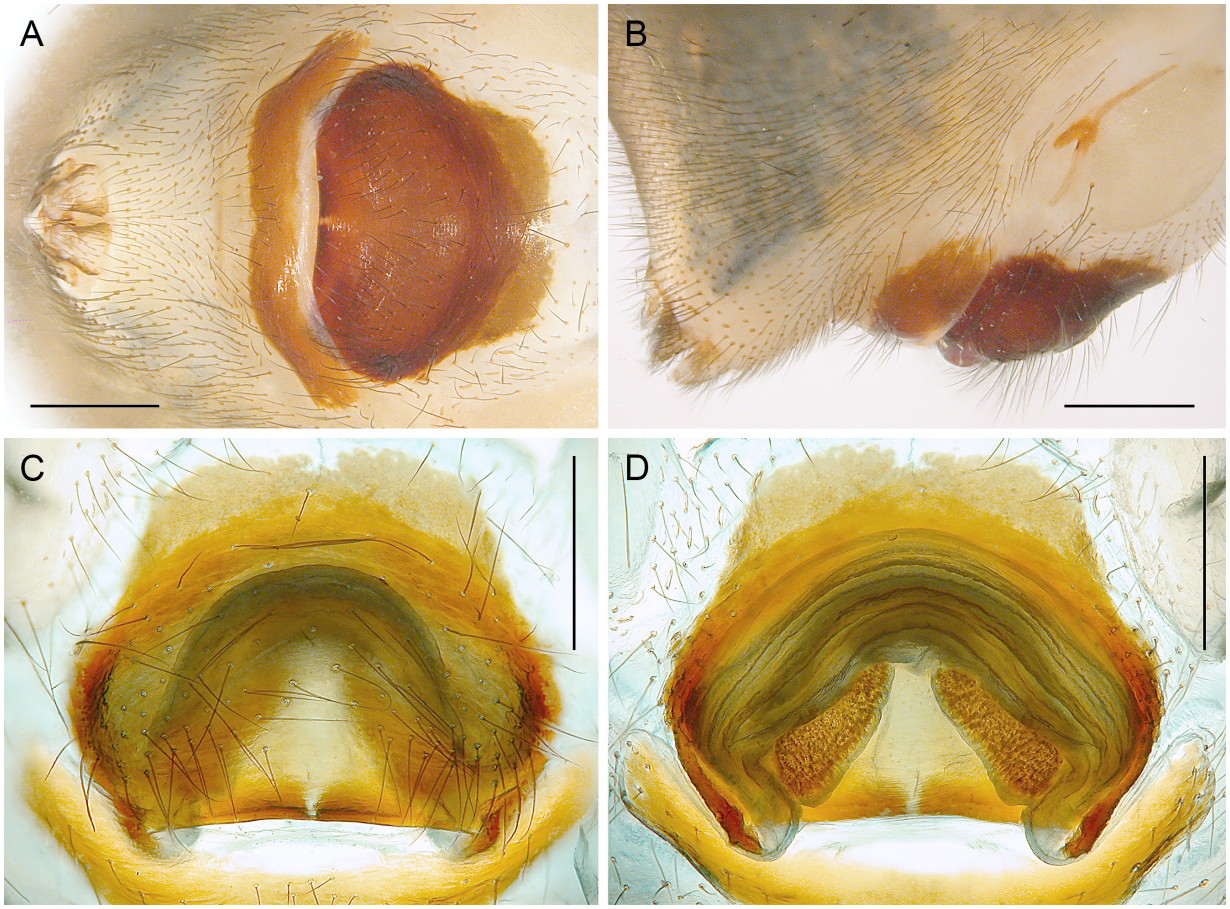

Fig. 11. *Priscula azuay* Huber sp. nov.; female paratype from between Guayaquil and Cuenca, 'loc. 2', ZFMK Ar 24098. **A–B.** Abdomen, ventral and lateral views. **C–D.** Cleared genitalia, ventral and dorsal views. Scale lines: 0.5 mm.

present on all leg tibiae; tarsi without regular pseudosegmentation but rather with many indistinct platelets.

Male (variation)

Tibia 1 in second male: 13.5.

Female

In general similar to male (Fig. 5B), but clypeus rim not sclerotized, hairs between eye triads shorter. Tibia 1: 6.8. Epigynum (Fig. 11A–B) main anterior plate trapezoidal, in lateral view anteriorly not protruding. Internal genitalia (Figs 10C, 11C–D) with pair of triangular pore plates converging anteriorly.

Distribution

Known from type locality only, in Azuay Province, Ecuador (Fig. 4A).

Natural history

The spiders were found in a tunnel under the road. In the neighboring forest, we found *P. espejoi* sp. nov.

Priscula llaviucu Huber sp. nov.

urn:lsid:zoobank.org:act:3010560D-557C-45B0-8455-A4F46A21F6D2

Figs 5C–D, 12–15

Diagnosis

Distinguished from known congeners by details of procursus (Fig. 13A–C; simple tip with strong prolateral-dorsal sclerite; without retrolateral process), genital bulb (Fig. 13D–F; main bulbal process

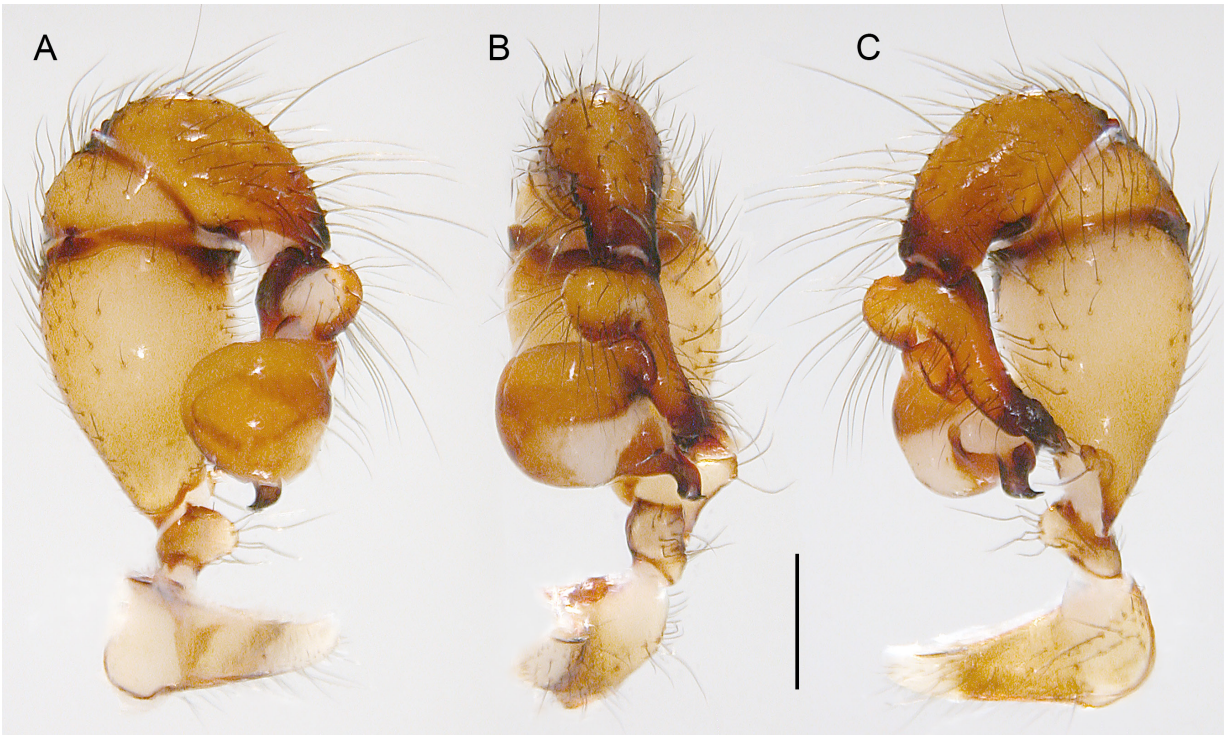

Fig. 12. *Priscula llaviucu* Huber sp. nov.; male paratype from Cajas N.P., ZFMK Ar 24099; left male palp, prolateral, dorsal, and retrolateral views. Scale line: 0.5 mm.

much smaller than in *P. azuay* sp. nov., similar to *P. espejoi* sp. nov.), male chelicerae (Fig. 14A–B; frontal apophyses in very proximal position), epigynum (Fig. 15A–B; in lateral view without anterior bulge similar to *P. azuay* but posterior bulge more prominent than in *P. azuay*), and female internal genitalia (Fig. 14C; pore plates oval, converging anteriorly – similar to *P. gularis*). From most congeners (from all known congeners in Ecuador) also distinguished by relatively short legs (male tibia 1 < 4 × carapace width).

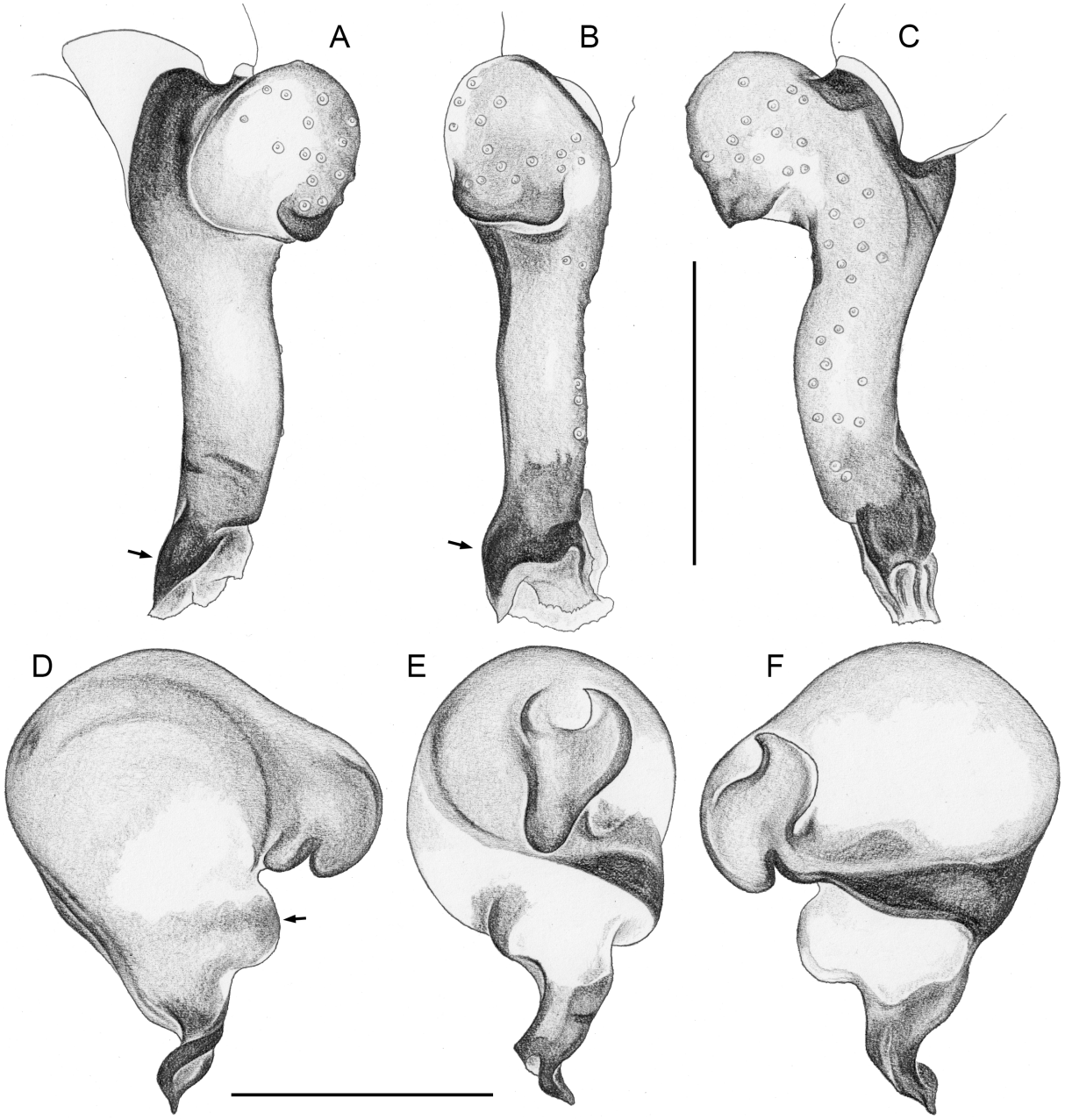

Fig. 13. *Priscula llaviucu* Huber sp. nov.; male paratype from Cajas N.P., ZFMK Ar 24099. **A–C.** Left tarsus and procursus, prolateral, dorsal, and retrolateral views; arrows point at distinctive prolateral-dorsal sclerite. **D–F.** Left genital bulb, dorsal, retrolateral, and ventral views; arrow points at sclerite that is narrower in male from near Zhud. Scale lines: 0.5 mm.

Note

This species is genetically close to several of our "*gularis*?" and "cf. *gularis*" specimens (8.7–9.2%) as well as to *P. azuay* sp. nov. (9.5%) and two undescribed species ("*P.* Ecu5" and "*P.* Dup55": 9.3–9.8%).

Type material

Holotype

ECUADOR – **Azuay** • ♂; Cajas N.P., eastern side of Laguna Llaviucu; 2.841–2.844° S, 79.144° W; 3160 m a.s.l.; 22 Sep. 2021; B.A. Huber and M. Herrera leg.; humid forest; MECN–ARAC–34–T.

Paratype

ECUADOR – **Azuay** • 1 ♂, together with one female abdomen; same collection data as for holotype; MECN–ARAC–35–T, in ZFMK Ar 24099.

Other material examined

ECUADOR – **Azuay** • 2 ♀♀, 3 juvs (in pure ethanol; one female abdomen transferred to ZFMK Ar 24099); same collection data as for holotype; ZFMK Ecu157 • **Cañar** 1 ♂, together with one female abdomen; S of Zhud, ravine above road; 2.4790° S, 78.9978° W; 2960 m a.s.l.; 22 Sep. 2021; B.A. Huber and M. Herrera leg.; MECN–ARAC–36–T, in ZFMK Ar 24100 • 1 ♀ (in pure ethanol; abdomen transferred to ZFMK Ar 24100); same collection data as for preceding; ZFMK Ecu163.

Etymology

The species name is derived from the type locality, noun in apposition.

Description

Male (holotype)

Measurements. Total body length 5.8, carapace width 2.25. Distance PME–PME 200 µm; diameter PME 175 µm; distance PME–ALE 125 µm; distance AME–AME 40 µm; diameter AME 55 µm. ALE and

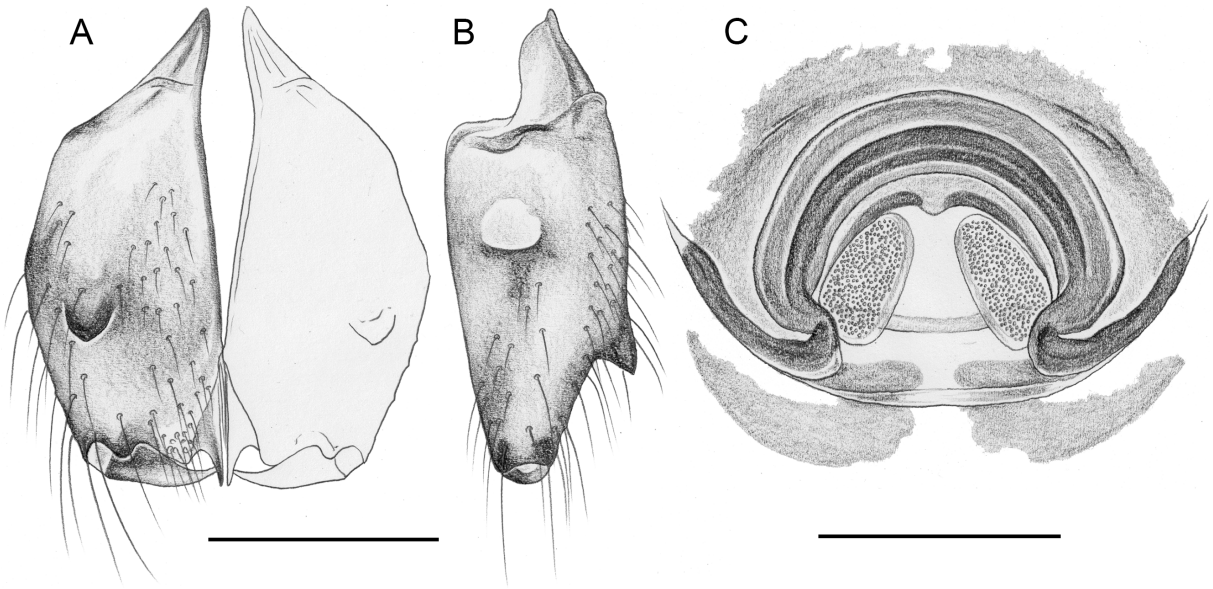

Fig. 14. *Priscula llaviucu* Huber sp. nov.; male paratype and female from Cajas N.P., ZFMK Ar 24099. **A–B.** Male chelicerae, frontal and lateral views. **C.** Cleared female genitalia, dorsal view. Scale lines: 0.5 mm.

PLE larger than PME (diameters ALE 230 µm, PLE 250 µm). Leg 1: 27.9 (7.1+0.9+7.3+10.6+2.0), tibia 2: 5.6, tibia 3: 4.1, tibia 4: 5.3; tibia 1 L/d: 32.

Color (in ethanol). Carapace pale ochre-yellow, with brown median and lateral marks not connected posteriorly (posterior area whitish), ocular area and clypeus dark ochre to brown; sternum brown with some lighter marks; legs light ochre-brown, with distinct dark rings subdistally on femora and proximally and subdistally on tibiae, further less distinct rings at half lengths of femora and tibiae and proximally on femora (partly only on ventral side); abdomen gray, dorsally and laterally densely covered with black marks and very small white marks in-between, ventrally with distinct brown plate in front of gonopore.

Body. Habitus as in Fig. 5C. Ocular area raised, with low hump on posterior side, with slightly stronger hairs at median side of each ocular triad. Deep thoracic groove. Clypeus unmodified except sclerotized rim. Sternum wider than long (1.50/1.05), unmodified. Abdomen higher than long, dorso-posteriorly rounded.

Chelicerae. As in Fig. 14A–B, with short entapophyses, pair of frontal apophyses in very proximal position, without stridulatory ridges.

Palps. As in Fig. 12A–C; coxa unmodified, trochanter with low rounded ventral protrusion, femur large, proximally with distinct retrolateral process, distal ventral rim protruding; patella ventrally reduced to

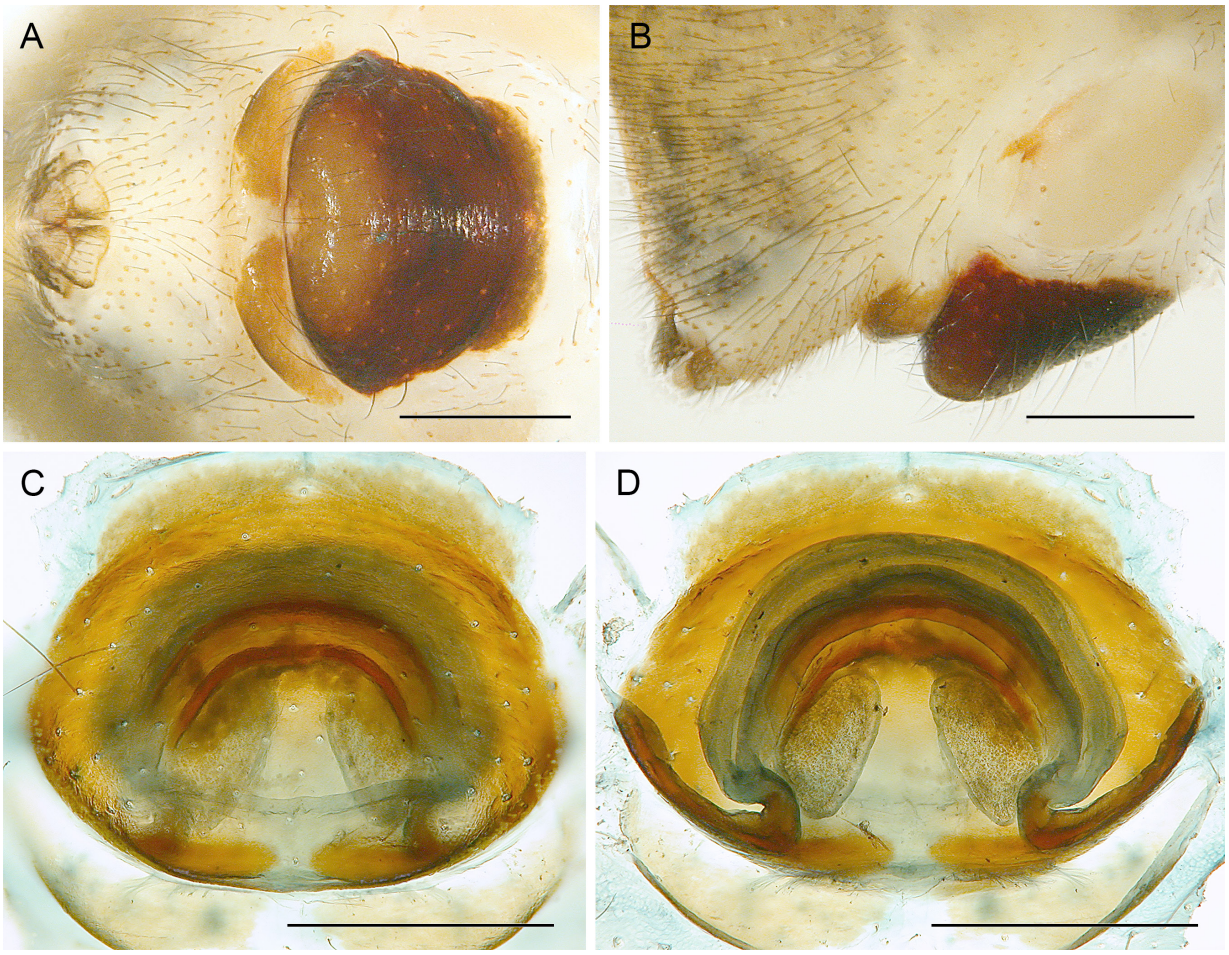

Fig. 15. *Priscula llaviucu* Huber sp. nov.; female from Cajas N.P., ZFMK Ar 24099. **A–B.** Abdomen, ventral and lateral views. **C–D.** Cleared genitalia, ventral and dorsal views. Scale lines: 0.5 mm.

strongly sclerotized narrow rim; tibia small relative to femur; procursus (Fig. 13A–C) relatively simple, without dorsal whitish or membranous element, distally with strong prolateral-dorsal sclerite and further partly membranous elements; genital bulb (Fig. 13D–F) with distinct process on proximal sclerite, with whitish area on retrolateral-ventral side, slightly spiraling main bulbal process with pointed tip.

Legs. Without spines; with many curved hairs on all tibiae and metatarsi, some weakly curved hairs also on anterior femora; with few short vertical hairs; retrolateral trichobothrium of tibia 1 at 9%; prolateral trichobothrium present on all leg tibiae; tarsi without regular pseudosegmentation but rather with many indistinct platelets.

Male (variation)

Tibia 1 in other male from type locality: 7.4; shape of median mark on carapace slightly variable. Male from near Zhud with slightly longer legs (tibia 1: 8.8), slightly narrower chelicerae (width 0.83 vs 0.87) and slightly more slender cheliceral apophyses (in lateral view), minimally wider distal element of procursus in retrolateral view, slightly narrower sclerite dorsally on genital bulb (arrow in Fig. 13D), and slightly shorter distal tip of main bulbal process.

Female

In general similar to male (Fig. 5D), but clypeus rim not sclerotized, dark rings at half lengths of femora and tibiae more distinct. Tibia 1 in two females from type locality: 5.2, 5.3; in female from near Zhud: 6.0. Epigynum (Fig. 15A–B) main anterior plate trapezoidal, very dark, posteriorly bulging; posterior epigynal plate medially divided by whitish area. Internal genitalia (Figs 14C, 15C–D) with pair of oval pore plates.

Distribution

Known from two localities in Azuay and Cañar Provinces, Ecuador (Fig. 4A).

Natural history

At the type locality, the spiders were found hidden in deep sheltered spaces at ground level. Near Zhud, the two specimens were hidden deeply in a large tussock. One egg-sac had a diameter of 4.3 mm, and contained ~50 eggs with an egg diameter of 1.05 mm.

Priscula gularis Simon, 1893

Priscula gularis Simon, 1893a: 319.
Priscula gularis – Simon 1893b: 477 — Huber 1997: 595, figs 17–19; 2000: 129, figs 495–500.
Physocyclus gularis – Brignoli 1981: 96, figs 8–10, 25.

Remarks

Our sample of sequenced material includes several specimens that appear very close to or even conspecific with the type species *P. gularis*. This species or species complex is badly in need of revision but this will require restudying the type material (a loan request remained unanswered) and more focused collecting. Here, we only point out the problematic identity of the type species, explaining the "*gularis*?" and "cf. *gularis*" in Fig. 1.

No detailed illustrations are available of the type material of *P. gularis*. The lectotype and the female paralectotype originate from "Quito" (without further specification), but the drawings in Brignoli (1981) and Huber (1997) are based on Eugène Simon's specimens from "Nariguel" (or "Narigual"), a locality we were not able to identify. Simon (1893a, b) never mentioned these specimens, meaning that they cannot

be considered types (contra Brignoli 1981). The drawings in Huber (2000) are based on specimens from Baños (~130 km S of Quito), which were collected in 1937 and which appear identical to a newly collected male from Desierto de Palmira (code of sequenced juvenile from this locality: EB083). We thus speculate that the male from Desierto de Palmira and the sequenced juvenile EB083 might be true *P. gularis*.

The sequenced juvenile from Desierto de Palmira is genetically closest to a female specimen from between Guano and Ilapo (EB020; distance 5.5%) but we have no male from this locality. Morphologically, the Desierto de Palmira male is also very similar to a newly collected male from near Zhud (EB077), but in this case, the genetic distance is already at 7.2%. Surprisingly, a newly collected male from Baños (EB084) is morphologically quite clearly different from the old (1937) Baños males, but the genetic distances to the previous specimens are almost the same as among those specimens, i.e. ~7–8%. Similar distances were also found between these specimens and a further "cf. *gularis*" specimen (EB127) from near El Ángel (~110 km NE of Quito), a further locality from which we have no male. Genetic distances between all these "*gularis*?" and "cf. *gularis*" specimens and the morphologically very distinct *P. llaviucu* sp. nov. are only slightly higher (8.7–9.2%) suggesting that several species might be represented by our "cf. *gularis*" specimens.

Two further closely related potential species ("*P.* Dup55" and "*P.* Ecu5") are included in our molecular dataset and shown in the distribution map (Fig. 4A), but not formally described because no males are available. The CO1 K2P–distance between the two sequenced specimens was 7.8%, and distances to other specimens of the *gularis* group ranged from 7.6–12.3%. The distribution map (Fig. 4A) shows a further potential species, "*P.* Dup140" that we tentatively assign to the *gularis* group, but we were not able to extract DNA from the single available female.

New material examined (identity unclear, see above)

"*gularis*?"

ECUADOR – **Chimborazo** • 1 ♂; Guamote, Desierto de Palmira; 2.0322° S, 78.7440° W; 3250 m a.s.l.; under rocks, deserted region; 27 Feb. 2017; E. Tapia, A. Tapia, and I. Tapia leg.; ZMH A2590 • 1 juv., in pure ethanol; Desierto de Palmira; 2.075° S, 78.758° W; 3230 m a.s.l.; under dead wood on the ground; 23 Sep. 2021; B.A. Huber and M. Herrera leg; ZFMK Ecu167 • 2 ♀♀; Guano, Via Guano-Ilapo; 1.6037° S, 78.5907° W; 2680 m a.s.l.; 7 Mar. 2020; N. Dupérré, A.A. Tapia, and E.E. Tapia leg.; ZMH A14888–9.

"cf. *gularis*"

ECUADOR – **Carchi** • 1 ♀; near El Ángel; 0.6178° N, 77.9261° W; 3240 m a.s.l.; degraded forest in ravine; 2 Oct. 2021; B.A. Huber and M. Herrera leg.; MECN–ARAC–31–T, in ZFMK Ar 24091 • 1 ♀, 1 juv., in pure ethanol; same collection data as for preceding; ZFMK Ecu222 – **Cañar** • 1 ♂; S Zhud, ravine above road; 2.4790° S, 78.9978° W; 2960 m a.s.l.; 22 Sep. 2021; B.A. Huber and M. Herrera leg.; MECN–ARAC–32–T, in ZFMK Ar 24092 • 2 juvs, in pure ethanol; same collection data as for preceding; ZFMK Ecu162 – **Tungurahua** • 1 ♂; S Baños; 1.4134° S, 78.4340° W; 2100 m a.s.l.; degraded forest along river; 24 Sep. 2021; B.A. Huber and M. Herrera leg.; MECN–ARAC–33–T, in ZFMK Ar 24093 and ZFMK Ecu168 (2 legs in pure ethanol) • 1 juv., in pure ethanol; same collection data as for preceding; ZFMK Ecu168.

"Ecu5"

ECUADOR – **Pichincha** • 1 ♀; between San Juan and Chiriboga, 'site 2'; 0.2327° S, 78.7497° W; 1900 m a.s.l.; forest at roadside; 15 Sep. 2021; B.A. Huber and M. Herrera leg.; ZFMK Ar 24113 • 3 juvs, in pure ethanol; same collection data as for preceding; ZFMK Ecu124.

"Dup55"
ECUADOR – **Cotopaxi** • 2 ♀♀; San Francisco de Las Pampas, OTONGA Natural Reserve; 0.4199° S, 79.0062° W; 1995 m a.s.l.; 4–7 Sep. 2014; N. Dupérré, E.E. Tapia, and C.A. Tapia leg.; QCAZ • 1 ♀; same collection data as for preceding but 12 Nov. 2014; QCAZ • 1 ♀; same collection data as for preceding but Jan. 2013; QCAZ • 1 ♀, sequenced specimen; same collection data as for preceding but 5–7 Sep. 2014; ZFMK Ar 24189.

"Dup140"
ECUADOR – **Azuay** • 1 ♀; Nabon; 3.3289° S, 79.0508° W; 2700 m a.s.l.; 5 Mar. 2020; N. Dupérré, A.A. Tapia, and E.E. Tapia leg.; ZFMK Ar 24190.

Priscula espejoi Huber sp. nov.
urn:lsid:zoobank.org:act:BF9F8559-152A-4541-8096-56EFDBBEB85C
Figs 5G–H, 16–20

Diagnosis

Distinguished from known congeners by details of procursus (Fig. 17A–C; distal ventral sclerite long and slender in lateral view, with distinctive bifid tip in dorsal view; distinctive dorsal membrane smaller than in similar *P. azuay* sp. nov.; without retrolateral process), genital bulb (Fig. 17D–F; main bulbal process with obtuse tip, similar to *P. llaviucu*, smaller than in *P. azuay*), male chelicerae (Fig. 18A–B; frontal apophyses in very distal position, longer than in most known congeners), epigynum (Fig. 19A–B; in lateral view with anterior bulge), and female internal genitalia (Fig. 18C; pore plates roughly triangular, narrower anteriorly than posteriorly and converging anteriorly – apparently indistinguishable from *P. azuay*).

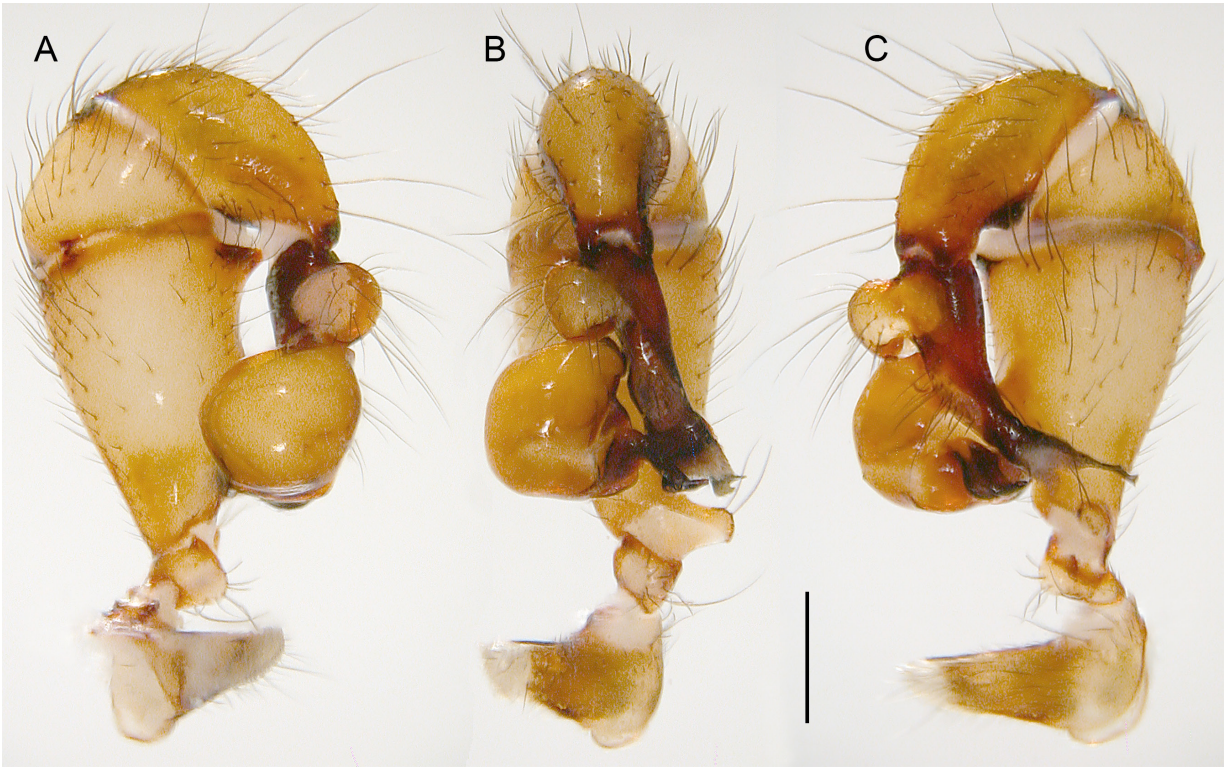

Fig. 16. *Priscula espejoi* Huber sp. nov.; male holotype from between Guayaquil and Cuenca, 'loc. 1', MECN-ARAC-28-T; left male palp, prolateral, dorsal, and retrolateral views. Scale line: 0.5 mm.

Etymology

The species is named for Francisco Javier Eugenio de Santa Cruz y Espejo (1747–1795), a scientist and writer of mestizo origin in colonial Ecuador.

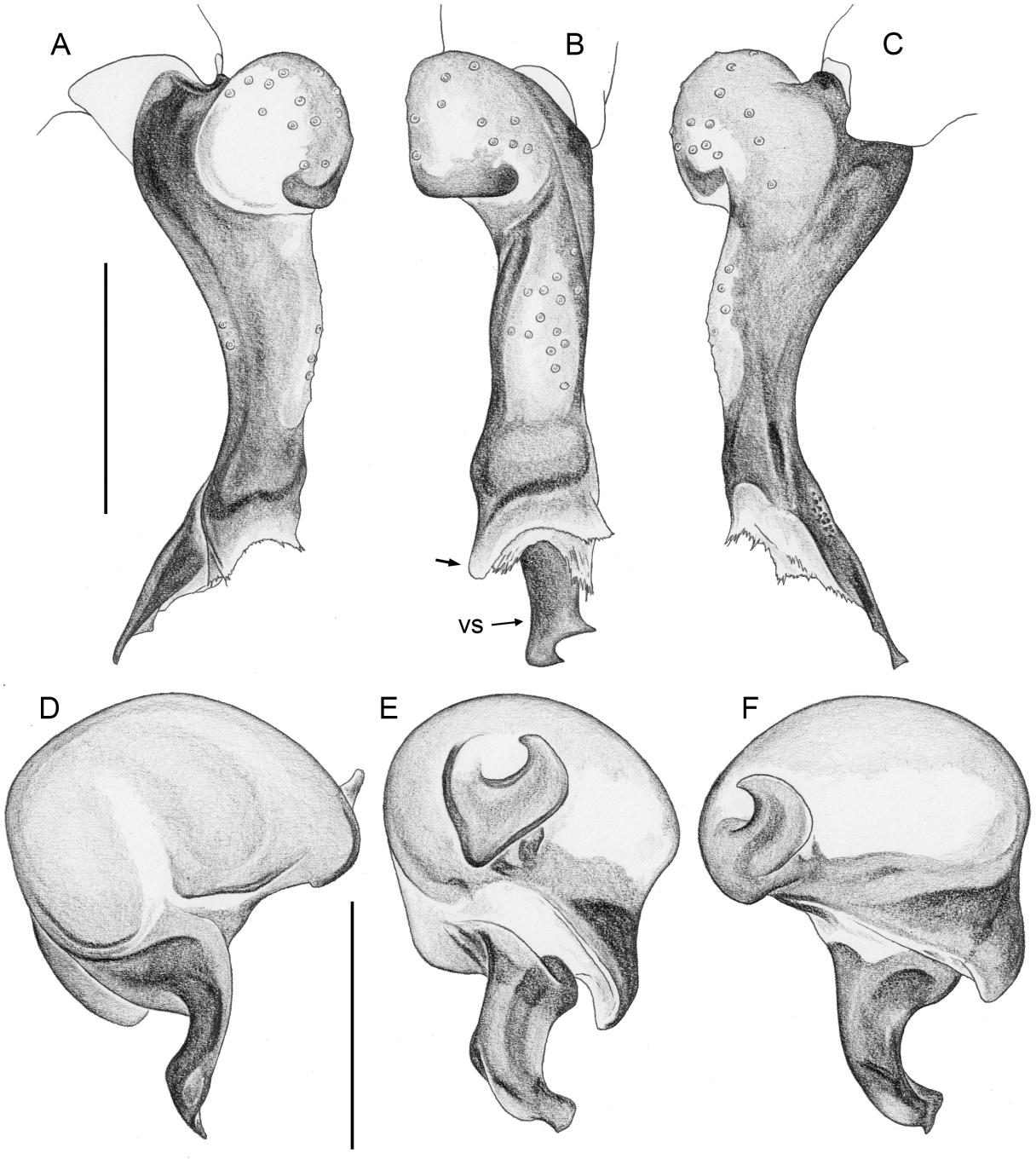

Fig. 17. *Priscula espejoi* Huber sp. nov.; male holotype from between Guayaquil and Cuenca, 'loc. 1', MECN-ARAC-28-T. **A–C.** Left tarsus and procursus, prolateral, dorsal, and retrolateral views; arrow points at distinctive dorsal membrane. **D–F.** Left genital bulb, dorsal, retrolateral, and ventral views (note that whitish area is slightly collapsed in this specimen). Abbreviation: vs = ventral sclerite. Scale lines: 0.5 mm.

Type material

Holotype

ECUADOR – **Azuay** • ♂; between Guayaquil and Cuenca, 'loc. 1'; 2.664° S, 79.445° W; 1100 m a.s.l.; 21 Sep. 2021; B.A. Huber and M. Herrera leg.; in tunnel under road; MECN–ARAC–28–T.

Paratype

ECUADOR – **Azuay** • 1 ♀; same collection data as for holotype but in forest at roadside; MECN–ARAC–29–T, in ZFMK Ar 24096.

Other material examined

ECUADOR – **Azuay** • 2 ♀♀, 3 juvs, in pure ethanol; same collection data as for paratype; ZFMK Ecu151 • 1 ♂, 1 ♀; between Guayaquil and Cuenca, 'loc. 2'; 2.706° S, 79.435° W; 2400 m a.s.l.; 21 Sep. 2021; B.A. Huber and M. Herrera leg.; ravine with forest remnant near road; MECN–ARAC–30–T, in ZFMK Ar 24097 • 3 ♀♀, in pure ethanol; same collection data as for preceding; ZFMK Ecu154.

Description

Male (holotype)

Measurements. Total body length 4.8, carapace width 2.25. Distance PME–PME 230 µm; diameter PME 220 µm; distance PME–ALE 130 µm; distance AME–AME 35 µm; diameter AME 65 µm. ALE and PLE larger than PME (diameters 270 µm). Leg 1: 41.2 (10.8+0.9+10.9+16.5+2.1), tibia 2: 7.5, tibia 3: 4.9, tibia 4: 6.9; tibia 1 L/d: 52.

Color (in ethanol). Carapace pale ochre-yellow, with brown median mark and lateral bands, ocular area and clypeus also dark brown; sternum brown with some lighter marks; legs ochre-yellow, with dark rings subdistally on femora and proximally and subdistally on tibiae; abdomen gray, dorsally and

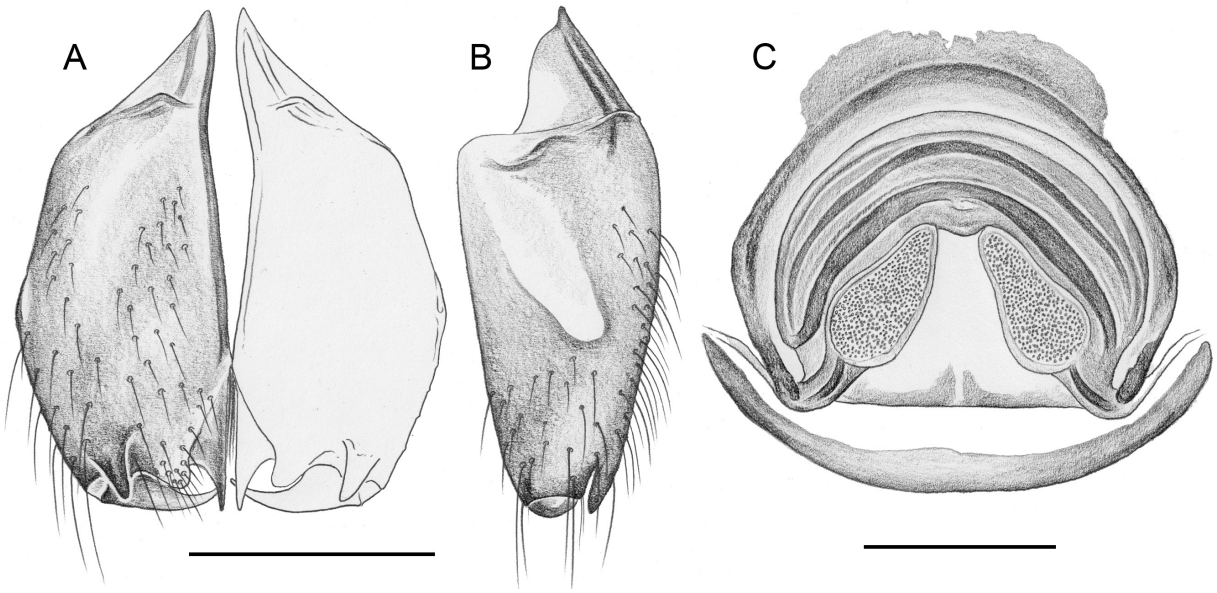

Fig. 18. *Priscula espejoi* Huber sp. nov.; male holotype and female paratype from between Guayaquil and Cuenca, 'loc. 1', MECN-ARAC-28-T (♂) and ZFMK Ar 24096 (♀). **A–B.** Male chelicerae, frontal and lateral views. **C.** Cleared female genitalia, dorsal view. Scale lines: 0.5 mm.

laterally densely covered with black marks and small white marks in-between, ventrally with distinct brown plate in front of gonopore and ochre mark between gonopore and pedicel.

Body. Habitus as in Fig. 5G. Ocular area raised, without hump on posterior side, with stronger hairs at median side of each ocular triad. Deep thoracic groove. Clypeus unmodified except sclerotized rim. Sternum wider than long (1.35/1.00), unmodified. Abdomen higher than long, dorso-posteriorly rounded.

Chelicerae. As in Fig. 18A–B, with short entapophyses, pair of frontal apophyses in very distal position and in lateral view pointing towards distal, without stridulatory ridges.

Palps. As in Fig. 16A–C; coxa unmodified, trochanter with low whitish rounded ventral protrusion, femur large, proximally with distinct retrolateral process, ventrally with low rounded process at half-length followed by whitish round area, distal ventral rim protruding, in ventral view with wide excavation; patella ventrally reduced to strongly sclerotized narrow rim; tibia small relative to femur; procursus (Fig. 17A–C) distally with dorsal transversal membranous element and distinctive ventral sclerite; genital bulb (Fig. 17D–F) with small process on proximal sclerite, with whitish area on retrolateral-ventral side (collapsed in holotype), slightly spiraling main bulbal process.

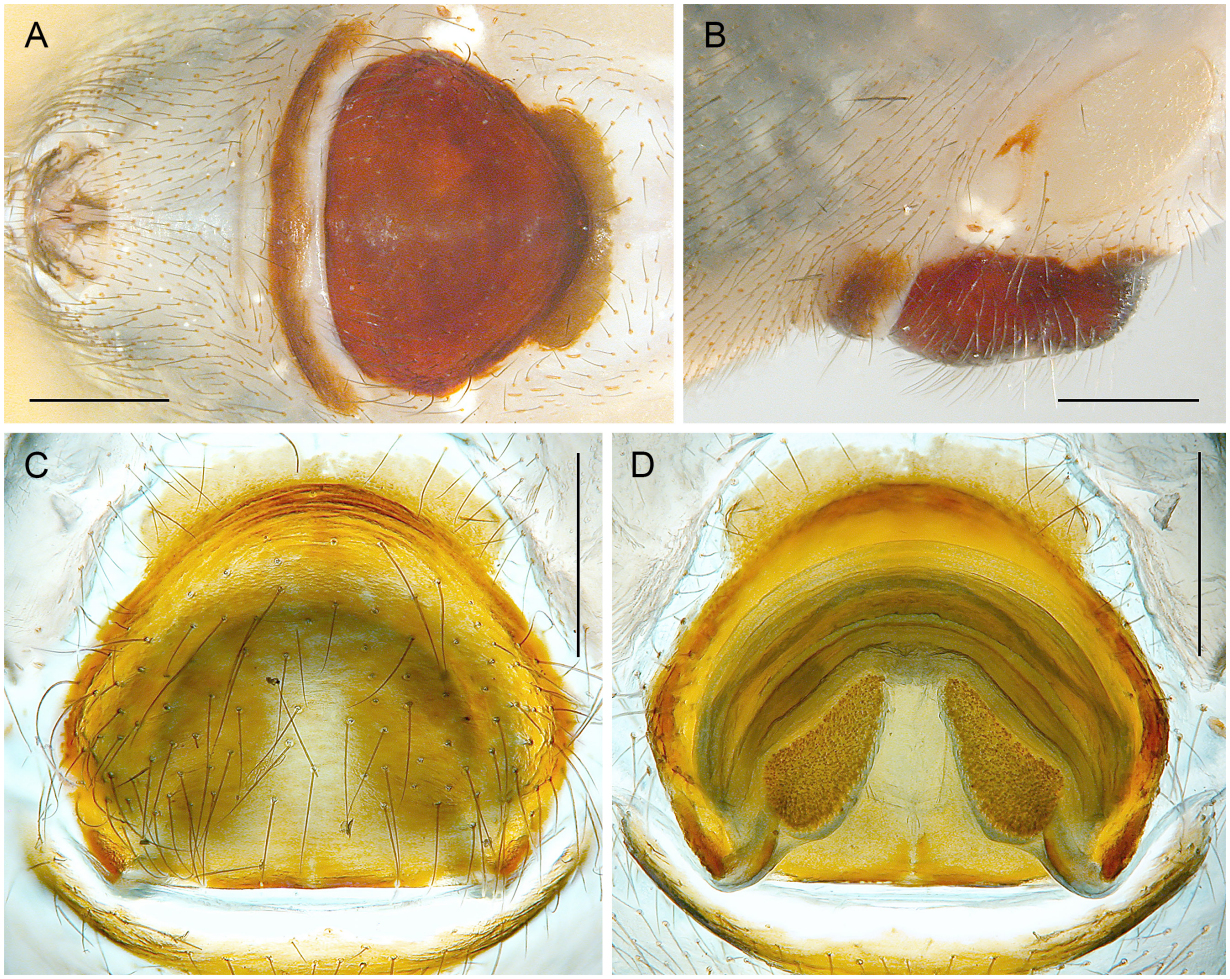

Fig. 19. *Priscula espejoi* Huber sp. nov.; female paratype from between Guayaquil and Cuenca, 'loc. 1', ZFMK Ar 24096. **A–B.** Abdomen, ventral and lateral views. **C–D.** Cleared genitalia, ventral and dorsal views. Scale lines: 0.5 mm.

Legs. Without spines; with curved hairs on metatarsi 1–3, some weakly curved hairs also on tibiae 1–2; with few short vertical hairs; retrolateral trichobothrium of tibia 1 at 6%; prolateral trichobothrium present on all leg tibiae; tarsi without regular pseudosegmentation but rather with many indistinct platelets.

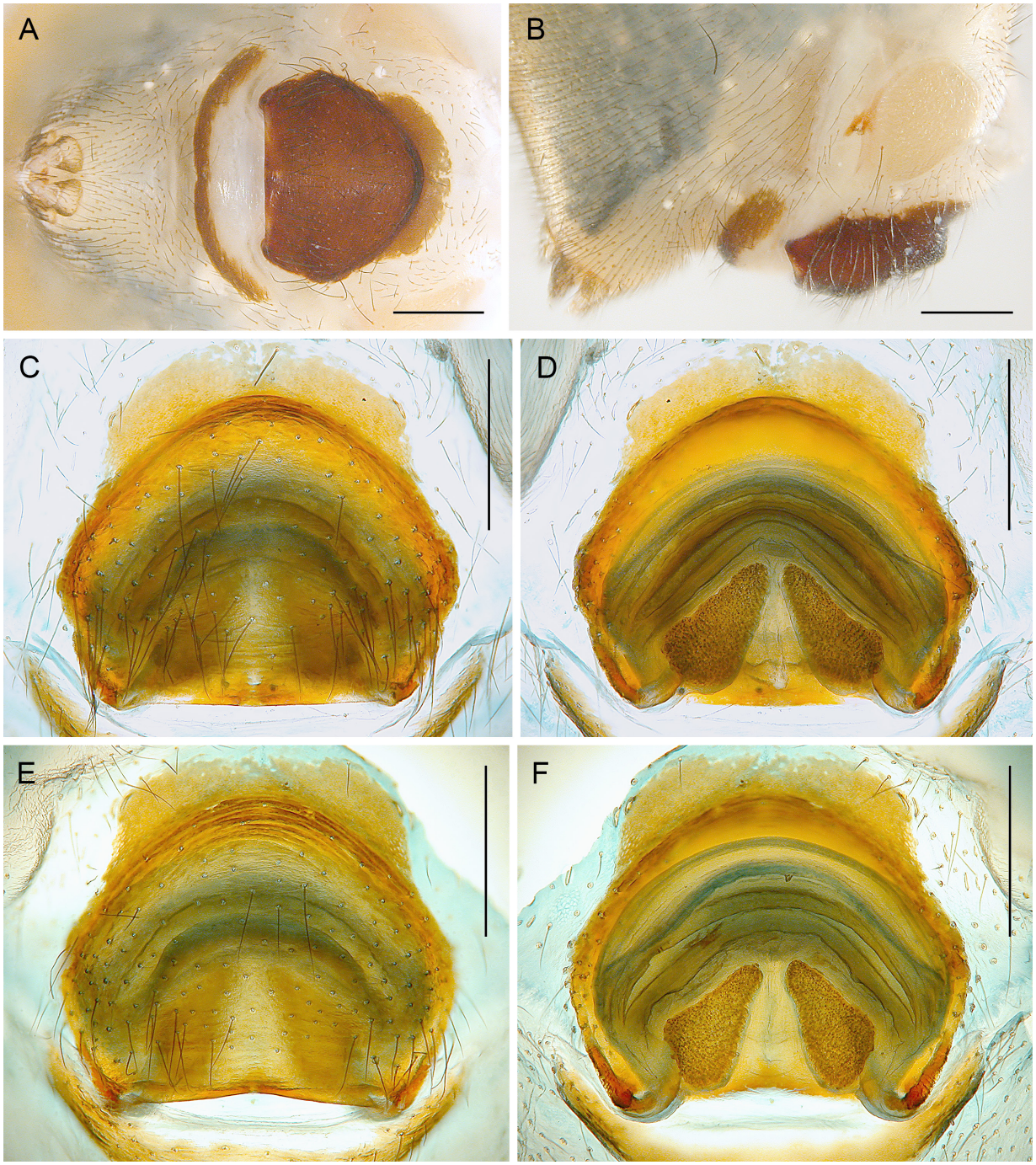

Fig. 20. *Priscula espejoi* Huber sp. nov.; females from between Guayaquil and Cuenca, 'loc. 2', ZFMK Ar 24097 (A–D), and from between Guayaquil and Cuenca, 'loc. 1', ZFMK Ecu151 (E–F). **A–B.** Abdomen, ventral and lateral views. **C–F.** Cleared genitalia, ventral and dorsal views. Scale lines: 0.5 mm.

Male (variation)

Tibia 1 in second male: 9.3.

Female

In general similar to male (Fig. 5H), but clypeus rim not sclerotized, hairs between eye triads shorter. Tibia 1 in seven females: 7.4–8.1 (mean 7.7). Epigynum (Figs 19A–B, 20A–B) main anterior plate trapezoidal, in lateral view anteriorly protruding and angular. Internal genitalia (Figs 18C, 19C–D, 20C–F) with pair of triangular pore plates at slightly variable distances, converging anteriorly.

Distribution

Known from two neighboring localities in Azuay Province, Ecuador (Fig. 4A). The two localities are close together (< 5 km straight line) but at very different altitudes (1100 and 2400 m a.s.l.).

Natural history

Most specimens were found deep in sheltered spaces in the ground; the male at the type locality was collected in a tunnel under the road. One egg-sac had a diameter of 4.5 mm, and contained ~40 eggs with a diameter of 1.20 mm.

Priscula esmeraldas Huber sp. nov.

urn:lsid:zoobank.org:act:C9A9D73A-0280-451D-8F95-69C6489E2ABD

Figs 21–24, 41D, G, 42A–C, 43A, F

Diagnosis

Distinguished from known congeners by details of procursus (Fig. 22A–C; distally with unique prolateral process), genital bulb (Fig. 22D–F; main bulbal process smaller than in most known congeners and strongly curved), epigynum (Fig. 24A–B; shorter than in most known congeners – similar to *P. chapintza* sp. nov.), and female internal genitalia (Fig. 23C; oval pore plates far apart, strongly converging anteriorly).

Type material

Holotype

ECUADOR – **Cotopaxi** • ♂; San Francisco de Las Pampas, Recinto Rio Esmeraldas, PRISTIRANA Natural Reserve; 0.4228° S, 78.9543° W; 1335 m a.s.l.; 25 Nov. 2019; E.E. Tapia and family leg.; QCAZ.

Paratypes

ECUADOR – **Cotopaxi** • 3 ♂♂, 9 ♀♀; same collection data as for holotype; QCAZ (12 vials) • 1 ♂, 4 ♀♀ (one female used for SEM); same locality as for holotype but 300 m NW; 0.4215° S, 78.9564° W; 1395 m a.s.l.; 12 Oct. 2021; N. Dupérré, E.E. Tapia, and A.A. Tapia leg; QCAZ • 1 ♂, 1 ♀; same collection data as for preceding; ZFMK Ar 24094.

Other material examined

ECUADOR – **Cotopaxi** • 4 juvs; same collection data as for holotype; QCAZ.

Etymology

The species name is derived from the type locality, noun in apposition.

Description

Male (holotype)

Measurements. Total body length 4.6, carapace width 2.1. Distance PME–PME 180 µm; diameter PME 160 µm; distance PME–ALE 80 µm; distance AME–AME 40 µm; diameter AME 40 µm. ALE and PLE larger than PME (diameter ALE 210 µm, diameter PLE 230 µm). Leg 1: 46.1 (11.1 + 0.9 + 11.3 + 20.3 + 2.5), tibia 2: 8.3, tibia 3: 6.0, tibia 4: 7.6; tibia 1 L/d: 48.

Color (in ethanol). Carapace ochre-yellow, with darker median mark and whitish marks beside ocular area, ocular area and clypeus dark ochre; sternum light ochre; legs ochre to light brown, with distinct dark rings on femora (subdistally) and tibiae (proximally and subdistally) each preceded and followed by lighter ring; abdomen dorsally and laterally densely covered with black marks separated by network of small white marks, ventrally with large brown mark in front of gonopore.

Body. Habitus similar to *P. bonita* sp. nov. (cf. Fig. 6C). Ocular area raised, without hump on posterior side, with comb of slightly stronger hairs at median side of each ocular triad. Deep thoracic groove. Clypeus unmodified except slightly sclerotized rim. Sternum wider than long (1.45/0.85), unmodified. Abdomen higher than long, dorso-posteriorly weakly angular.

Chelicerae. As in Fig. 23A–B, with short entapophyses, pair of short frontal apophyses close to fang joints, without stridulatory ridges.

Palps. As in Fig. 21A–C; coxa unmodified, trochanter slightly protruding ventrally, femur large, with unsclerotized retrolateral process proximally followed distally by deep indentation, femur distally ventrally

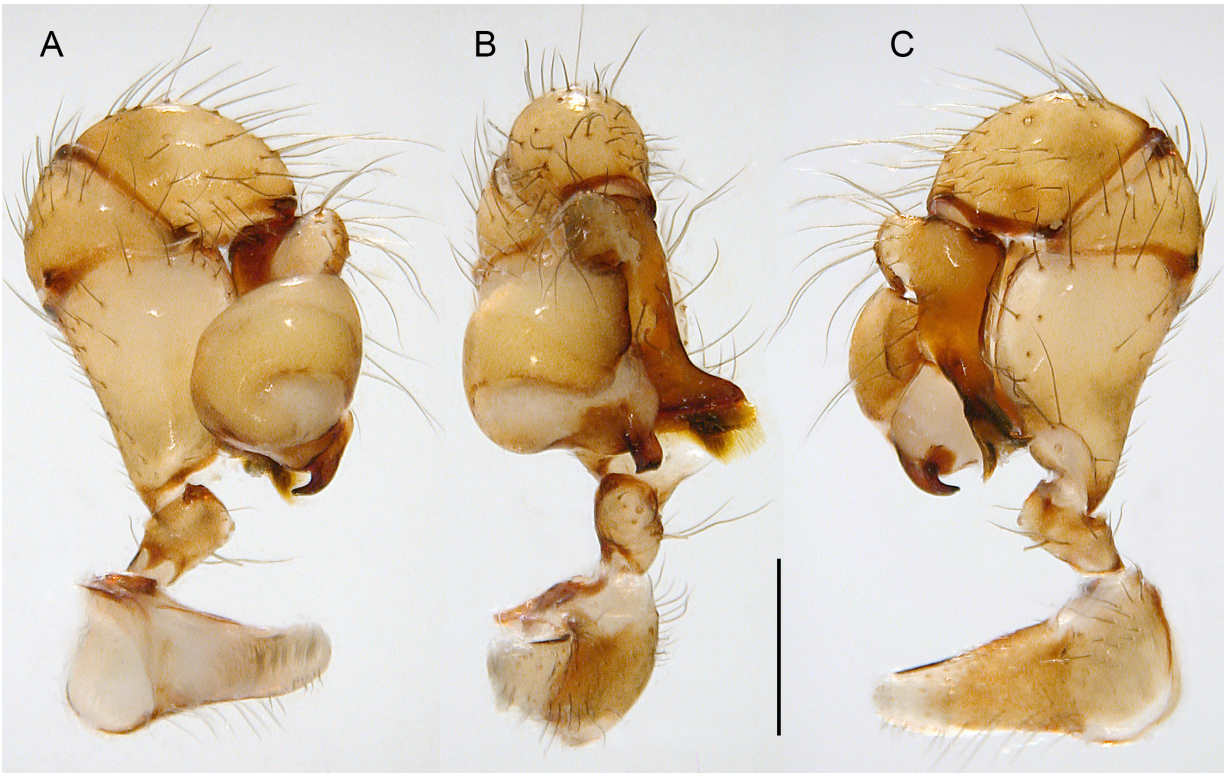

Fig. 21. *Priscula esmeraldas* Huber sp. nov.; male paratype from San Francisco de Las Pampas, QCAZ; left male palp, prolateral, dorsal, and retrolateral views. Scale line: 0.5 mm.

protruding but without additional protrusion of rim; patella ventrally reduced to strongly sclerotized narrow rim; tibia small relative to femur; procursus (Fig. 22A–C) with distinct slightly protruding whitish area dorsally, distal part distinctively T-shaped in dorsal view (Fig. 42B), with long prolateral process and retrolateral process divided into dorsal and ventral flat elements, prolateral and retrolateral processes set with membranous cushions composed of fringes and hair-like processes (Fig. 42B–C); genital bulb (Fig. 22D–F) with small proximal sclerite connecting to tarsus, with large whitish area on retrolateral-ventral side, relatively small and strongly curved main bulbal process with obtuse tip.

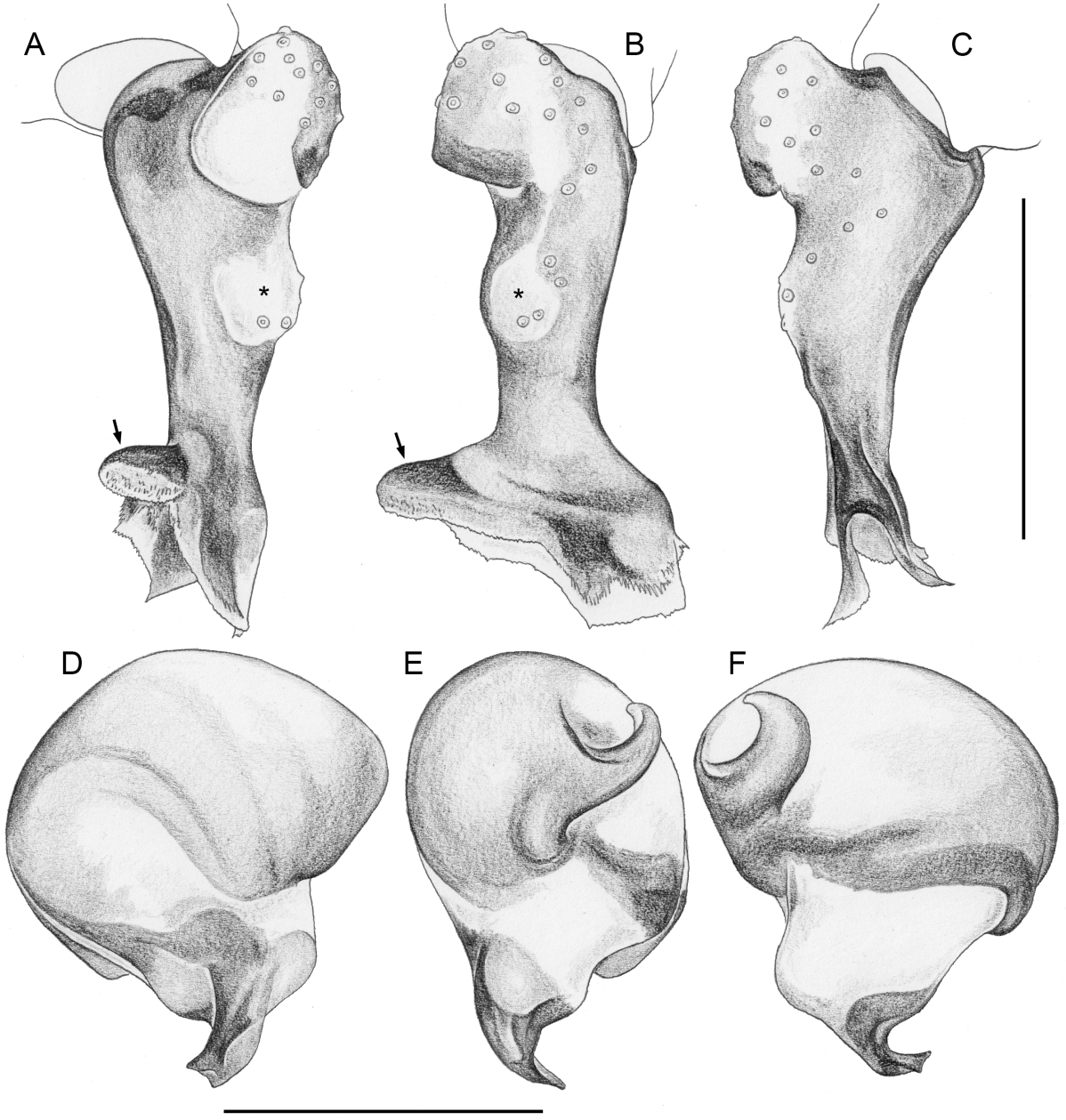

Fig. 22. *Priscula esmeraldas* Huber; sp. nov., male paratype from San Francisco de Las Pampas, QCAZ. **A–C.** Left tarsus and procursus, prolateral, dorsal, and retrolateral views; arrows point at distinctive prolateral process, asterisks: whitish protruding area. **D–F.** Left genital bulb, dorsal, retrolateral, and ventral views. Scale lines: 0.5 mm.

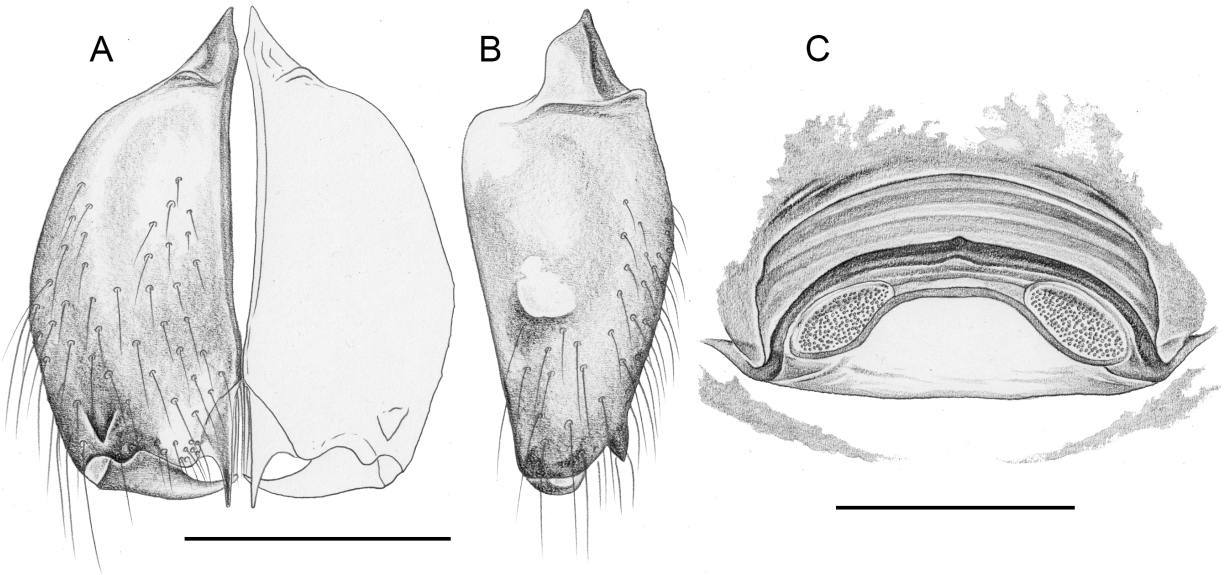

Fig. 23. *Priscula esmeraldas* Huber sp. nov.; male and female paratypes from San Francisco de Las Pampas, QCAZ. **A–B.** Male chelicerae, frontal and lateral views. **C.** Cleared female genitalia, dorsal view. Scale lines: 0.5 mm.

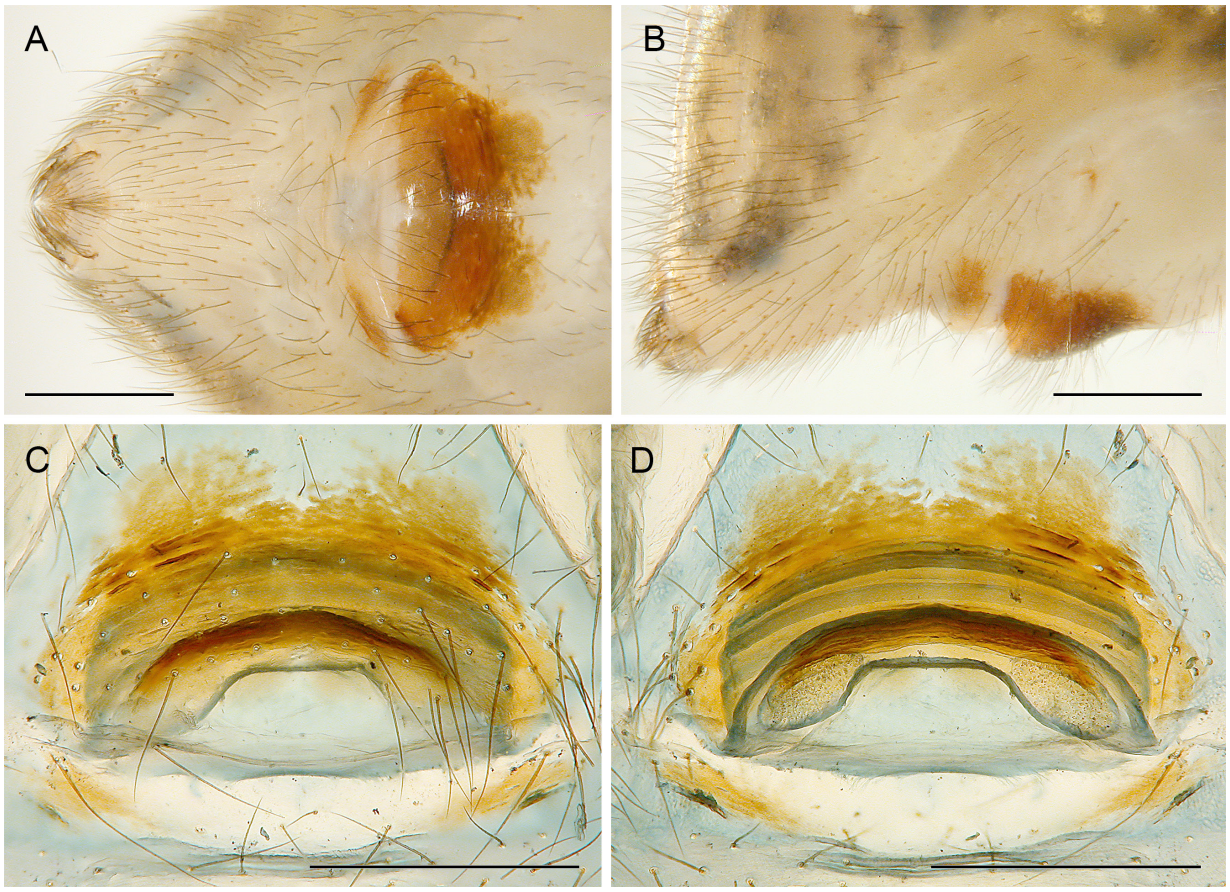

Fig. 24. *Priscula esmeraldas* Huber sp. nov.; female paratype from San Francisco de Las Pampas, QCAZ. **A–B.** Abdomen, ventral and lateral views. **C–D.** Cleared genitalia, ventral and dorsal views. Scale lines: 0.5 mm.

Legs. Without spines; with curved hairs on metatarsi 1–3; with few short vertical hairs; retrolateral trichobothrium of tibia 1 at 6%; prolateral trichobothrium present on all leg tibiae; tarsi without regular pseudosegmentation but rather with many irregular platelets.

Male (variation)

Tibia 1 in six males (incl. holotype): 11.1–12.0 (mean 11.5).

Female

In general similar to male but clypeus rim unsclerotized, hairs on ocular area slightly less strong. Tibia 1 in 14 females: 7.7–9.2 (mean 8.6). Tip of palp simple, pointed, with dorsal invagination (Fig. 43A). Tarsal organs on palps and legs exposed (Fig. 43F). ALS with one strongly widened spigot, one pointed spigot, and one large and four small cylindrical spigots (Fig. 41D); with distinctively sculptured area medially in front of ALS (Fig. 41G). Epigynum (Fig. 24A–B) main anterior plate trapezoidal, wider than long, slightly protruding, internal arc visible through cuticle; posterior epigynal plate medially divided by wide whitish area. Internal genitalia (Figs 23C, 24C–D) with simple sclerotized arc, membranous 'valve', and pair or oval pore plates far apart.

Distribution

Known from two neighboring sites in San Francisco de Las Pampas, Cotopaxi Province, Ecuador (Fig. 4B).

Natural history

The spiders were collected from little cracks and crevices in an outcrop along the river bank. One egg-sac had a diameter of 3.7 mm, and contained ~40 eggs with an egg diameter of 0.95 mm.

Priscula chapintza Huber sp. nov.

urn:lsid:zoobank.org:act:D8155AE4-4752-4DF4-B3F3-A6BC5C02F01E

Figs 25–28, 41F, 44G-H

Diagnosis

Distinguished from known congeners by details of procursus (Fig. 26A–C; long ventral distal sclerite slender in lateral view, wide in dorsal view, with simple tip; distinctive dorsal process with bifid tip), genital bulb (Fig. 26D–F; main bulbal process with unique prolateral hook), epigynum (Fig. 28A–B; shorter than in most known congeners – similar to *P. esmeraldas* sp. nov.), and female internal genitalia (Fig. 27C; almost round pore plates far apart).

Type material

Holotype

ECUADOR – **Pastaza** • ♂; Via Puyo-Macas, Comunidad Chuwitayo 7 km via Comunidad Chapintza, Cueva de los Tallos; 1.9512° S, 77.7885° W; 640 m a.s.l.; 5 Oct. 2021; E.E. and A.A. Tapia leg.; QCAZ.

Paratypes

ECUADOR – **Pastaza** • 1 ♀, 1 juv., together with holotype; QCAZ • 1 ♂, 1 juv.; same collection data as for holotype; QCAZ • 1 ♂; same locality and date as for holotype; N. Dupérré, E.E. and A.A. Tapia leg.; QCAZ • 1 ♂, 1 ♀; same collection data as for preceding; ZFMK Ar 24095 • 5 ♀♀ (one female used for SEM), 3 juvs; same collection data as for preceding; QCAZ • 1 ♀, 2 juvs; same collection data as for preceding; QCAZ • 1 ♀, 1 juv.; same collection data as for preceding; QCAZ.

Etymology

The species name is derived from the type locality, noun in apposition.

Description

Male (holotype)

Measurements. Total body length 3.8, carapace width 2.0. Distance PME–PME 260 µm; diameter PME 150 µm; distance PME–ALE 80 µm; distance AME–AME 40 µm; diameter AME 35 µm. ALE and PLE larger than PME (diameters ALE 200 µm, PLE 190 µm). Leg 1: 49.3 (12.0+0.9+12.4+21.1+2.9), tibia 2: 9.3, tibia 3 missing, tibia 4: 8.3; tibia 1 L/d: 62.

Color (in ethanol). Carapace whitish, with light brown median band and radial marks, ocular area brown, clypeus light brown; sternum pale ochre with light brown margins; legs whitish, with darker rings subdistally on femora and proximally and subdistally on tibiae; abdomen pale ochre-gray, dorsally and laterally densely covered with black and white marks, ventrally monochromous, very indistinct ochre mark in front of gonopore.

Body. Habitus similar to *P. pastaza* (cf. Fig. 6A). Ocular area raised, without hump on posterior side, with pair of brushes of stronger hairs between ocular triads. Deep thoracic groove. Clypeus unmodified except sclerotized rim. Sternum slightly damaged, unmodified. Abdomen as high as long, dorso-posteriorly rounded.

Chelicerae. As in Fig. 27A–B, with short entapophyses, pair of slender frontal apophyses in very distal and lateral position, without stridulatory ridges.

Palps. As in Fig. 25A–C; coxa unmodified, trochanter with low rounded ventral protrusion, femur large, proximally with distinct retrolateral process followed by deep furrow, ventral rim distally straight (in ventral view) and not protruding; patella ventrally reduced to strongly sclerotized narrow rim; tibia

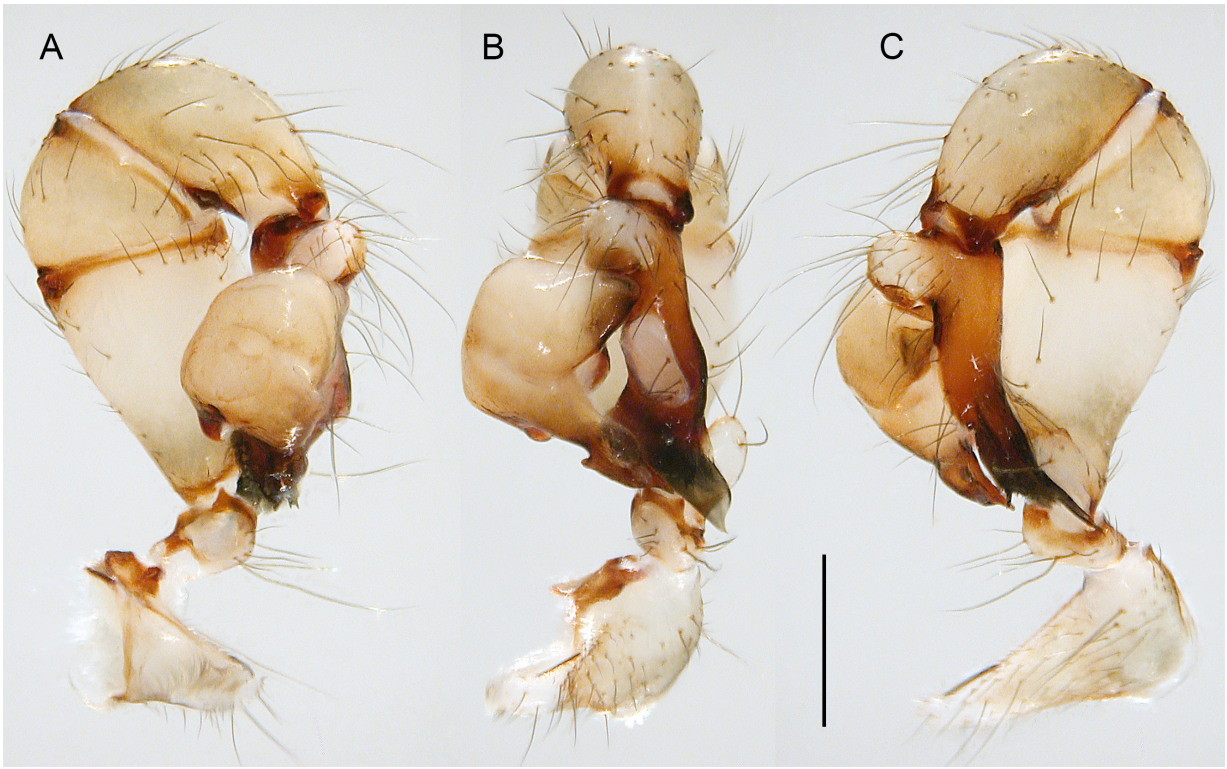

Fig. 25. *Priscula chapintza* Huber sp. nov.; male holotype from Cueva de los Tallos, QCAZ; left male palp, prolateral, dorsal, and retrolateral views. Scale line: 0.5 mm.

small relative to femur; procursus (Fig. 26A–C) with large protruding dorsal whitish element, distally with large prolateral-dorsal band of fringes, distinctive dorsal process with bifid tip, and flat triangular ventral sclerite; genital bulb (Fig. 26D–F) with simple proximal sclerite, with distinctive ventral hook on main bulbal process.

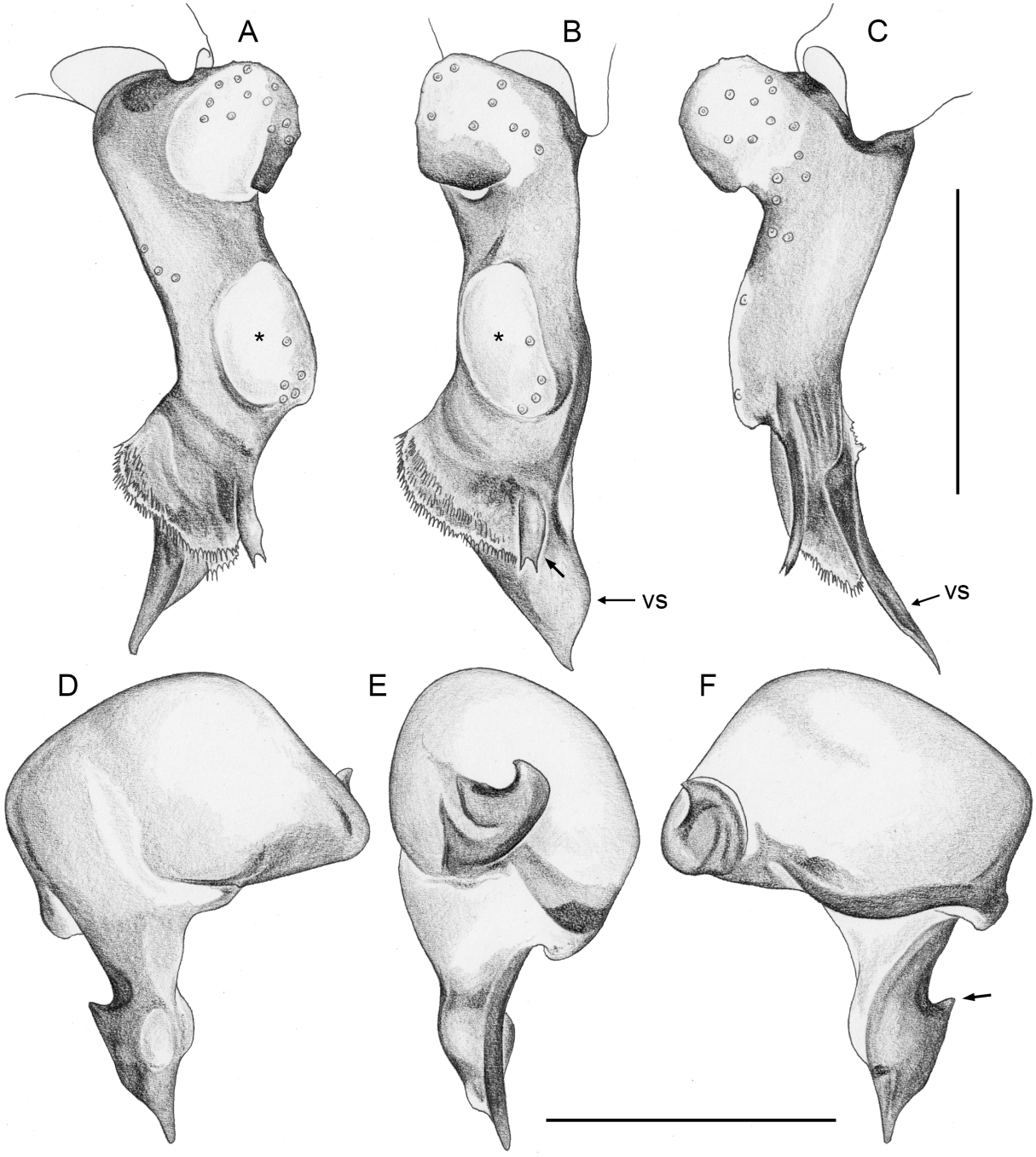

Fig. 26. *Priscula chapintza* Huber sp. nov.; male holotype from Cueva de los Tallos, QCAZ. **A–C.** Left tarsus and procursus, prolateral, dorsal, and retrolateral views; arrow points at distinctive dorsal process; asterisks: whitish protruding area. **D–F.** Left genital bulb, dorsal, retrolateral, and ventral views; arrow points at distinctive prolateral hook. Abbreviation: vs = ventral sclerite. Scale lines: 0.5 mm.

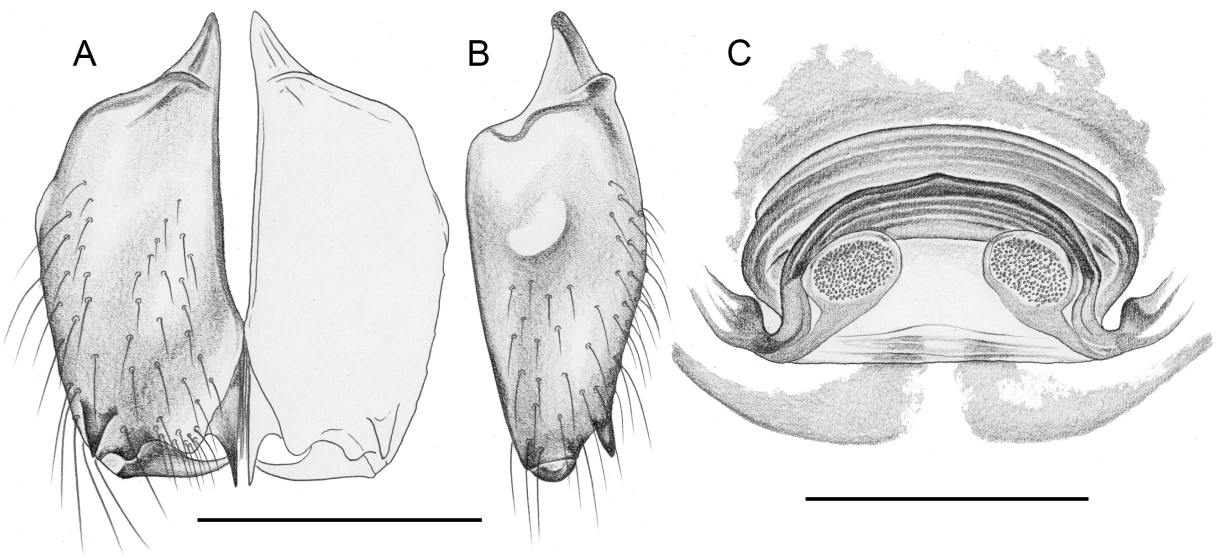

Fig. 27. *Priscula chapintza* Huber sp. nov.; paratypes from Cueva de los Tallos, ZFMK Ar 24095 (♂) and QCAZ (♀). **A–B.** Male chelicerae, frontal and lateral views. **C.** Cleared female genitalia, dorsal view. Scale lines: 0.5 mm.

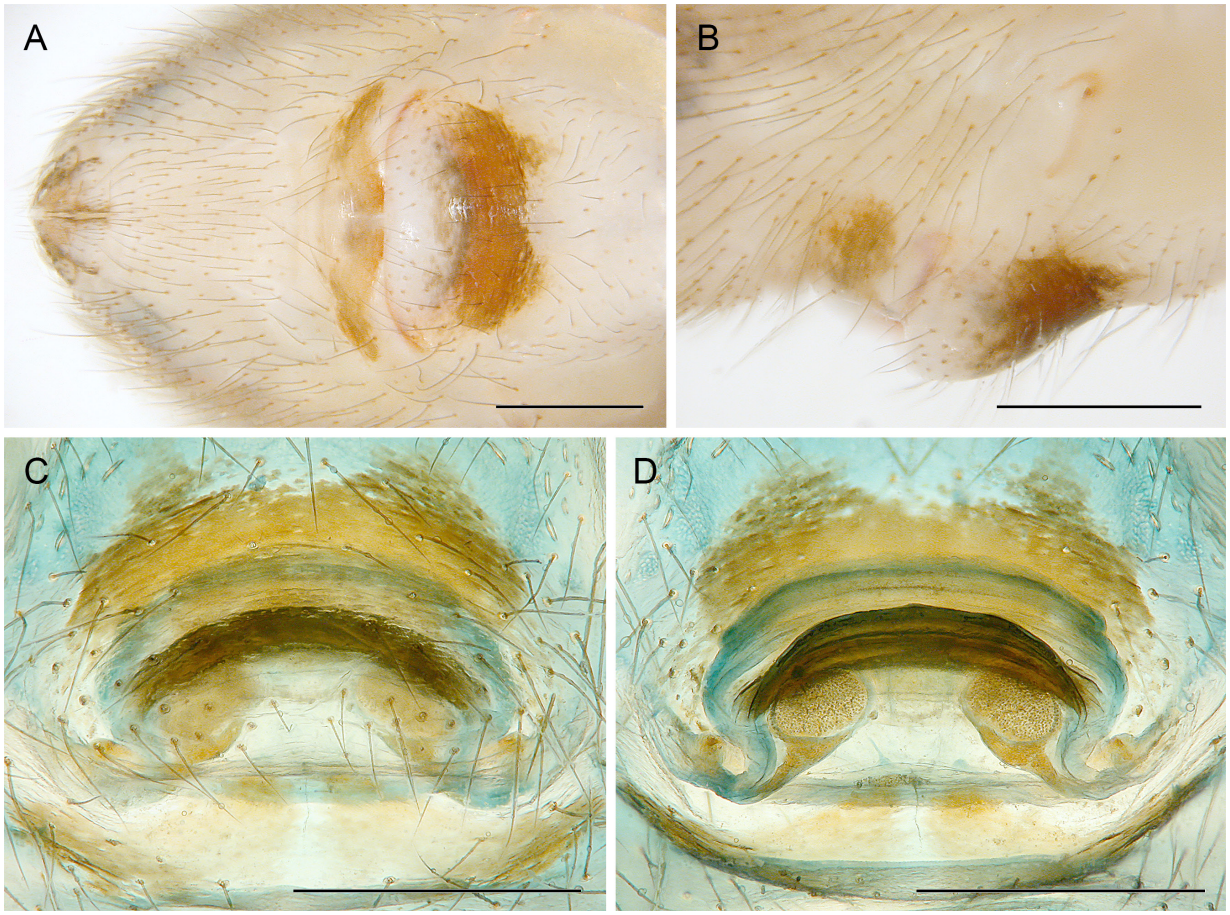

Fig. 28. *Priscula chapintza* Huber sp. nov.; female paratype from Cueva de los Tallos, QCAZ. **A–B.** Abdomen, ventral and lateral views. **C–D.** Cleared genitalia, ventral and dorsal views. Scale lines: 0.5 mm.

Legs. Without spines; without curved hairs; with few short vertical hairs; retrolateral trichobothrium of tibia 1 at 5%; prolateral trichobothrium present on all leg tibiae; tarsi without regular pseudosegmentation but rather with many indistinct platelets.

Male (variation)

Tibia 1 in three other males: 9.3, 10.8, 11.2. Other males (and most females) without or with very indistinct dark marks on abdomen.

Female

In general similar to male but clypeus rim not sclerotized and brushes of hairs between eye triads much shorter. Tibia 1 in six females: 8.1–8.5 (mean 8.2). ALS with one strongly widened spigot, one pointed spigot, and one large and four small cylindrical spigots; with distinctively sculptured area medially in front of ALS (Fig. 41F). Epigynum (Fig. 28A–B) main anterior plate trapezoidal, posterior half whitish and protruding; posterior epigynal plate medially divided by whitish area (indistinct) and with wide shallow depression. Internal genitalia (Figs 27C, 28C–D) with strong transversal sclerite and pair of roundish pore plates connected to pair of lateral sclerites posteriorly.

Distribution

Known from type locality only, in Pastaza Province, Ecuador (Fig. 4B).

Natural history

Cueva de los Tallos is a cave with a sinkhole in the middle (~20m × 20m, 50m deep). Five species of Pholcidae were collected at the bottom of the sinkhole. Most of the Pholcidae, presumably all the *Priscula* specimens, were collected in the sinkhole under or between large to median boulders, a few possibly in the entrance area, also between boulders.

Priscula pastaza Huber sp. nov.
urn:lsid:zoobank.org:act:DADCE77E-4843-45FC-B14E-B20C35764BE3
Figs 6A–B, 29–32, 41A, C, H, 42D–E, H, 43C, G–H, 44B–D, F

Diagnosis

Distinguished from known congeners by details of procursus (Fig. 30A–C; tip with two large membranous elements: wide dorsal flap and long ventral flap with pointed tip), genital bulb (Fig. 30D–F; main bulbal process weakly curved with obtuse tip), epigynum (Fig. 32A–B; semicircular, longer than in putatively closest known relatives, *P. esmeraldas* sp. nov. and *P. chapintza* sp. nov.), and female internal genitalia (Fig. 31C; round pore plates similar to *P. chapintza* but not connected to sclerites posteriorly).

Type material

Holotype

ECUADOR – **Pastaza** • ♂; Cavernas del Anzu Forest Reserve, Caverna de los Continentes; 1.4067° S, 78.0449° W; 1160 m a.s.l.; 25 Sep. 2021; B.A. Huber and M. Herrera leg.; in cave; MECN–ARAC–37–T.

Paratypes

ECUADOR – **Pastaza** • 1 ♂, 2 ♀♀ (one female used for SEM); same collection data as for holotype; MECN–ARAC–38–T, in ZFMK Ar 24101.

Other material examined

ECUADOR – **Pastaza** • 3 ♀♀, 2 juvs (in pure ethanol); same collection data as for holotype; ZFMK Ecu174 • 2 ♂♂ (one palp used for SEM), 1 ♀, 2 juvs; Cavernas del Anzu Forest Reserve, Cueva Copa del Mundo; 1.4054° S, 78.0433° W; 1140 m a.s.l.; 26 Sep. 2021; B.A. Huber and M. Herrera leg.; in cave; MECN–ARAC–39–T, in ZFMK Ar 24102 • 1 ♀ with egg-sac; same collection data as for preceding; MECN–ARAC–40–T, in ZFMK Ar 24103 • 1 juv. (in pure ethanol); same collection data as for preceding; ZFMK Ecu183 • 1 ♀, 2 juvs; same locality as for preceding; 17 Jul. 2013; M. Archambault leg.; QCAZ.

Etymology

The species name is derived from the type locality, noun in apposition.

Description

Male (holotype)

Measurements. Total body length 4.2, carapace width 1.7. Distance PME–PME 200 µm; diameter PME 130×150 µm; distance PME–ALE 50 µm; AME absent (cf. female: Fig. 41A). ALE and PLE larger than PME (diameter ALE 180 µm, PLE 160 µm). Leg 1: 41.4 (10.3+0.8+10.4+17.5+2.4), tibia 2: 7.7, tibia 3: 5.7, tibia 4: 7.3; tibia 1 L/d: 69.

Color (in ethanol). Carapace light-brown, with whitish marks beside ocular area, clypeus with large light brown band narrowing towards chelicerae; sternum light brown with thin darker brown margins; legs monochromous light brown, without darker rings; abdomen monochromous pale gray, only ventrally with darker ochre mark in gonopore area.

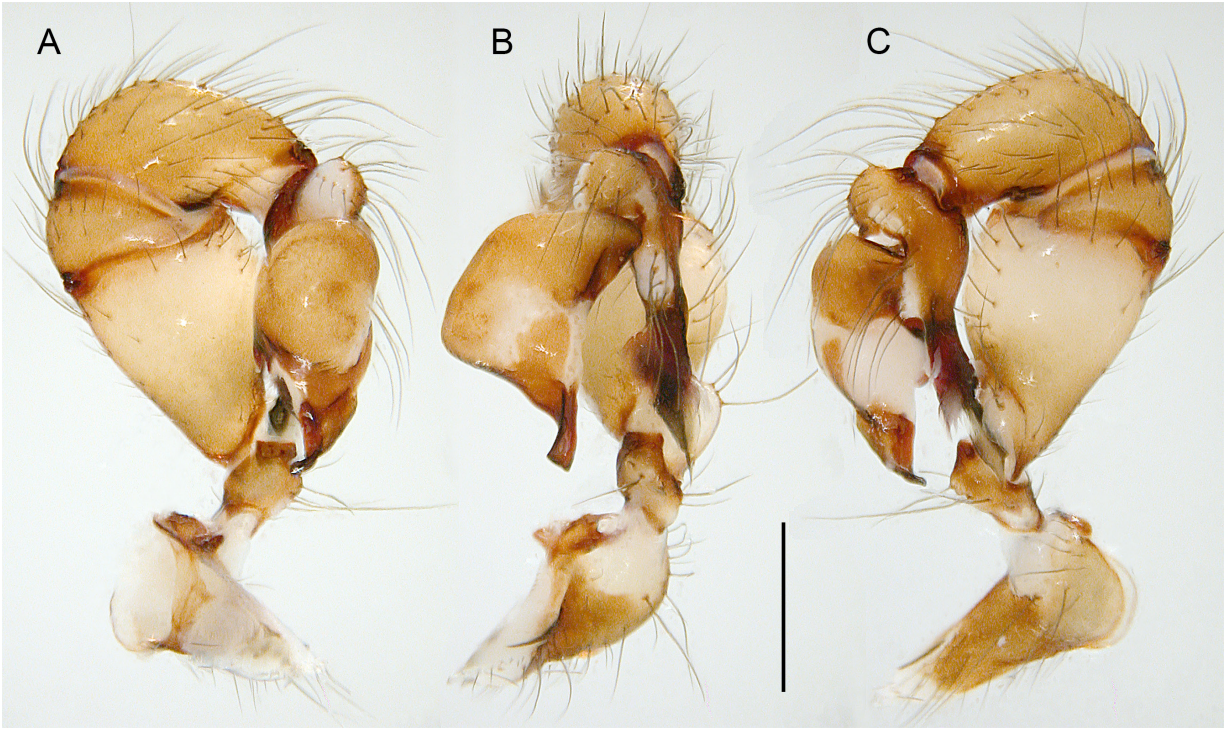

Fig. 29. *Priscula pastaza* Huber sp. nov.; male paratype from Cavernas del Anzu Forest Reserve, ZFMK Ar 24101; left male palp, prolateral, dorsal, and retrolateral views. Scale line: 0.5 mm.

Body. Habitus as in Fig. 6A. Ocular area raised, without hump on posterior side, with comb of stronger hairs at median side of each ocular triad. Deep thoracic groove. Clypeus unmodified except sclerotized rim. Sternum wider than long (1.15/0.80), unmodified. Abdomen globular to slightly higher than long, dorso-posteriorly rounded.

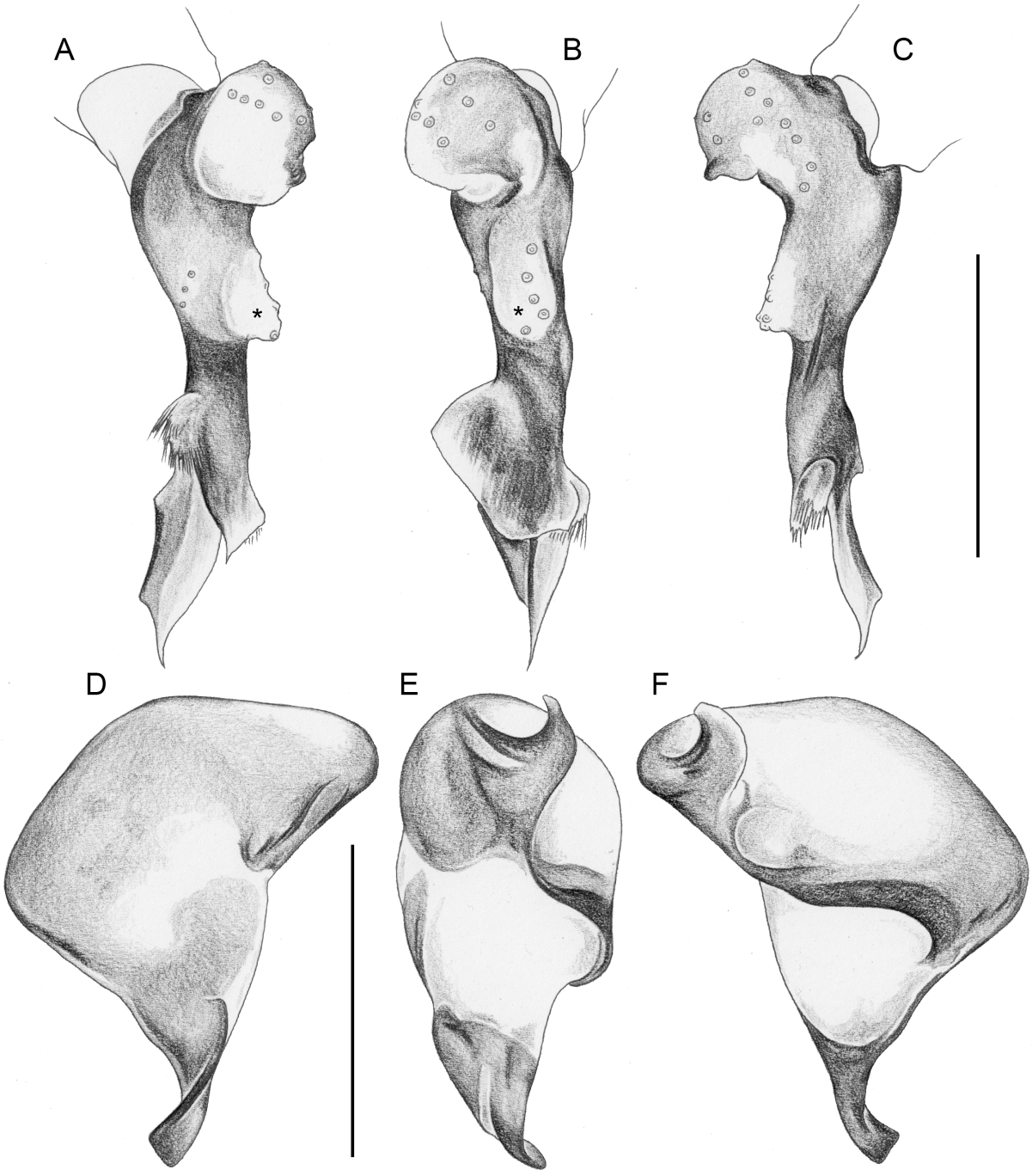

Fig. 30. *Priscula pastaza* Huber sp. nov.; male paratype from Cavernas del Anzu Forest Reserve, ZFMK Ar 24101. **A–C.** Left tarsus and procursus, prolateral, dorsal, and retrolateral views; asterisks: whitish protruding area. **D–F.** Left genital bulb, dorsal, retrolateral, and ventral views. Scale lines: 0.5 mm.

Chelicerae. As in Fig. 31A–B, with short entapophyses, pair of short frontal apophyses close to fang joints; without stridulatory ridges.

Palps. As in Fig. 29A–C; coxa unmodified, trochanter slightly protruding ventrally, femur large, with unsclerotized retrolateral process proximally followed distally by sclerotized indentation, distal ventral rim not protruding; patella ventrally reduced to strongly sclerotized narrow rim; tibia small relative to femur; palpal tarsal organ exposed, weakly raised (Fig. 43C); procursus (Fig. 30A–C) with distinct whitish protruding area dorsally, distinctive prolateral and dorsal membranous elements composed of hair-like processes (dorsal part shown in Fig. 42D–E), distal ventral sclerite flat and weakly sclerotized; genital bulb (Fig. 30D–F) with small proximal sclerite connecting to tarsus, with large whitish area on retrolateral-ventral side, strong and slightly spiraling main bulbal process with subdistal sperm duct opening (arrow in Fig. 42H) and obtuse tip.

Legs. Without spines; with curved hairs on tibiae and metatarsi (mainly legs 1 and 2); with few short vertical hairs; retrolateral trichobothrium of tibia 1 at 6%; prolateral trichobothrium present on all leg tibiae; tarsi without regular pseudosegmentation but rather with many indistinct platelets.

Male (variation)

Tibia 1 in three other males: 9.3, 11.0, 11.3. AME pigment always present but lenses tiny (~20 μm diameter) or absent.

Female

In general similar to male (Fig. 6B) but clypeus rim not sclerotized and hairs on ocular area unmodified. AME variable as in males. Tibia 1 in five females: 7.7–8.8 (mean 8.2). Tarsal organs exposed (Fig. 43G–H); main tarsal claws with ~14–17 tines, tarsus 4 claws more evenly curved and with shorter tines than tarsi 1–3 claws (Fig. 44C–D, F). ALS with one strongly widened spigot, one pointed spigot, and one large and four small cylindrical spigots (Fig. 41C); with distinctively sculptured area medially in front of ALS (Fig. 41H). Epigynum (Fig. 32A–B) main anterior plate

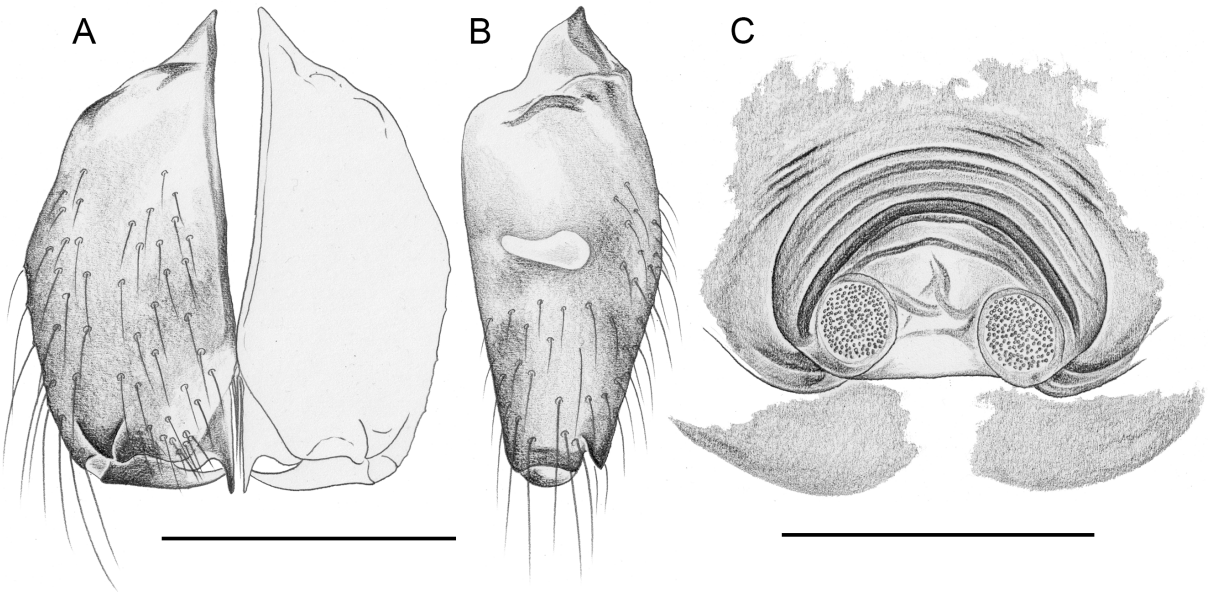

Fig. 31. *Priscula pastaza* Huber sp. nov.; male and female paratypes from Cavernas del Anzu Forest Reserve, ZFMK Ar 24101. **A–B.** Male chelicerae, frontal and lateral views. **C.** Cleared female genitalia, dorsal view. Scale lines: 0.5 mm.

semicircular, slightly protruding, posteriorly with lighter semicircular area; posterior epigynal plate medially divided by whitish area. Internal genitalia (Fig. 31C) with simple sclerotized arc, membranous 'valve', and pair or roundish pore plates.

Distribution

Known from two neighboring caves in the Cavernas del Anzu Forest Reserve, Pastaza Province, Ecuador (Fig. 4B).

Natural history

All spiders were collected in the interior of two caves; adults were only found in the aphotic zones, but juveniles were also found in the twilight area (the first meters of the entrance areas of both caves were occupied by a different species that also occurs in the neighboring forest; see *P. bonita* sp. nov.). No specimens of *P. pastaza* sp. nov. were found in the well-preserved neighboring forest, suggesting that the species might be a troglobite, i.e. strictly bound to underground habitats. The spiders were hanging in very fine and barely visible webs, freely exposed among rocks or in wall niches. Two egg-sacs contained six and seven eggs, respectively, with an egg diameter of 0.95 mm.

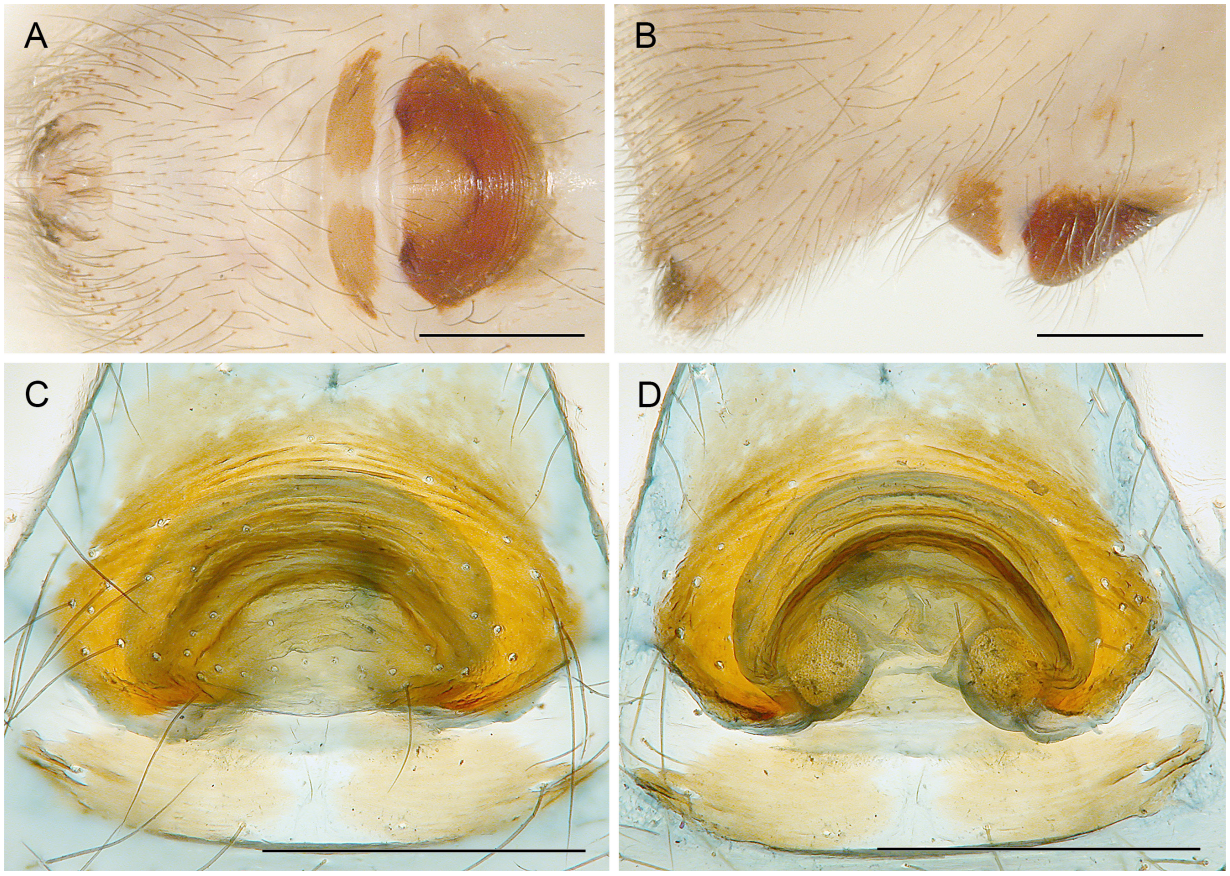

Fig. 32. *Priscula pastaza* Huber sp. nov.; female paratype from Cavernas del Anzu Forest Reserve, ZFMK Ar 24101. **A–B.** Abdomen, ventral and lateral views. **C–D.** Cleared genitalia, ventral and dorsal views. Scale lines: 0.5 mm.

Priscula bonita Huber sp. nov.
urn:lsid:zoobank.org:act:E8DC917E-0778-4C1B-AA97-F59DB99B3A6A
Figs 6C–D, 33–36, 42F–G, 44E

Priscula sp. n. 'Ecu93' – Dederichs *et al.* 2022: 46 (sperm ultrastructure).

Diagnosis

Distinguished from known congeners by details of procursus (Fig. 34A–C; distinctive distal sclerite with two pointed processes; slender proximal part – similar to *P. annulipes* (Keyserling, 1877) and *P. venezuelana*), genital bulb (Fig. 34D–F; main bulbal process longer than in most known congeners, with pointed tip), and female internal genitalia (Fig. 35C; pore plates roughly triangular, narrower posteriorly than anteriorly – similar to *P. bolivari*). From most known congeners in Ecuador (except *P. lumbaqui* sp. nov.) also by very large male palpal femur (Fig. 33C; 1.7 times longer than palpal tibia; *P. lumbaqui*: 2.0; other species in Ecuador. 1.1–1.3).

Type material

Holotype

ECUADOR – **Sucumbíos** • ♂; near La Bonita; 0.474° N, 77.558° W; 1870 m a.s.l.; 1 Oct. 2021; B.A. Huber and M. Herrera leg.; humid forest; MECN–ARAC–41–T.

Paratypes

ECUADOR – **Sucumbíos** • 1 ♂, 1 ♀; same collection data as for holotype; MECN–ARAC–42–T, in ZFMK Ar 24104.

Other material examined

ECUADOR – **Sucumbíos** • 1 ♀, 1 juv. (in pure ethanol); same collection data as for holotype; ZFMK Ecu214 • 1 ♂; between La Bonita and Santa Barbara; 0.6470° N, 77.4910° W; 2720 m a.s.l., 1 Oct. 2021; B.A. Huber and M. Herrera leg.; humid forest; MECN–ARAC–43–T • 1 ♂ (1 palp used for SEM); same collection data as for preceding; MECN–ARAC–44–T, in ZFMK Ar 24105 • 1 ♀, 1 juv. (in pure ethanol); same collection data as for preceding; ZFMK Ecu216. **Napo** • 1 ♂, 4 ♀♀ (one female used for SEM); Gruta de Los Tayos, in 'cave' (canyon); 0.2186° S, 77.7402° W; 1590 m a.s.l.; 29 Sep. 2021; B.A. Huber and M. Herrera leg.; MECN–ARAC–45–T, in ZFMK Ar 24106–07 • 2 ♀♀, 3 juvs (in pure ethanol); same collection data as for preceding; ZFMK Ecu205 • 1 ♀; Antisana N.P.; 0.6409° S, 77.8086° W; 2000 m a.s.l.; 28 Sep. 2021; B.A. Huber and M. Herrera leg.; humid forest; MECN–ARAC–46–T, in ZFMK Ar 24108 • 1 ♀, 1 juv. (in pure ethanol); same collection data as for preceding; ZFMK Ecu201.

Assigned tentatively (see below)

ECUADOR – **Napo** • 1 ♂ (in pure ethanol); SE Archidona, Rio Hollin; 0.955° S, 77.748° W; 660 m a.s.l.; 29 Nov. 2009; P. Michalik leg.; ZFMK Mich35. **Pastaza** • 1 ♂, 1 ♀ abdomen; Cavernas del Anzu Forest Reserve, at cave entrance of Cueva Copa del Mundo; 1.4054° S, 78.0433° W; 1140 m a.s.l.; 26 Sep. 2021; B.A. Huber and M. Herrera leg.; MECN–ARAC–47–T, in ZFMK Ar 24109 • 1 ♀ (in pure ethanol; abdomen transferred to ZFMK Ar 24109); same collection data as for preceding; ZFMK Ecu184 • 3 ♀♀ (in pure ethanol); Cavernas del Anzu Forest Reserve; between 1.406° S, 78.043° W and 1.416° S, 78.049° W; 1140–1270 m a.s.l.; 26 Sep. 2021; B.A. Huber and M. Herrera leg., ZFMK Ecu185.

Etymology

The species name is derived from the type locality, noun in apposition.

Description

Male (holotype)

Measurements. Total body length 5.2, carapace width 2.1. Distance PME–PME 270 µm; diameter PME 170 µm; distance PME–ALE 180 µm; distance AME–AME 45 µm; diameter AME 45 µm. ALE and PLE larger than PME (diameters 250 µm). Leg 1: 46.1 (11.7+0.9+11.5+18.7+3.3), tibia 2: 8.1, tibia 3: 5.7, tibia 4: 7.3; tibia 1 L/d: 55.

Color (in ethanol). Carapace pale ochre-yellow, with large brown median mark and three pairs of lateral marks, ocular area also brown, clypeus with large brown band narrowing towards chelicerae; sternum light brown with thin darker margins; legs pale ochre, with 3–4 variably distinct dark rings on each femur and tibia; abdomen dorsally and laterally densely covered with black marks, with some small white marks in-between, ventrally with large brown mark in front of gonopore and light brown sclerite in front of spinnerets.

Body. Habitus as in Fig. 6C. Ocular area raised, without hump on posterior side, without comb of stronger hairs at median side of each ocular triad. Deep thoracic groove. Clypeus unmodified except sclerotized rim. Sternum wider than long (1.45/1.00), unmodified. Abdomen slightly higher than long, dorso-posteriorly pointed.

Chelicerae. As in Fig. 35A–B, with short entapophyses, with pair of very small frontal apophyses near fang joints, whitish lateral area slightly protruding; without stridulatory ridges.

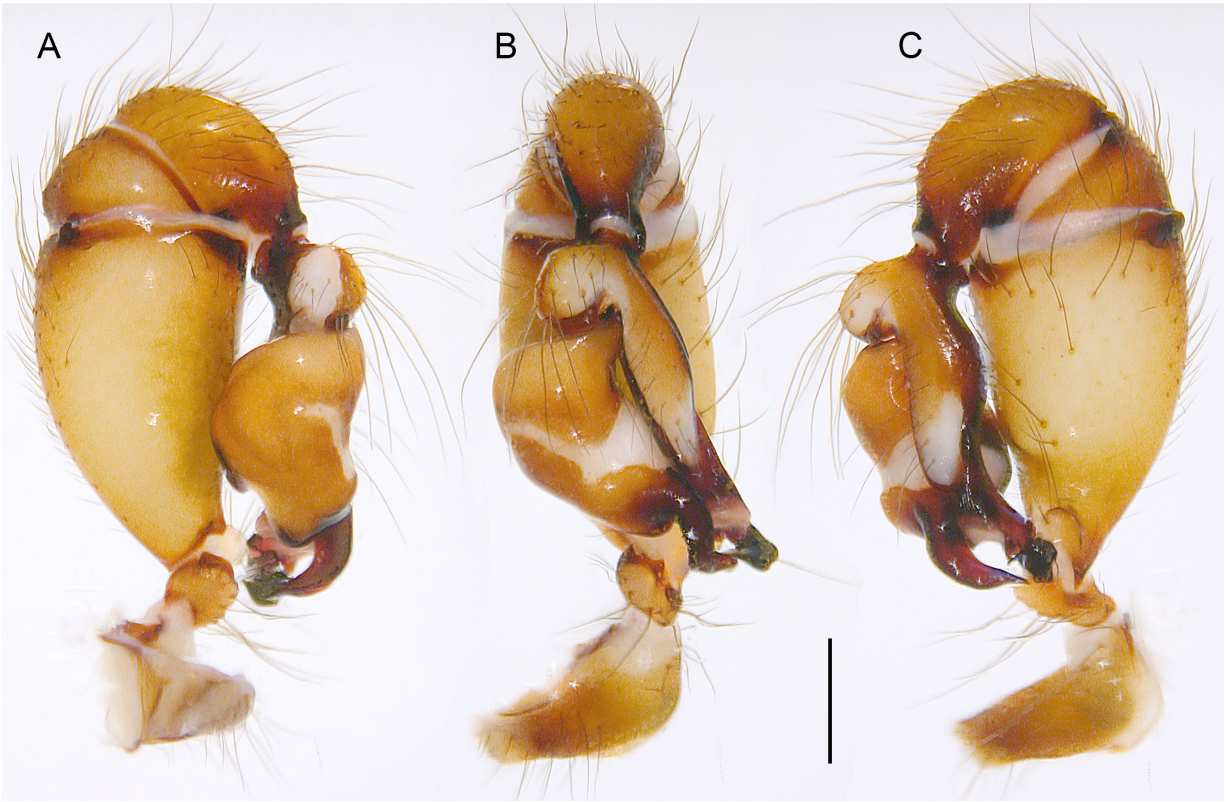

Fig. 33. *Priscula bonita* Huber sp. nov.; male paratype from near La Bonita, ZFMK Ar 24104; left male palp, prolateral, dorsal, and retrolateral views. Scale line: 0.5 mm.

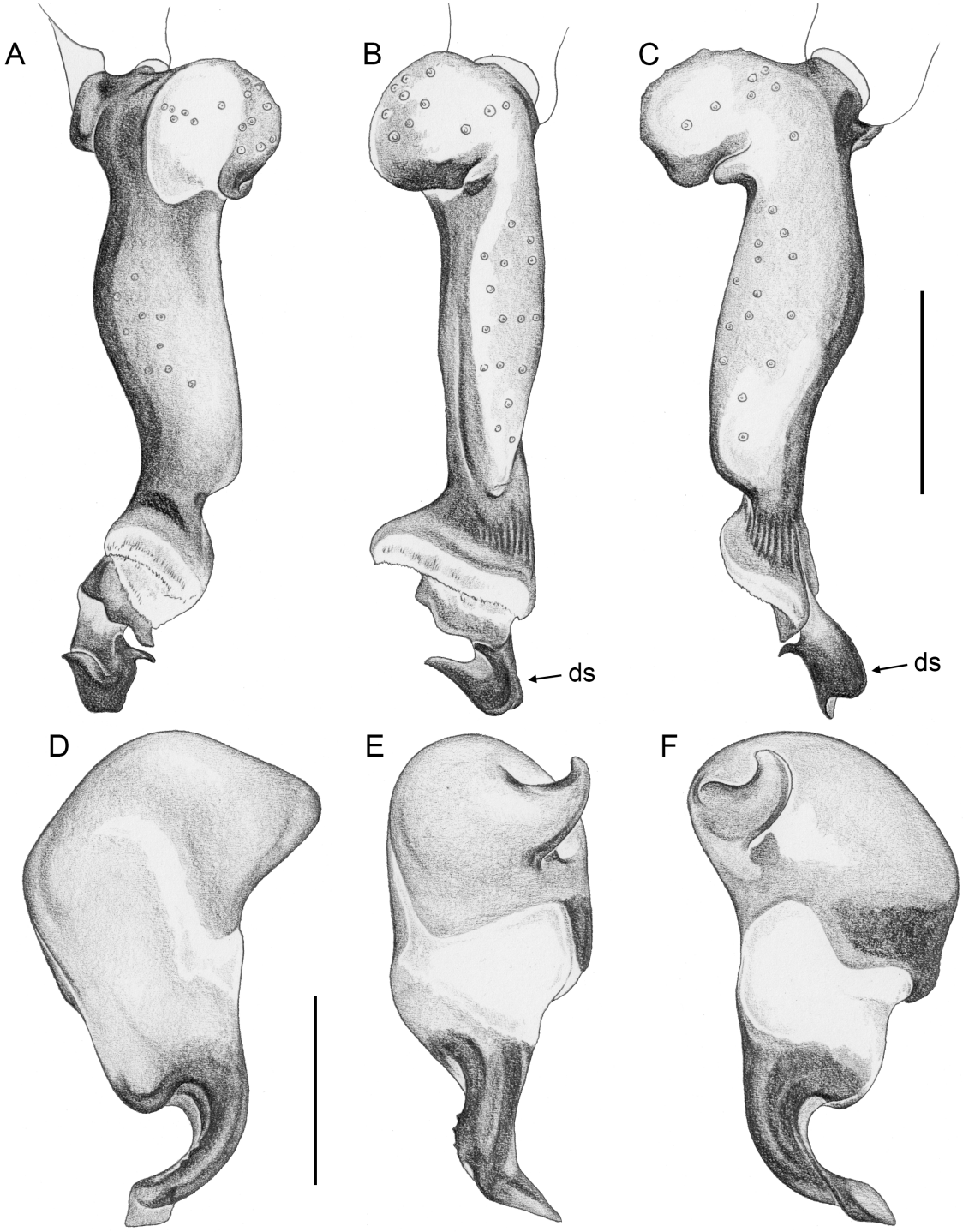

Fig. 34. *Priscula bonita* Huber sp. nov.; male paratype from near La Bonita, ZFMK Ar 24104. **A–C.** Left tarsus and procursus, prolateral, dorsal, and retrolateral views. **D–F.** Left genital bulb, dorsal, retrolateral, and ventral views. Abbreviation: ds = distal sclerite. Scale lines: 0.5 mm.

Palps. As in Fig. 33A–C; coxa unmodified, trochanter slightly protruding ventrally, femur very large, proximally with distinct retrolateral process and prolateral-ventral ridge, distal ventral rim not protruding; patella ventrally reduced to strongly sclerotized narrow rim; tibia small relative to femur; procursus (Fig. 34A–C) slender, proximally with exposed tarsal organ (arrow in Fig. 42F), distally with prolateral-dorsal band of whitish membranous and fringed elements, with strongly sclerotized distal sclerite apparently moveable against proximal part of procursus; genital bulb (Fig. 34D–F) with small proximal sclerite connecting to tarsus, with large whitish area on retrolateral-ventral side, strong and slightly spiraling main bulbal process with subdistal sperm duct opening (arrow in Fig. 42G) and pointed tip.

Legs. Without spines; with curved hairs on all tibiae and metatarsi, few weakly curved hairs also on femora; with few short vertical hairs; retrolateral trichobothrium of tibia 1 at 7%; prolateral trichobothrium present on all leg tibiae; tarsi without regular pseudosegmentation but rather with many indistinct platelets.

Male (variation)

Tibia 1 in seven males (incl. holotype): 9.9–12.4 (mean 11.4). Lateral marks on carapace variably separated or connected with each other at carapace margin; sternum sometimes with light marks. Males from southern Napo and Pastaza are very similar but have slightly smaller palps and the distal sclerite on the procursus is slightly narrower in retrolateral view. This is also reflected in the relatively large CO1 distances between the sequenced specimen from Pastaza and the sequenced specimens from Sucumbíos and central to northern Napo (8.1–8.8%). Distances among the Sucumbíos and central to northern Napo specimens are 5.3% or lower.

Female

In general similar to male (Fig. 6D) but clypeus rim not sclerotized but with median ochre mark. Ventral sclerite in front of spinnerets variably divided medially or undivided. Tibia 1 in 13 females: 6.1–7.7 (mean 7.2). ALS with one strongly widened spigot, one pointed spigot, and one large and four small cylindrical spigots; with distinctively sculptured area medially in front of ALS (similar to Fig. 41G).

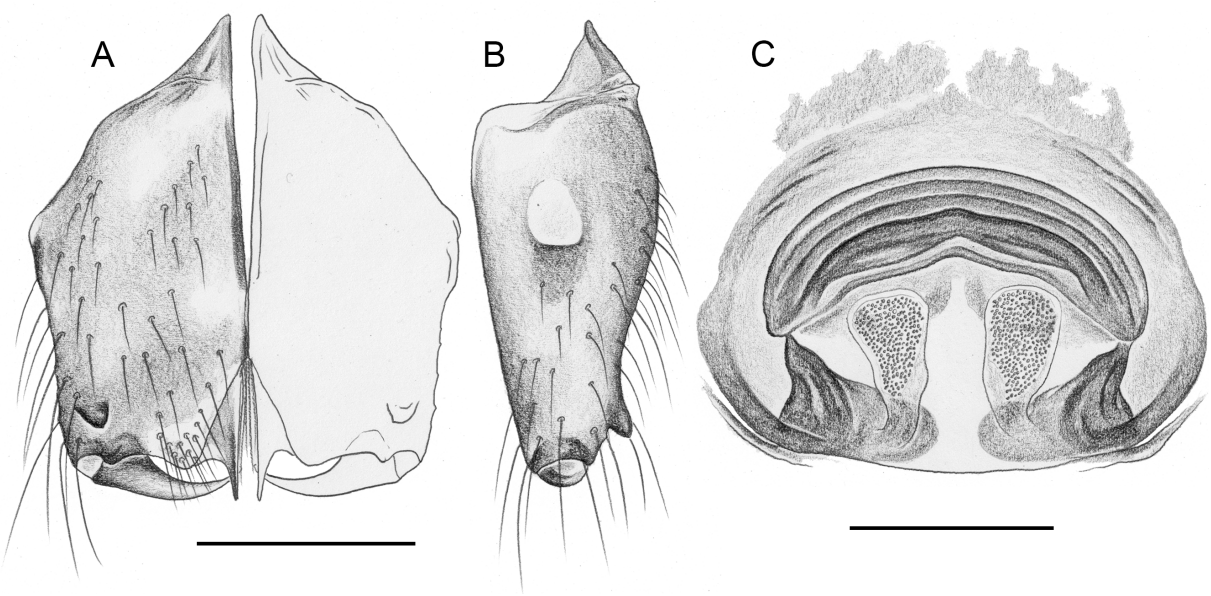

Fig. 35. *Priscula bonita* Huber sp. nov.; male and female paratypes from near La Bonita, ZFMK Ar 24104. **A–B.** Male chelicerae, frontal and lateral views. **C.** Cleared female genitalia, dorsal view. Scale lines: 0.5 mm.

Epigynum (Fig. 36A–B) main anterior plate trapezoidal, slightly protruding, posteriorly medially slightly indented; posterior epigynal plate reduced to pair of small lateral sclerites. Females from Pastaza with similar anterior plate but less reduced posterior plate (Fig. 36E–F). Internal genitalia (Figs 35C, 36C–D) with pair of large pore plates in almost parallel position, narrowing posteriorly.

Distribution

Apparently widely distributed along the eastern Andean slopes of Ecuador (Fig. 4B).

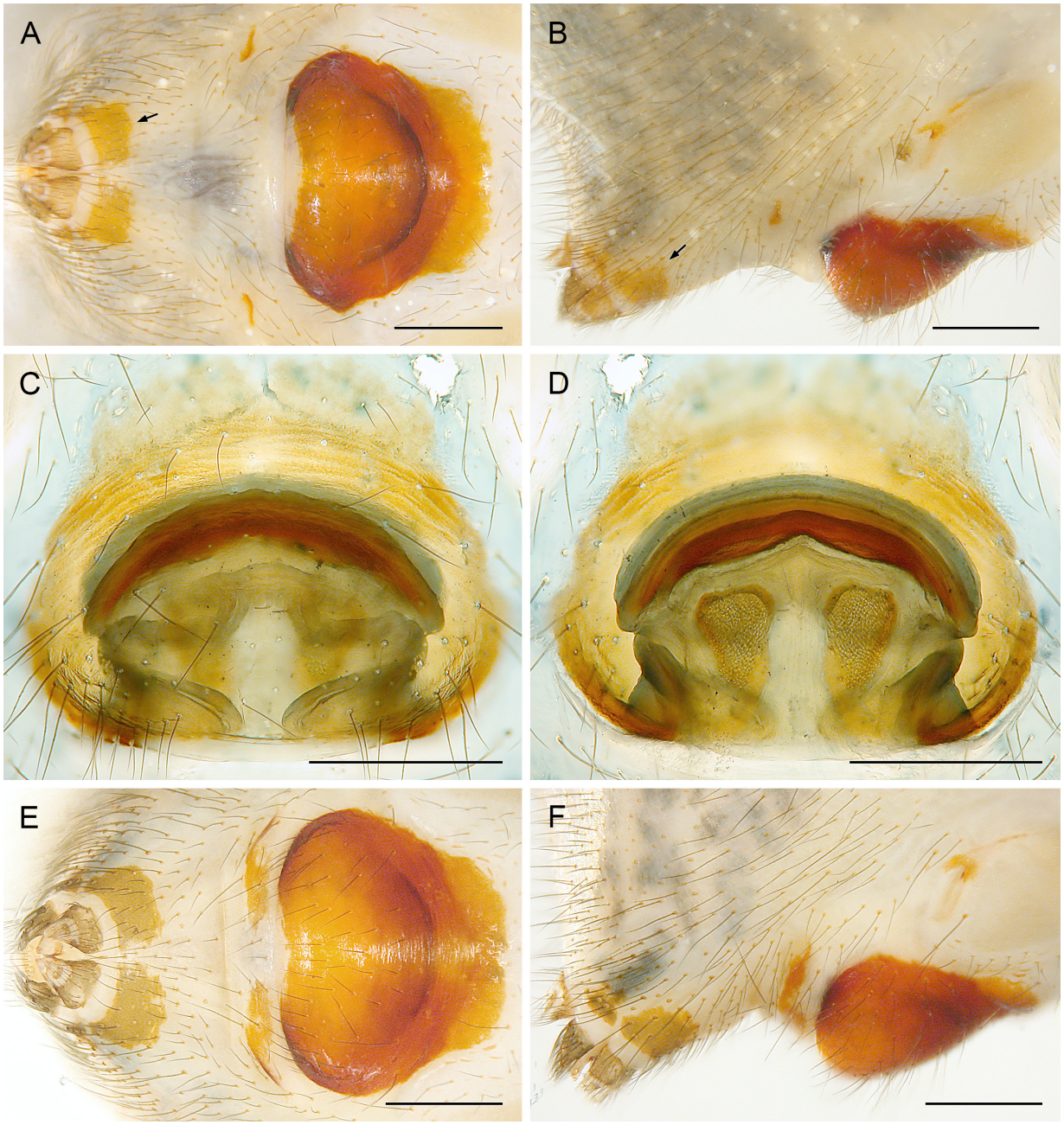

Fig. 36. *Priscula bonita* Huber sp. nov.; female paratype from near La Bonita, ZFMK Ar 24104 (A–D) and female from Cavernas del Anzu Forest Reserve, ZFMK Ar 24109 (E–F). **A–B, E–F.** Abdomens, ventral and lateral views; arrows point at sclerite in front of spinnerets. **C–D.** Cleared genitalia, ventral and dorsal views. Scale lines: 0.5 mm.

Natural history

At the type locality and between La Bonita and Santa Barbara, the spiders were found hidden in deep sheltered spaces at ground level. In Antisana National Park, one specimen was found in thick mosses covering a tree trunk, the second one in a crevice of a rock wall. In the canyon of the Gruta de Los Tayos, the spiders were fairly abundant, usually under small ledges on the rock wall, up to several meters above the ground; no specimens were found in the neighboring forest. In Cavernas del Anzu Forest Reserve, some specimens were found in the entrance areas of caves (whose deeper parts were occupied by *P. pastaza*). Others were found in the neighboring forest; among the latter, one female was found in the mosses covering a tree trunk. Two egg sacs had diameters of 3.3 and 4.5 mm, respectively, and contained ~25/65 eggs with an egg diameter of 1.00 mm.

Priscula lumbaqui Huber sp. nov.

urn:lsid:zoobank.org:act:748651F8-E634-4F74-A11C-B44D27BE59E9

Figs 6E–F, 37–40, 41B, E, 43B, D–E, 44A

Diagnosis

Easily distinguished from known congeners by extremely widened procursus in lateral view (Fig. 38C) and by large triangular sclerite in female internal genitalia (Fig. 40D). Also by further details of procursus (Fig. 38A–C; distinctive distal sclerite with retrolateral process), genital bulb (Fig. 38D–F; main bulbal process shorter than in most congeners, with wide obtuse tip), male chelicerae (Fig. 39A–B; very small frontal apophyses – similar only in some Venezuelan species of the *limonensis* group), and female internal genitalia (Fig. 40C–D; pair of processes on ventral arc; pore plates almost round, far apart).

Type material

Holotype

ECUADOR – **Sucumbíos** • ♂; near Lumbaquí; 0.0349° N, 77.3106° W; 810 m a.s.l.; 30 Sep. 2021; B.A. Huber and M. Herrera leg.; humid forest on hill; MECN–ARAC–48–T.

Paratypes

ECUADOR – **Sucumbíos** • 1 ♀; together with holotype; MECN–ARAC–48–T • 1 ♂, 4 ♀♀ (one female used for SEM); same collection data as for holotype; MECN–ARAC–49–T, in ZFMK Ar 24110.

Other material examined

ECUADOR – **Sucumbíos** • 3 ♀♀ (in pure ethanol); same collection data as for holotype; ZFMK Ecu210.

Etymology

The species name is derived from the type locality, noun in apposition.

Description

Male (holotype)

Measurements. Total body length 4.3, carapace width 2.0. Distance PME–PME 240 µm; diameter PME 190 µm; distance PME–ALE 150 µm; distance AME–AME 50 µm; diameter AME 60 µm. ALE larger than PLE and PME (diameter ALE 260 µm). Leg 1: 54.3 (13.5+0.9+13.3+23.3+3.3), tibia 2: 9.3, tibia 3: 6.4, tibia 4: 8.4; tibia 1 L/d: 74.

Color (in ethanol). Carapace pale ochre-yellow, with dark ochre median and lateral marks connected by irregular radial lines, ocular area dark ochre to brown, clypeus with large dark ochre band narrowing

towards chelicerae; sternum dark ochre with thin brown margins; legs pale ochre, with dark rings on femora (subdistally) and tibiae (proximally and subdistally); abdomen dorsally and laterally densely covered with black marks separated by network of small white marks, ventrally with large brown mark in front of gonopore and ochre to light brown sclerite in front of spinnerets.

Body. Habitus as in Fig. 6E. Ocular area raised (cf. female: Fig. 41B), without hump on posterior side, without comb of stronger hairs at median side of each ocular triad. Deep thoracic groove. Clypeus unmodified except sclerotized rim. Sternum wider than long (1.30/0.80), unmodified. Abdomen slightly higher than long, dorso-posteriorly pointed.

Chelicerae. As in Fig. 39A–B, with short entapophyses, pair of lateral processes proximally and pair of very small frontal apophyses near fang joints; without stridulatory ridges.

Palps. As in Fig. 37A–C; coxa unmodified, trochanter slightly protruding ventrally, femur very large, proximally with distinct retrolateral process and indistinct prolateral-ventral process, distal ventral rim not protruding; patella ventrally reduced to strongly sclerotized narrow rim; tibia small relative to femur; procursus (Fig. 38A–C) very wide in lateral view, distally with prolateral-dorsal band of whitish membranous and fringed elements, with strongly sclerotized distal sclerite provided with long retrolateral process and apparently moveable against proximal part of procursus; genital bulb (Fig. 38D–F) with small proximal sclerite connecting to tarsus, large whitish area on retrolateral-ventral side, strong and curved main bulbal process with wide obtuse tip.

Legs. Without spines; with very weakly curved hairs on all tibiae and metatarsi; with few short vertical hairs; retrolateral trichobothrium of tibia 1 at 5%; prolateral trichobothrium present on all leg tibiae; tarsi without regular pseudosegmentation but rather with many indistinct platelets.

Fig. 37. *Priscula lumbaqui* Huber sp. nov.; male paratype from near Lumbaqui, ZFMK Ar 24110; left male palp, prolateral, dorsal, and retrolateral views. Scale line: 0.5 mm.

Male (variation)

Tibia 1 in other male: 12.0.

Female

In general similar to male (Fig. 6F) but clypeus slightly less protruding than in male and clypeus rim not sclerotized but with median ochre mark. Ventral sclerite in front of spinnerets variably divided medially or undivided. Tibia 1 in five females: 7.5–8.7 (mean 7.9). Tip of palp simple, pointed, with dorsal invagination (Fig. 43B). Tarsal organs on palps and legs exposed (Fig. 43D, E). ALS with one strongly widened spigot, one pointed spigot, and one large and four small cylindrical spigots (Fig. 41E);

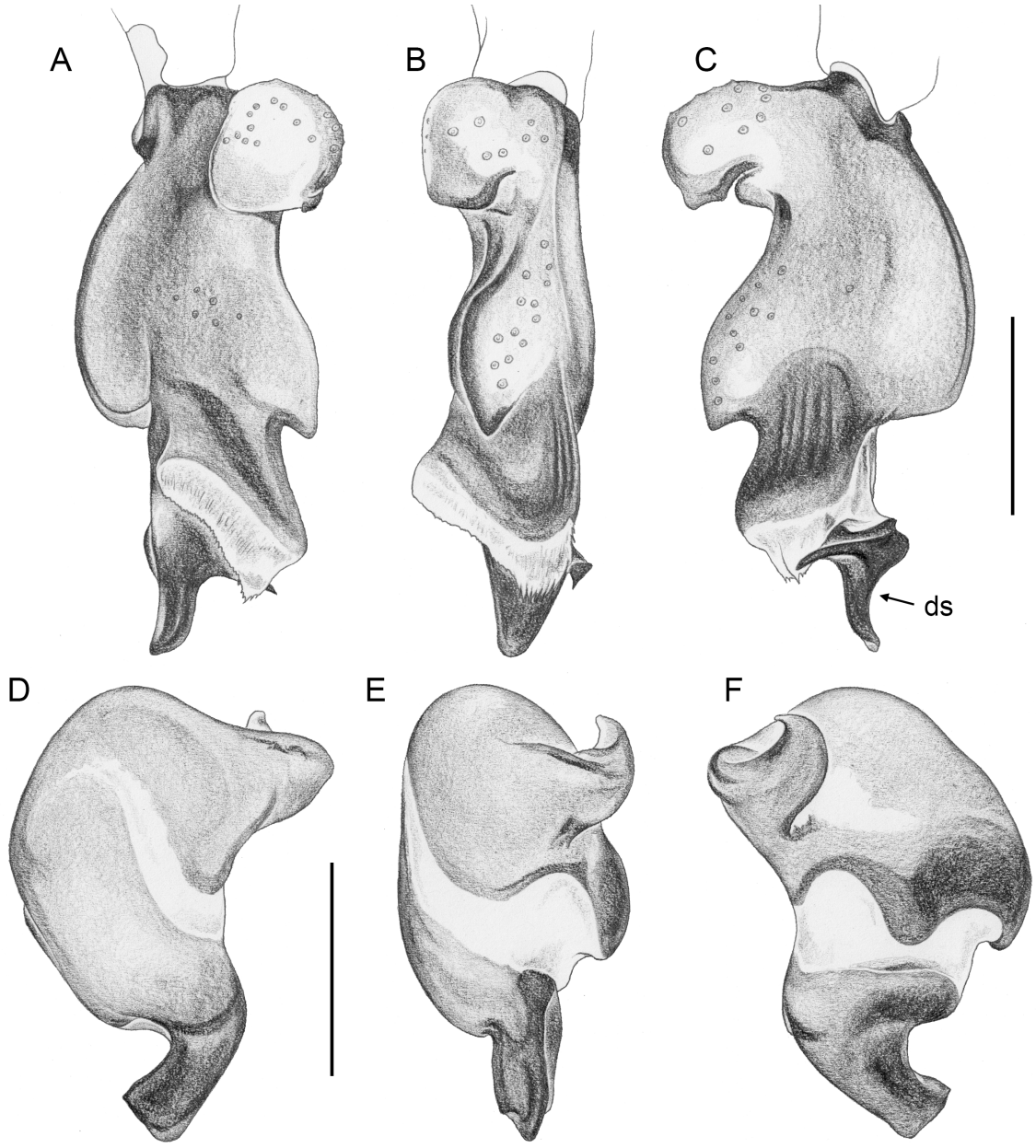

Fig. 38. *Priscula lumbaqui* Huber sp. nov.; male paratype from near Lumbaqui, ZFMK Ar 24110. **A–C.** Left tarsus and procursus, prolateral, dorsal, and retrolateral views. **D–F.** Left genital bulb, dorsal, retrolateral, and ventral views. Abbreviation: ds = distal sclerite. Scale lines: 0.5 mm.

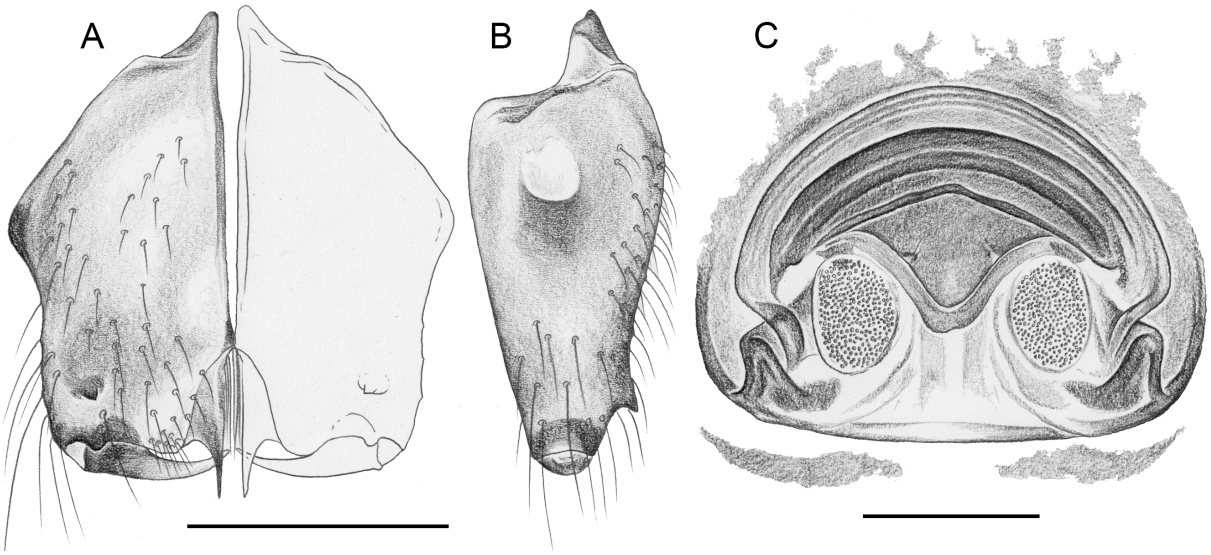

Fig. 39. *Priscula lumbaqui* Huber sp. nov.; male and female paratypes from near Lumbaqui, ZFMK Ar 24110. **A–B.** Male chelicerae, frontal and lateral views. **C.** Cleared female genitalia, dorsal view. Scale lines: 0.5 mm.

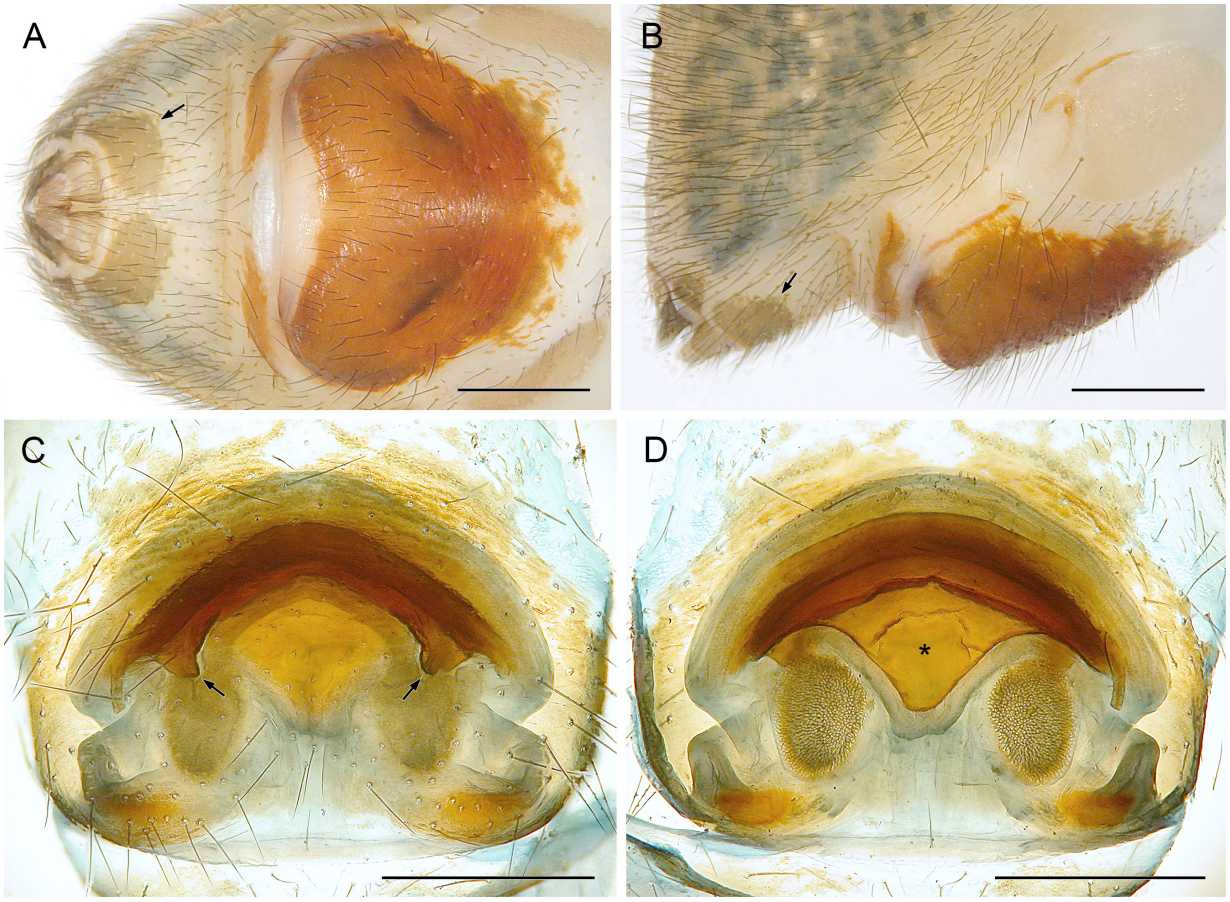

Fig. 40. *Priscula lumbaqui* Huber sp. nov.; female paratype from near Lumbaqui, ZFMK Ar 24110. **A–B.** Abdomen, ventral and lateral views; arrows point at sclerite in front of spinnerets. **C–D.** Cleared genitalia, ventral and dorsal views; arrows point at processes of ventral arc; asterisk marks distinctive triangular sclerite. Scale lines: 0.5 mm.

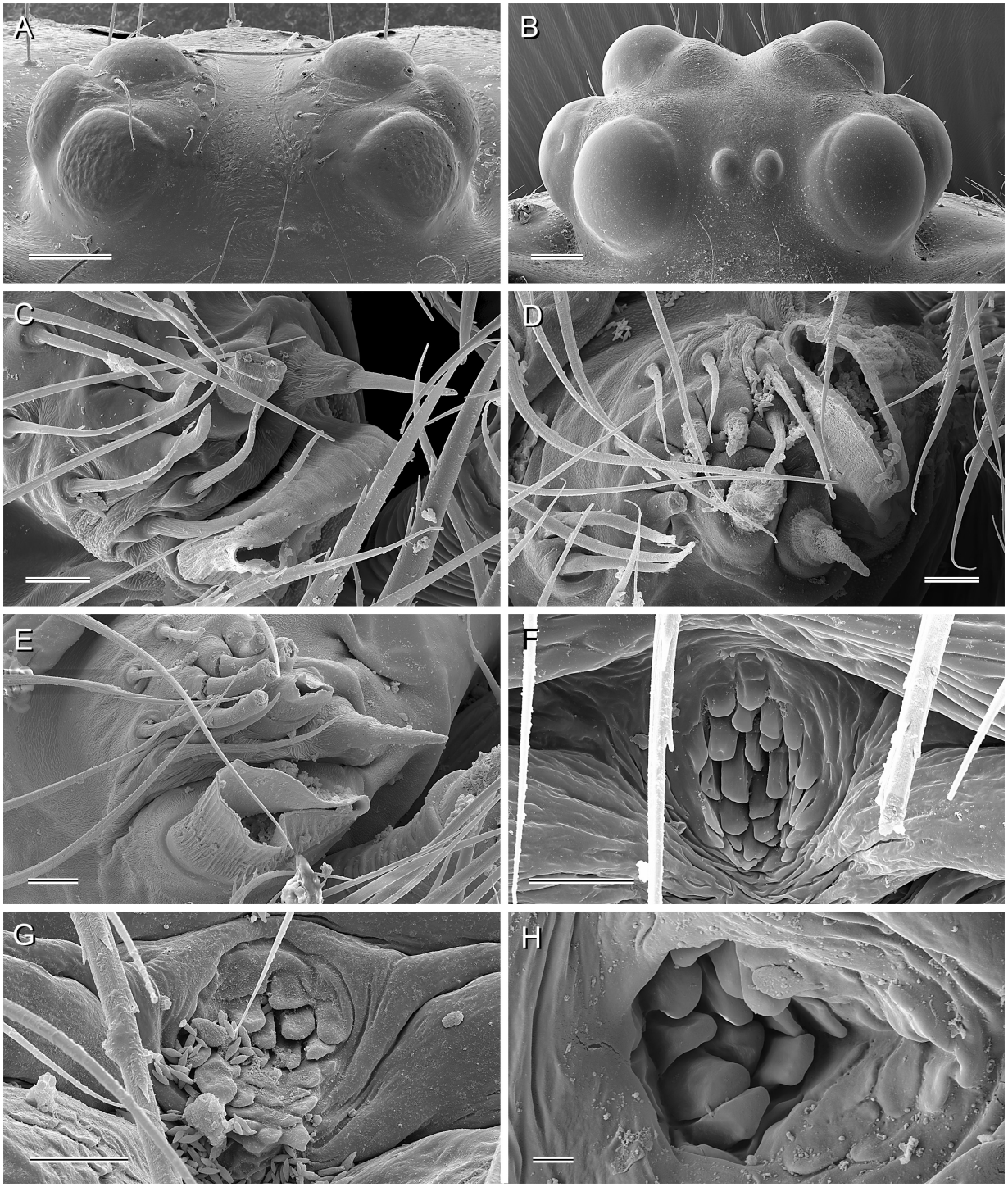

Fig. 41. *Priscula* spp., SEM photographs of female ocular areas and spinnerets. **A–B**. Ocular areas, frontal views; *Priscula pastaza* Huber sp. nov. (A) and *P. lumbaqui* Huber sp. nov. (B). **C–E**. ALS, *P. pastaza* (C), *P. esmeraldas* Huber sp. nov. (D), and *P. lumbaqui* sp. nov. (E). **F–H**. Distinctive structures in front of spinnerets (in place of colulus); *P. chapintza* Huber sp. nov. (F), *P. esmeraldas* (G), and *P. pastaza* (H). Scale lines: 100 µm (A–B); 10 µm (C–G); 2 µm (H).

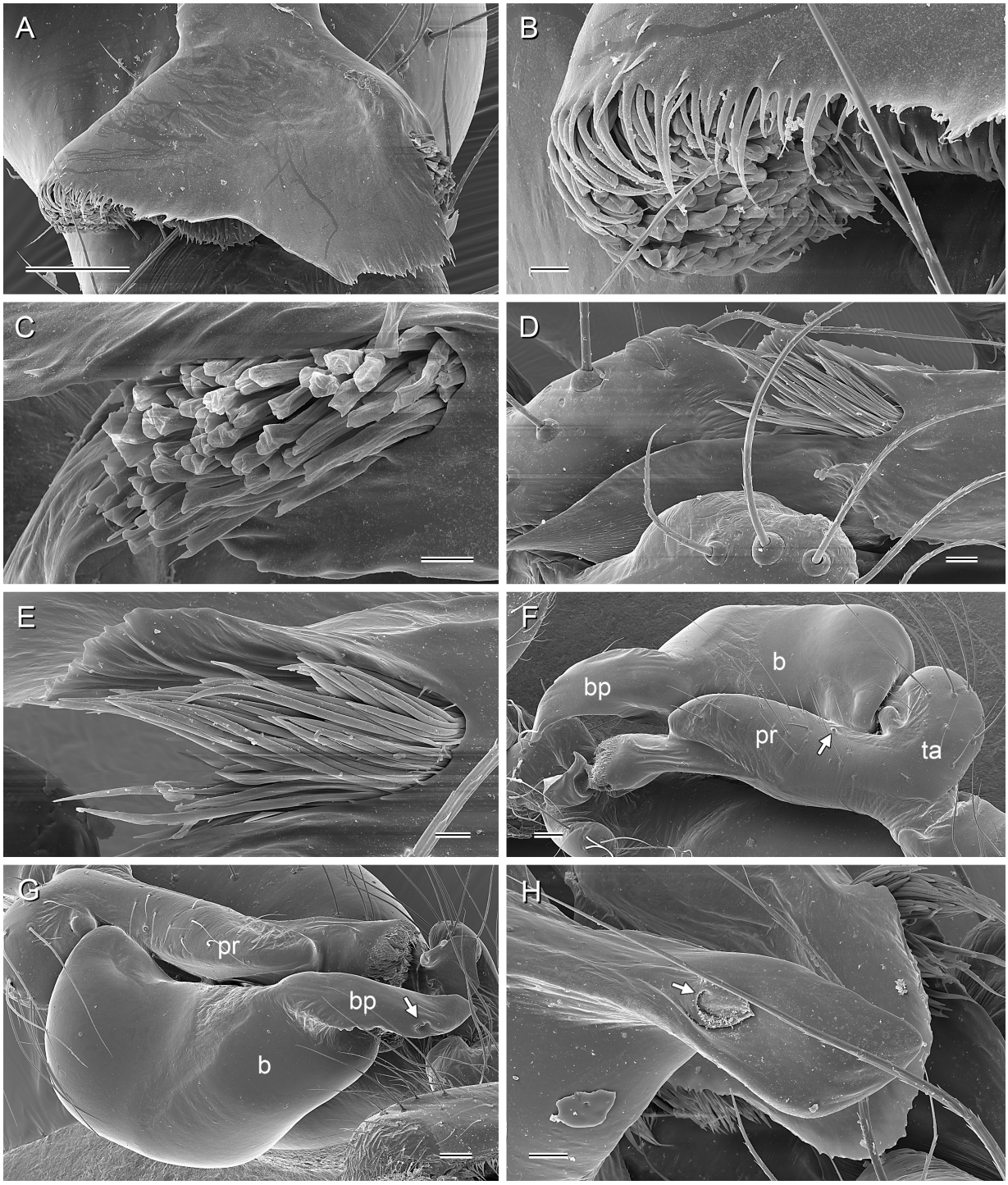

Fig. 42. *Priscula* spp., SEM photographs of male pedipalps. **A–C**. Tip of left procursus in dorsal view (A) and hair-like processes on its prolateral (B) and retrolateral (C) sides; *P. esmeraldas* Huber sp. nov. **D–E**. Tip of left procursus in retrolateral view (D) and hair-like processes in more detail (E); *P. pastaza* Huber sp. nov. **F–G**. Left procursus and bulb of *P. bonita* Huber sp. nov., showing position of tarsal organ (arrow in F) and position of sperm duct opening (arrow in G). **H**. Sperm duct opening (arrow) on bulbal process in *P. pastaza*. Scale lines: 100 µm (A, F–G); 10 µm (B–C, E); 20 µm (D, H).

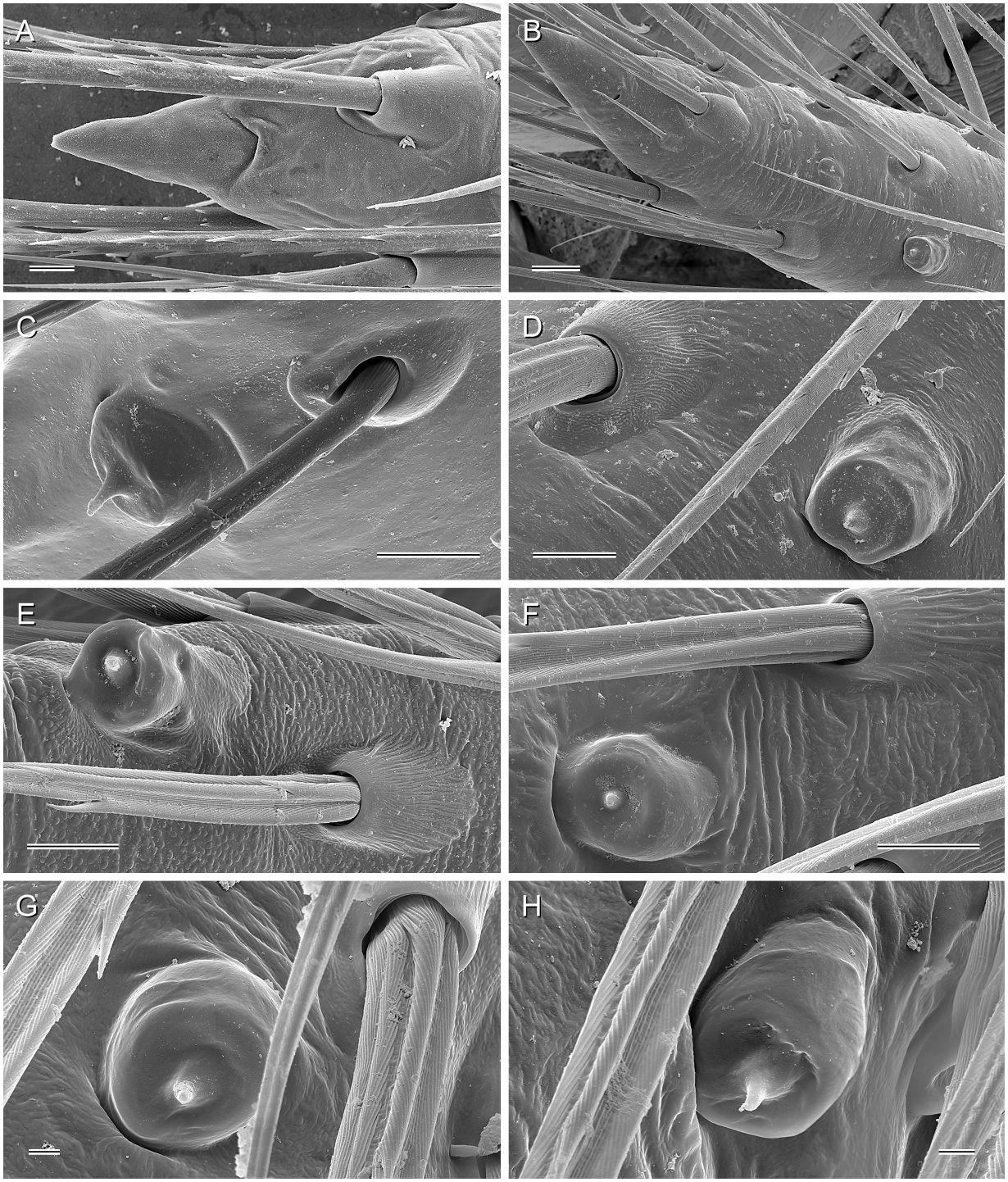

Fig. 43. *Priscula* spp., SEM photographs of female palps and of male and female tarsal organs. A–B. Tips of female palps in dorsal views; *Priscula esmeraldas* Huber sp. nov. (A) and *P. lumbaqui* Huber sp. nov. (B). C. Male palpal tarsal organ, *P. pastaza* Huber sp. nov. D. Female palpal tarsal organ, *P. lumbaqui*. E–H. Female tarsal organs on leg 1 (E, *P. lumbaqui*), leg 2 (F, *P. esmeraldas*), leg 3 (G, *P. pastaza*), and leg 4 (H, *P. pastaza*). Scale lines: 10 µm (A, C–F); 20 µm (B); 2 µm (G–H).

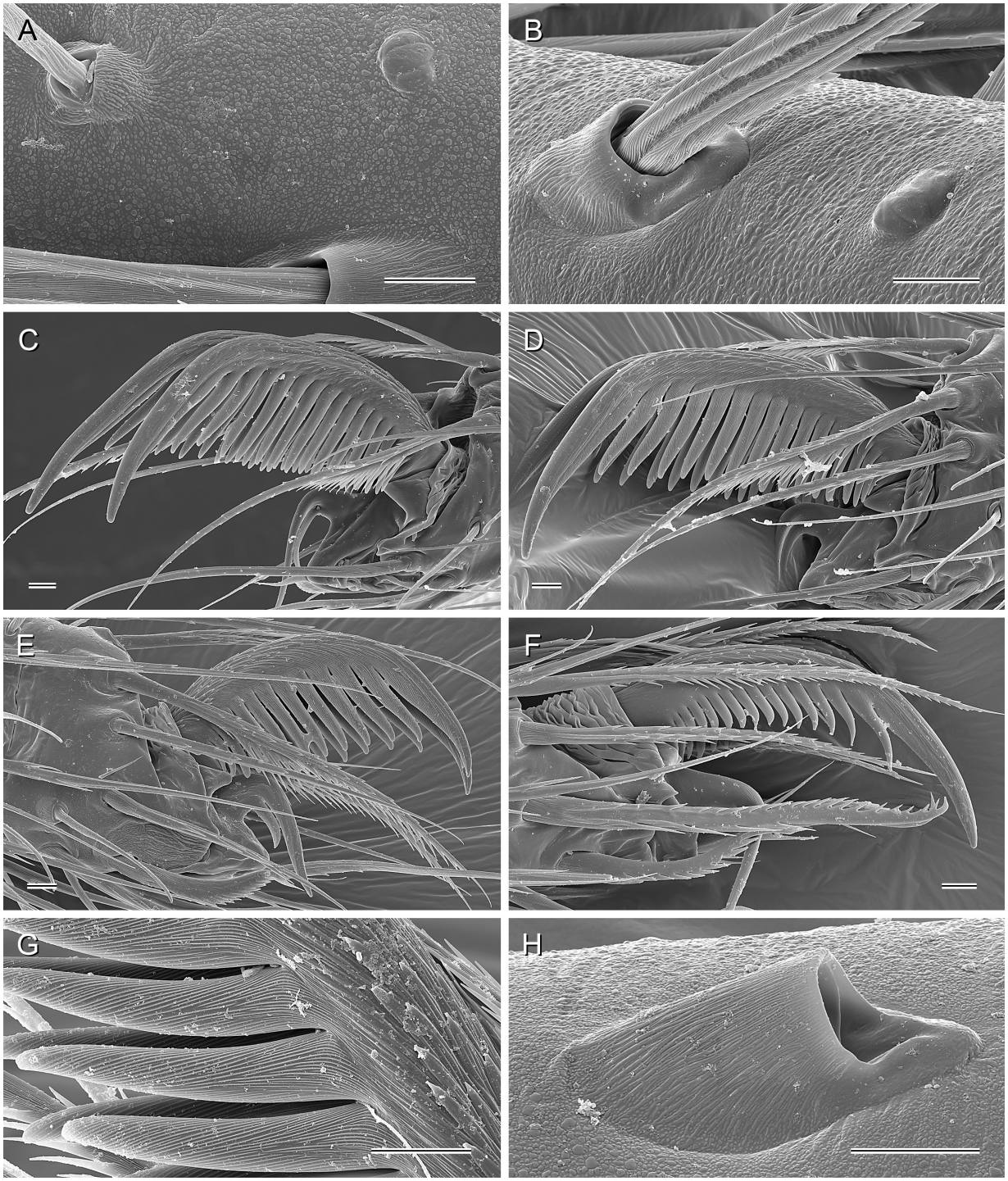

Fig. 44. *Priscula* spp., SEM photographs of female legs. A–B. Oval plates of unknown function, in *Priscula lumbaqui* Huber sp. nov. (A, metatarsus 4) and *P. pastaza* Huber sp. nov. (B, metatarsus 4). C–F. Tarsal claws of leg 1 (C, *P. pastaza*), leg 2 (D, *P. pastaza*), leg 3 (E, *P. bonita* Huber sp. nov.), and leg 4 (F, *P. pastaza*). G. Microstructure of claw tines (*P. chapintza* Huber sp. nov.). H. Basis of mechanoreceptive hair (*P. chapintza*; metatarsus 4), showing distal bulge (on right side). Scale lines: 10 μm.

with distinctively sculptured area medially in front of ALS (similar to Fig. 41G but smaller). Epigynum (Fig. 40A–B) main anterior plate semicircular to trapezoidal, slightly protruding, with pair of low humps at posterior margin, posteriorly medially slightly indented; posterior epigynal plate medially divided by whitish area. Internal genitalia (Figs 39C, 40C–D) with pair or oval pore plates, with pair of small processes on ventral arc, and with large median triangular sclerite between pore plates on dorsal arc.

Distribution

Known from type locality only, in Sucumbíos Province, Ecuador (Fig. 4B). The ZMH (A2591) has a single female specimen from Napo, "Misahualli via Yuralpa", 1.0901° S, 77.5434° W, which might belong to this species. In the map in Fig. 4B it is shown as "*P.* Dup134".

Natural history

Most specimens were collected from webs that were hidden deeply in sheltered spaces at ground level; one female was found on the underside of a large dead tree trunk suspended over a brook; one pair was found under small overhangs of a roadcut. One egg-sac had a diameter of 4.5 mm, and contained ~65 eggs with an egg diameter of 1.00 mm.

Discussion

Monophyly

All our analyses supported the monophyly of *Priscula*, with moderate to high support (SH–aLRT supports 81–99). This is also the case in our preliminary UCE dataset (G. Meng, B.A. Huber, L. Podsiadlowski, unpubl. data), which includes fewer species of *Priscula* but many more other genera. The monophyly of *Priscula* is equally uncontested on morphological grounds. Surprisingly, however, few synapomorphies are known to support this monophyly. An exposed male palpal tarsal organ situated on a turret was proposed as the only synapomorphy in Huber (2000). This character has previously been studied with SEM in only two species (Huber 2000). Our new data show that this is not a general character in the genus: in *P. pastaza* sp. nov. and in *P. bonita* sp. nov. the male palpal tarsal organ is exposed but not situated on a stalk (Fig. 43C). Potential synapomorphies are (1) the whitish areas laterally on the male chelicerae (Figs 10B, 14B, etc.); (2) the whitish areas on the genital bulbs that allow for considerable movement of the distal sclerite against the main part of the bulb (Figs 8B, 9E–F; see also Huber & Villarreal 2020: figs 892–897); (3) the irregular tarsal pseudosegmentation (Huber 2000: fig. 101; a character state that is shared with all Smeringopinae except *Cenemus* Saaristo, 2001; Huber & Meng 2023); (4) the distinctive structure medially in front of the spinnerets (in place of the colulus; Fig. 41F–H); and (5) the reduction of epiandrous spigots (Huber 2000: fig. 140). The latter have been reduced convergently several times within Pholcidae, and their absence has been confirmed with SEM in only three species (Huber 2000).

Other traits that characterize *Priscula* and make it easily distinguishable among Neotropical pholcids are all presumably plesiomorphies. The large size and the large male palpal femora (relative to the palpal tibiae) are shared with *Artema*, which, according to our preliminary UCE data (G. Meng, B.A. Huber, L. Podsiadlowski, unpubl. data), may be the sister of *Priscula*. A dense egg sac cover is shared with certain species in the genera *Artema*; *Cantikus* Huber, 2018; and *Physocyclus* Simon, 1893 (Huber & Eberle 2021). And the full set of spigots on the spinnerets is considered plesiomorphic for the entire family (Huber 2000).

Species limits

In a previous study on molecular taxonomy in pholcid spiders (Astrin *et al.* 2006), intra- and interspecific genetic (CO1) variation was found to overlap between 8.7 and 10.9%. This is almost

exactly the range that includes the inconclusive cases in the present study. Values below and above this range usually characterize specimens that are morphologically unambiguous conspecifics or unambiguous allospecifics, respectively. Three remarkable exceptions exist in our dataset: (1) A *P. acarite* specimen from Lara had a distance of 12.8% to a specimen from the type locality in Falcón (both Venezuela). The original description emphasizes explicitly that the genitalia are indistinguishable (Huber & Villarreal 2020). (2) A female identified as *P. piapoco* Huber, 2000 had distances between 3.0 and 5.9% to the sequenced *P. andinensis* specimens. However, the identification of this female rested mainly on the facts that it had been collected at the type locality of *P. piapoco* and that an unambiguous *P. piapoco* male had been collected in the same collecting event. Our sequence data suggest that this female is either not conspecific with the *P. piapoco* male or that a contamination occurred (EB161 and EB167 were in neighboring tubes in the sequencing plate). (3) A female from Bolivia (La Paz) identified as *P. binghamae* by Astrin *et al.* (2006) had a distance of 11.1% to a newly sequenced specimen from Argentina. Males are available from the Argentinean locality, and *P. binghamae* has been reported from La Paz before (Huber 2000), suggesting that this is not a case of misidentification. *Priscula binghamae* is supposedly the species with the widest geographic distribution in the genus (~2700 km). Our data suggest that this species should be restudied.

Noteworthy cases that fall in the problematic overlap area between about 8 and 11% are the following: (1) The specimens supposed to be conspecific or close to *P. gularis* had distances to the sequenced specimen of *P. llaviucu* sp. nov. between 8.7 and 9.2%; morphologically, the available males appear clearly allospecific. The same is true for the pair *P. llaviucu* and *P. azuay* sp. nov. (9.5%). (2) The southernmost sequenced specimen of *P. bonita* sp. nov. (EB096) had a distance to the other sequenced specimens between 8.1 and 8.8%. In this case, morphology is equally ambiguous, which is why we assigned specimens from two southern localities tentatively to this species. (3) A female specimen that we tentatively identified as "*P.* cf. *limonensis*" (from Venezuela, Miranda) had a distance of 8.9% to an unambiguous *P. limonensis* González-Sponga, 1999 specimen from the type locality (Venezuela, La Guaira). The sequenced female is the only specimen available of the dubious 'species', so the collection of males is required to help solve its taxonomic status.

Species groups

The five species groups we propose are preliminary in the sense that they are based on a very limited molecular data set and geographically biased towards species from Ecuador and Venezuela. However, the groups seem to be concentrated in different geographic regions along the Andes, and morphology seems to support several of them. We thus consider these groups as useful working hypotheses, guiding further collecting efforts and future systematic work on the genus. In the absence of a formal cladistic analysis, it remains unknown whether the morphological similarities below are synapomorphies or not. Equally, some of the assignments to species groups of species not included in our molecular dataset are based on similarity only and must be treated with caution.

***gularis* group**

The only potential morphological synapomorphy for this possibly most 'basal' group (i.e. sister to all other groups) is the process on the proximal bulbal sclerite (e.g., Fig. 9E–F). Species in this group share with species in the *binghamae* group the (presumably plesiomorphic) absence of sclerites ventrally in front of the spinnerets (Figs 11A, 15A, etc.) and the relatively short male palpal femur (only ~1.5–1.6 times longer than wide; other groups: 1.8–2.0). The *gularis* group is distinguished from the *binghamae* group by the absence of a protruding whitish area on the procursus (see below). Composition: *P. gularis*; *P. azuay* sp. nov.; *P. espejoi* sp. nov.; *P. llaviucu* sp. nov. (all Ecuador); possibly also *P. paeza* Huber, 2000 (Colombia) and *P. pallisteri* Huber, 2000 (Peru).

***binghamae* group**

Species in this group share a protruding whitish area dorsally on the procursus (asterisks in Figs 22B, 26B, 30A; see also Huber 2000: fig. 509). Beyond that, the group shares plesiomorphic characters with the *gularis* group (see above). Composition: *P. binghamae* (Peru to Argentina); *P. esmeraldas* sp. nov.; *P. pastaza* sp. nov.; *P. chapintza* sp. nov. (all Ecuador).

***limonensis* group**

Species in this group share very small cheliceral apophyses (convergently in *P. lumbaqui* sp. nov.). Composition: *P. limonensis*; *P. lagunosa* González-Sponga, 1999; *P. paila* Huber, 2020 (all Venezuela). An undescribed species from the Island of Trinidad ("*P.* Tri18-11") also belongs in this group; it shares with *P. lagunosa* a distinct sclerotized dorsal process on the procursus.

***salmeronica* group**

Species in this group share the tendency to reduce the AME (convergently in *P. pastaza* and *P. limonensis*). In addition, *P. salmeronica* and *P. acarite* share a distinct ventral process on the male palpal femur. Composition: *P. acarite*; *P. salmeronica*; *P. ulai* González-Sponga, 1999 (all Venezuela); possibly also *P. taruma* (Guyana?).

***andinensis* group**

Species in this group share a distinctive narrow distal element on the procursus, often with a complex sclerite at the tip (e.g. Figs 34A–C, 38A–C). Composition: *P. andinensis*; *P. venezuelana*; *P. bolivari* (all Venezuela); *P. bonita* sp. nov.; *P. lumbaqui* sp. nov. (both Ecuador); probably also *P. annulipes* and *P. huila* (both Colombia), *P. piapoco*; *P. tunebo* Huber, 2000; *P. chejapi* González-Sponga, 1999; *P. piedraensis* González-Sponga, 1999 (all Venezuela).

Finally, a clade consisting of the three latter groups (*limonensis*, *salmeronica*, and *andinensis* groups) is supported by the presence of a pair of sclerites in front of the spinnerets (e.g., Figs 36A–B, 40A–B).

Conservatism and cave adaptations

It has been argued that evolutionary ecological flexibility or 'evolvability' may have been among the main drivers of species diversification in certain pholcid taxa (Eberle *et al.* 2018). In several species-rich genera, individual species have adapted to different microhabitats, leading to an extraordinary morphological diversity of closely related species. This is particularly true for numerous genera in Pholcinae and Modisiminae. *Priscula* does not follow this pattern and is in this respect more similar to genera in Ninetinae, Arteminae, and Smeringopinae. Most species newly described in this study strongly resemble each other in their general morphology (body shape, leg length, coloration) and in their preferred microhabitat (dark sheltered spaces). The same is true for most known Venezuelan species (Huber & Villarreal 2020) and for recently collected material from Argentina and Colombia (B.A. Huber unpubl. data). A notable exception is *P. venezuelana*, a species that was sometimes found on live leaves, where it tended to be lighter-colored than specimens collected at ground level (compare figs 939–940 in Huber & Villarreal 2020); in particular, juveniles were often found higher in the vegetation and tended to be light greenish in life. Our molecular dataset includes two such light *P. venezuelana* specimens (codes BH126: juvenile; and BH127: adult female). In addition, the sister group of *P. venezuelana* in our analyses was always composed of a pair of specimens that were also particularly light (illustrated in Huber & Villarreal 2020: figs 943–944). Their genetic distance from each other was 7.4%, and their distances from *P. venezuelana* specimens ranged from 9.6 to 12.5%, suggesting that one or two further species might be involved. Unfortunately, these two specimens are juveniles and no males are known from their localities of origin.

The cave-dwelling *P. pastaza* sp. nov. fits this image of a morphologically conservative group of spiders. Even though adult specimens were restricted to cave-sections that were absolutely lightless, the morphological adaptations (troglomorphisms) are modest. The spiders are slightly lighter-colored than congeners but by no means as pale or even whitish as many cave-dwelling Pholcinae and Modisiminae; they do not have particularly elongated legs (tibia 1 / carapace width: 5.7 - other species: 2.9–6.2; tibia 1 L/d: 69 - other congeners: 23–73); they have strongly reduced AME, but the AME have been reduced or lost many times convergently in epigean Pholcidae, even in a few other species of *Priscula* (*P. limonensis*, *P. salmeronica*, *P. acarite*, *P. ulai*); the other eyes of *P. pastaza* are barely reduced in size (PLE diameter / carapace width: 0.09; in other species 0.08–0.14). Surprisingly, however, our anecdotal observations on two egg sacs suggest that *P. pastaza* may follow a general prediction about eggs in cave-dwelling animals: *P. pastaza* seems to produce fewer but larger eggs than its epigean relatives. This is surprising because a recent study involving strongly troglomorphic (entirely blind) *Metagonia* spiders did not find such a relationship (Huber & Eberle 2021; Huber *et al.* 2022). The sample size for *Metagonia* was as inadequate as it is in the present case, but the preliminary results in *P. pastaza* suggest that this species and its epigean relatives might be a rewarding topic for a focused study on the evolution of life history parameters in cave spiders.

Acknowledgments

We greatly appreciate the help of Francisco José Prieto Albuja, Lucia Paguay, Alex Pazmino, and Diego Javier Inclán Luna (INABIO) with permits, logistics, and fieldwork in Ecuador; Ecuador specimens were collected under permits MAAE-DNB-CM-2020-0136 and MAE-DNB-CM-2020-0130. We thank the EcoMinga Foundation for allowing us to enter Rio Anzu Reserve. BAH thanks the directors of the Museo del Instituto de Zoología Agrícola (MIZA, UCV, Maracay), Vilma Savini and José Clavijo, for facilitating field work in Venezuela; Osvaldo Villarreal and Quintin Arias for help with logistics and collecting in Venezuela; Abel Pérez González for help with getting a collection permit; and the Dirección General de Fauna y Oficina Nacional de Diversidad Biológica in Caracas for issuing permit No 01-11-0966; and Laura von der Mark and Lars Podsiadlowski (ZFMK) for support with molecular work. We thank Abel Pérez González and an anonymous reviewer for valuable comments on the manuscript. Field work in Ecuador was partly funded by the Alexander Koenig Stiftung (AKS, Bonn).

References

Astrin J.J. & Stüben P.E. 2008. Phylogeny in cryptic weevils: molecules, morphology and new genera of western Palaearctic Cryptorhynchinae (Coleoptera: Curculionidae). *Invertebrate Systematics* 22 (5): 503–522. https://doi.org/10.1071/IS07057

Astrin J.J., Huber B.A., Misof B. & Kluetsch C.F.C. 2006. Molecular taxonomy in pholcid spiders (Pholcidae, Araneae): evaluations of species identification methods using CO1 and 16S rRNA. *Zoologica Scripta* 35: 441–457. https://doi.org/10.1111/j.1463-6409.2006.00239.x

Astrin J.J., Höfer H., Spelda J., Holstein J., Bayer S., Hendrich L., Huber B.A., Kielhorn K.-H., Krammer H.-J., Lemke M., Monje J.C., Morinière J., Rulik B., Petersen M., Janssen H. & Muster C. 2016. Towards a DNA barcode reference database for spiders and harvestmen of Germany. *PLoS One* 11 (9): e0162624. https://doi.org/10.1371/journal.pone.0162624

Brignoli P.M. 1981. Studies on the Pholcidae, I. Notes on the genera *Artema* and *Physocyclus* (Araneae). *Bulletin of the American Museum of Natural History* 170: 90–100.

Bruvo-Mađarić B., Huber B.A., Steinacher A. & Pass G. 2005. Phylogeny of pholcid spiders (Araneae: Pholcidae): combined analysis using morphology and molecules. *Molecular Phylogenetics and Evolution* 37 (3): 661–673. https://doi.org/10.1016/j.ympev.2005.08.016

Capella-Gutiérrez S., Silla-Martínez J.M. & Gabaldón T. 2009. trimAl: a tool for automated alignment trimming in large-scale phylogenetic analyses. *Bioinformatics* 25 (15): 1972–1973. https://doi.org/10.1093/bioinformatics/btp348

Cock P.J.A., Antao T., Chang J.T., Chapman B.A., Cox C.J., Dalke A., Friedberg I., Hamelryck T., Kauff F., Wilczynski B. & de Hoon M.J. 2009. Biopython: freely available Python tools for computational molecular biology and bioinformatics. *Bioinformatics* 25 (11): 1422–1423. https://doi.org/10.1093/bioinformatics/btp163

Dederichs T.M., Huber B.A. & Michalik P. 2022. Evolutionary morphology of sperm in pholcid spiders (Pholcidae, Synspermiata). *BMC Zoology* 7: 52. https://doi.org/10.1186/s40850-022-00148-3

Eberle J., Dimitrov D., Valdez-Mondragón A. & Huber B.A. 2018. Microhabitat change drives diversification in pholcid spiders. *BMC Evolutionary Biology* 18: 141. https://doi.org/10.1186/s12862-018-1244-8

González-Sponga M.A. 1999. Arácnidos de Venezuela. Ocho especies nuevas del género *Priscula* y descripción de *Priscula venezuelana* Simon, 1893 (Arachnida: Araneae: Pholcidae). *Boletín de la Academia de Ciencias Fisicas, Matematicas y Naturales* 54: 123–168.

Guindon S., Dufayard J.-F., Lefort V., Anisimova M., Hordijk W. & Gascuel O. 2010. New algorithms and methods to estimate maximum-likelihood phylogenies: assessing the performance of PhyML 3.0. *Systematic Biology* 59: 307–321. https://doi.org/10.1093/sysbio/syq010

Huber B.A. 1997. Redescriptions of Eugène Simon's neotropical pholcids (Araneae, Pholcidae). *Zoosystema* 19 (3): 573–612.

Huber B.A. 2000. New World pholcid spiders (Araneae: Pholcidae): a revision at generic level. *Bulletin of the American Museum of Natural History* 254: 1–348. https://doi.org/10.1206/0003-0090(2000)254<0001:NWPSAP>2.0.CO;2

Huber B.A. 2014. Pholcidae. *In*: Roig-Juñent S., Claps L.E. & Morrone J.J. (eds) *Biodiversidad de Artrópodos Argentinos*, *Vol. 3*: 131–140. Sociedad Entomológica Argentina.

Huber B.A. 2021. First Northwest African species of the spider genus *Artema*, from caves in Morocco, with notes on body size in pholcid spiders (Araneae, Pholcidae). *Zootaxa* 4984: 324–334. https://doi.org/10.11646/zootaxa.4984.1.23

Huber B.A. 2022. Revisions of *Holocnemus* and *Crossopriza*: the spotted-leg clade of Smeringopinae (Araneae, Pholcidae). *European Journal of Taxonomy* 795: 1–241. https://doi.org/10.5852/ejt.2022.795.1663

Huber B.A. & Eberle J. 2021. Mining a photo library: Eggs and egg sacs in a major spider family. *Invertebrate Biology* 140 (4): e12349, 1–13. https://doi.org/10.1111/ivb.12349

Huber B.A. & Meng G. 2023. On the mysterious Seychellois endemic spider genus *Cenemus* (Araneae, Pholcidae). *Arthropod Systematics and Phylogeny* 81: 179–200. https://doi.org/10.3897/asp.81.e86793

Huber B.A. & Villarreal O. 2020. On Venezuelan pholcid spiders (Araneae, Pholcidae). *European Journal of Taxonomy* 718: 1–317. https://doi.org/10.5852/ejt.2020.718.1101

Huber B.A., Meng G., Acurio A.E., Astrin J.J., Inclán D.J., Izquierdo M. & Valdez-Mondragón A. 2022. *Metagonia* spiders of Galápagos: blind cave-dwellers and their epigean relatives (Araneae, Pholcidae). *Invertebrate Systematics* 36 (7): 647–678. https://doi.org/10.1071/IS21082

Kalyaanamoorthy S., Minh B.Q., Wong T.K.F., von Haeseler A. & Jermiin L.S. 2017. ModelFinder: fast model selection for accurate phylogenetic estimates. *Nature Methods* 14: 587–589. https://doi.org/10.1038/nmeth.4285

Katoh K. & Standley D.M. 2013. MAFFT multiple sequence alignment software version 7: improvements in performance and usability. *Molecular Biology and Evolution* 30 (4): 772–780. https://doi.org/10.1093/molbev/mst010

Kearse M., Moir R., Wilson A., Stones-Havas S., Cheung M., Sturrock S., Buxton S., Cooper A., Markowitz S., Duran C., Thierer T., Ashton B., Meintjes P. & Drummond A. 2012. Geneious Basic: an integrated and extendable desktop software platform for the organization and analysis of sequence data. *Bioinformatics* 28 (12): 1647–1649. https://doi.org/10.1093/bioinformatics/bts199

Kimura M. 1980. A simple method for estimating evolutionary rates of base substitutions through comparative studies of nucleotide sequences. *Journal of Molecular Evolution* 16: 111–120. https://doi.org/10.1007/BF01731581

Letunic I. & Bork P. 2021. Interactive Tree Of Life (iTOL) v5: an online tool for phylogenetic tree display and annotation. *Nucleic Acids Research* 49 (W1): W293–W296. https://doi.org/10.1093/nar/gkab301

Minh B.Q., Nguyen M.A.T. & von Haeseler A. 2013. Ultrafast approximation for phylogenetic bootstrap. *Molecular Biology and Evolution* 30 (5): 1188–1195. https://doi.org/10.1093/molbev/mst024

Minh B.Q., Schmidt H.A., Chernomor O., Schrempf D., Woodhams M.D., von Haeseler A. & Lanfear R. 2020. IQ-TREE 2: New models and efficient methods for phylogenetic inference in the genomic era. *Molecular Biology and Evolution* 37 (5): 1530–1534. https://doi.org/10.1093/molbev/msaa015

Ratnasingham S. & Hebert P.D.N. 2007. BOLD: The Barcode of Life Data System (http://www.barcodinglife.org). *Molecular Ecology Notes* 7: 355–364. https://doi.org/10.1111/j.1471-8286.2007.01678.x

Simon E. 1893a. Descriptions d'espèces et de genres nouveaux de l'ordre des Araneae. *Annales de la Société Entomologique de France* 62: 299–330.

Simon E. 1893b. *Histoire Naturelle des Araignées*. 2nd edition, 1 (2): 256–488. Roret, Paris.

Steenwyk J.L., Buida III T.J., Li Y., Shen X.-X. & Rokas A. 2020. ClipKIT: A multiple sequence alignment trimming software for accurate phylogenomic inference. *PLoS Biology* 18: e3001007. https://doi.org/10.1371/journal.pbio.3001007

Suyama M., Torrents D. & Bork P. 2006. PAL2NAL: robust conversion of protein sequence alignments into the corresponding codon alignments. *Nucleic Acids Research* 34: W609–W612. https://doi.org/10.1093/nar/gkl315

Tabei Y., Kiryu H., Kin T. & Asai K. 2008. A fast structural multiple alignment method for long RNA sequences. *BMC Bioinformatics* 9: 33. https://doi.org/10.1186/1471-2105-9-33

Talavera G. & Castresana J. 2007. Improvement of phylogenies after removing divergent and ambiguously aligned blocks from protein sequence alignments. *Systematic Biology* 56 (4): 564–577. https://doi.org/10.1080/10635150701472164

Tamura K., Stecher G. & Kumar S. 2021. MEGA11: Molecular Evolutionary Genetics Analysis Version 11. *Molecular Biology and Evolution* 38 (7): 3022–3027. https://doi.org/10.1093/molbev/msab120

Torres-Carvajal O., Pazmiño-Otamendi G. & Salazar-Valenzuela D. 2019. Reptiles of Ecuador: a resource-rich online portal, with dynamic checklists and photographic guides. *Amphibian and Reptile Conservation* 13 (1): 209–229.

Yang C., Zheng Y., Tan S., Meng G., Rao W., Yang C., Bourne D.G., O'Brien P.A., Xu J., Liao S., Chen A., Chen X., Jia X., Zhang A. & Liu S. 2020. Efficient COI barcoding using high throughput single-end 400 bp sequencing. *BMC Genomics* 21: 862. https://doi.org/10.1186/s12864-020-07255-w

Manuscript received: 7 February 2023
Manuscript accepted: 9 June 2023
Published on: 28 November 2023
Topic editor: Magalie Castelin
Subject editor: Rudy Jocqué
Desk editor: Thomas Guyomard

Printed versions of all papers are also deposited in the libraries of the institutes that are members of the *EJT* consortium: Muséum national d'histoire naturelle, Paris, France; Meise Botanic Garden, Belgium; Royal Museum for Central Africa, Tervuren, Belgium; Royal Belgian Institute of Natural Sciences, Brussels, Belgium; Natural History Museum of Denmark, Copenhagen, Denmark; Naturalis Biodiversity Center, Leiden, the Netherlands; Museo Nacional de Ciencias Naturales-CSIC, Madrid, Spain; Leibniz Institute for the Analysis of Biodiversity Change, Bonn – Hamburg, Germany; National Museum of the Czech Republic, Prague, Czech Republic.

Supplementary files

Table S1. GenBank accessions of all gene sequences used in the study. Gray background genes were obtained from Eberle *et al.* 2018. The other genes were sequenced in this study.
https://doi.org/10.5852/ejt.2023.909.2351.10259

Table S2. CO1 genetic distances calculated from the untrimmed alignment using MEGA. The Kimura 2-parameter model was applied with uniform rates among sites. Homogeneous pattern of rates among lineages was assumed. Pairwise deletion strategy was used to deal with gaps/missing data in the alignment. https://doi.org/10.5852/ejt.2023.909.2351.10261

Figure S1. Maximum likelihood tree from ClipKIT_kpic-smart-gap-trimmed alignments and unpartitioned analysis using IQ-TREE. Numbers on the branches are SH-aLRT support (%). Best-fit model according to BIC for the reference tree: SYM+I+G4.
https://doi.org/10.5852/ejt.2023.909.2351.10263

Figure S2. Summary tree of all trees constructed from unpartitioned analyses. All trees were constructed from the same gene set but with different multiple-sequence-alignment (MSA) trimming strategies or from the untrimmed MSA using IQ-TREE. The ClipKIT_kpic-smart-gap tree was used as the reference tree. The trees (query trees) from other MSA-trimming strategies were compared to the reference tree, with '+' or '-' indicating that the query trees agree or disagree, respectively with the branching events of the reference tree. Numbers on the branches are SH-aLRT support (%). Best-fit model according to BIC for the reference tree: SYM+I+G4. https://doi.org/10.5852/ejt.2023.909.2351.10265

Figure S3. Summary tree of all trees constructed from partitioned analyses. All trees were constructed from the same gene set but with different multiple-sequence-alignment (MSA) trimming strategies or from the untrimmed MSA using IQ-TREE. The Gblocks tree was used as the reference tree. The trees (query trees) from other MSA-trimming strategies were compared to the reference tree, with '+' or '-' indicating that the query trees agree or disagree, respectively with the branching events of the reference tree. Numbers on the branches are SH-aLRT support (%). For the partitioned analyses, the initial partition was locus-wise, but subsequently the best partitioning scheme was determined by allowing the merge of different loci (-m MFP+MERGE); at the same time, the best-fit model of each partition was also determined. The best partitioning scheme and the best-fit model of each partition of the reference tree: (1) CO1 partition: TIM3+F+I+G4; (2) H3+18S+28S partition: TN+F+G4; (3) 12S+16S partition: GTR+F+G4. https://doi.org/10.5852/ejt.2023.909.2351.10267

Figure S4. CO1 NJ tree calculated using MEGA. The untrimmed CO1 alignment was used. The Kimura 2-parameter (K80) model was applied with uniform rates among sites. Homogeneous pattern of rates among lineages was assumed. Pairwise deletion strategy was used to deal with gaps/missing data in the alignment. Numbers on the branches are the standard bootstrap supports calculated from 500 replicates.
https://doi.org/10.5852/ejt.2023.909.2351.10269